*Stacked image of registered **Aurigids** during the night of August 31 – September 1, 2021 from the camera located in **Derazhnoye, Belarus** Read more page 16.*

Contents

An outburst of Andromedids (AND#0018) in 2021

Peter Jenniskens

SETI Institute, 189 Bernardo Avenue, Mountain View, CA 94043, USA

pjenniskens@seti.org

Northern hemisphere networks of the CAMS video orbit survey are detecting higher than expected rates of Andromedids (IAU shower 18) in recent days. Starting on November 20, 2021, rates have been significantly above the usual level and reversing a trend of decreasing Andromedid activity after November 9. On November 22, the geocentric radiant was located in the constellation Andromeda at R.A. = 25.2 ± 1.0°, Decl. = +39.5 ± 0.7°, while meteors entered the atmosphere with a slow geocentric speed v_g = 17.9 ± 2.2 km/s. Activity may continue for a few more days.

1 Introduction

The Andromedids are known from spectacular meteor storms in 1872 and 1885 that occurred shortly after the fragmentation of parent comet 3D/Biela. These storms appear to have resulted from normal comet (fragment) activity in the 1846 and 1852 returns, rather than from the breakup of 3D/Biela itself (Jenniskens and Vaubaillon, 2007). The shower was only briefly sighted in later years, but was recovered in photographic data in 1959 (Hawkins et al., 1959). More recently, it was found that the Andromedids are an annual meteor shower in low-light video data in early November (Jenniskens et al., 2016).

In most years, modest rates are detected in the first two weeks of November, but in some years the shower has episodes of enhanced activity in the final weeks of November and in early December. Andromedid outbursts in 2011 and 2013 were ascribed to the crossing of the 17th century dust trails from comet 3D/Biela (Wiegert et al., 2013; Brown, 2013). Based on that hypothesis, no enhanced activity was predicted for 2021.

2 Methods

The 2021 Andromedid activity was detected mostly by the northern hemisphere networks of the CAMS video-based meteoroid orbit survey, in particular by the networks in the BeNeLux (coordinated by C. Johannink and M. Breukers), Turkey (O. Unsalan), the United Arab Emirates (M. Odeh), Florida (A. Howell), Texas (W. Cooney, D. Samuels), Arkansas (L. Juneau), Arizona (N. Moskovitz), and California (J. Albers, T. Beck). Methods are described in Jenniskens et al. (2011).

3 The observations

The Andromedid shower ("AND" in *Figure 1*) was first detected on 2021 Oct. 28, when the radiant was near the ecliptic plane. The radiant slowly rose to higher ecliptic latitudes while rates increased until a broad maximum around November 9, when on average one Andromedid was triangulated for every 68 sporadic meteors. After that, rates declined until a reversal occurred (see *Figure 1* and the website[1]).
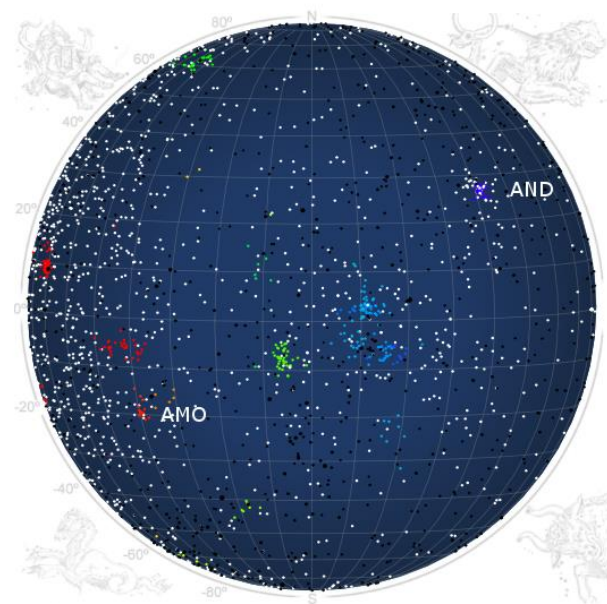
Figure 1 – The radiant plot obtained by CAMS for 2021 November 22 ± 0.5.

Starting on November 20, Andromedid rates have been significantly above the previous trend. On November 22, there was one Andromedid triangulated for every 42 sporadic meteors and rates appeared to be rising (*Figure 2*).

On that day, the geocentric radiant was located in the constellation Andromeda at R.A. = 25.2 ± 1.0°, Decl. = +39.5 ± 0.7°, while meteors entered the atmosphere with speed v_g = 17.9 ± 2.2 km/s (apparent speed v_{inf} = 21.0 km/s). Median orbital elements were:

- a = 4.5 AU;
- q = 0.828 ± 0.013 AU;
- e = 0.816 ± 0.128;
- i = 12.9 ± 1.2°;
- ω = 230.7 ± 1.0°;
- Ω = 239.8 ± 0.1° (Equinox J2000.0).

---

[1] http://cams.seti.org/FDL/ for dates of 2021 Nov. 20 to 22.

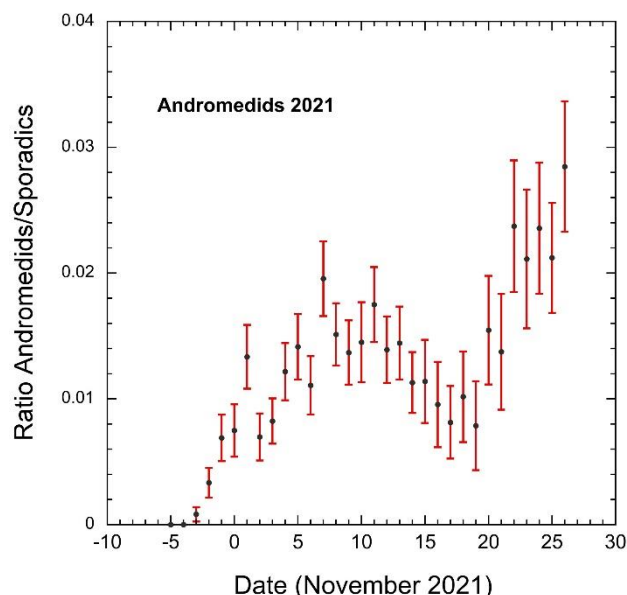*Figure 2* – The preliminary activity profile of the Andromedids based on all low-light video data reported before November 23, 2021 (see website[2]). This graph does not take into account varying coverage due to weather and technical issues. [Updated: 2021 Nov 26].

The unexpected outburst will shed new light on the past activity of comet 3D/Biela. Activity may continue for a few more days, a faint echo of past meteor storms. Further observations are encouraged. It is interesting to note that the historic Andromedid storms from 1872 and 1885 radiated from R.A. = 27° and Decl. = +45° on November 27, but no such high activity is expected this year.

Based on unusual Andromedid activity in prior years, the shower may remain visible until about December 6.

References

Brown P. (2013). "Andromedid Meteors". CBET 3741, D. W. E. Green (ed.), Central Bureau for Astronomical Telegrams, pp 1–1.

Hawkins G. S., Southworth R. B., Stienon F. F. (1959). "Recovery of the Andromedids". *Astronomical Journal*, **64**, 183–188.

Jenniskens P., Vaubaillon J. (2007). "3D/Biela and the Andromedids: Fragmenting versus sublimating comets". *Astronomical Journal*, **134**, 1037–1045.

Jenniskens P., Gural P. S., Dynneson L., Grigsby B. J., Newman K. E., Borden M., Koop M., Holman D. (2011). "CAMS: Cameras for Allsky Meteor Surveillance to establish minor meteor showers". *Icarus*, **216**, 40–61.

Jenniskens P., Nénon Q., Albers J., Gural P. S., Haberman B., Morales R., Grigsby B. J., Samuels D., Johannink C. (2016). "The established meteor showers as observed by CAMS". *Icarus*, **266**, 331–354.

Wiegert P. A., Brown P. G., Weryk R. J., Wong D. K. (2013). "The return of the Andromedids meteor shower". *Astronomical Journal*, **145**, 70–81.

[2] http://cams.seti.org/FDL/

An outburst of Andromedids on November 28, 2021

Peter Jenniskens[1] **and Nick Moskovitz**[2]

[1] **SETI Institute, 189 Bernardo Avenue, Mountain View, CA 94043, USA**

pjenniskens@seti.org

[2] **Lowell Observatory, USA**

In addition to enhanced Andromedid (AND#0018) activity since November 20, 2021, we report here that an outburst of mainly faint meteors was detected over Northern America by northern hemisphere networks of the CAMS video orbit survey on November 28. The outburst was centered on solar longitude $245.887 \pm 0.007°$ ($05^h18^m \pm 0^h10^m$ UTC) and had a Full Width at Half Maximum of 4.0 ± 0.5 h. The mean magnitude was $+1.6$ and magnitude distribution index was 3.8 ± 0.3.

1 Introduction

During most years the Andromedids display a low annual activity in early November. This meteor shower is best known from the impressive meteor storms in 1872 and 1885 that occurred shortly after the fragmentation of parent comet 3D/Biela (Jenniskens, 2006). In recent years, unusual Andromedid activity has been detected in late November and early December in 2011 and 2013 (Wiegert et al., 2013; Brown, 2013). The exact cause of those events is a topic of active research. Now, a new outburst was detected that may help find an answer.

2 Methods

The Andromedid activity, a northern hemisphere shower, was monitored by the northern hemisphere networks of the CAMS video-based meteoroid orbit survey. Meteor trajectories were calculated from low-light video observations (Jenniskens et al., 2011). Most video-detected meteors are of magnitude $+4$ to -5. Radiant positions and speed are reported in near-real time at the CAMS-website[3].

In recent years, the CAMS BeNeLux and LO-CAMS networks have included the use of the CAMS-compatible RMS cameras and the triangulations among those RMS cameras are also reported by the Global Meteor Network (Vida et al., 2021). That network also detected the enhanced Andromedid activity. Results are reported at Global Meteor Network website[4].

Northern hemisphere meteor showers are also monitored by the Canadian Meteor Orbit radar (Brown et al., 2008). The radar is sensitive to about $+5^{th}$ to $+10^{th}$ magnitude meteors caused by smaller particles than are detected by video. Radiant and speed results are reported in near-real time at the CMOR website[5].

3 Results

We reported earlier that the first Andromedid activity in 2021 was detected on October 28, gradually increasing to a broad maximum around November 9. After that, rates declined until a reversal occurred and rates started to increase again (Jenniskens, 2021a, 2021b).

On November 28, CMOR detected a strong outburst from the Andromedid shower (*Figure 1*). Brown (2021[6]) reported by tweet that the outburst was "*very rich in fainter meteors. Peak occurred between $6^h–7^h$ UT, November 28 with ZHRs in excess of 100. Hundreds of AND orbits have been recorded. Strongest outburst of AND ever detected by CMOR. AND activity has been high as measured by CMOR the last 10 days, but plateaued in previous 4 days. Last night's sharp outburst was several times above the broad outburst peak of the last days.*"

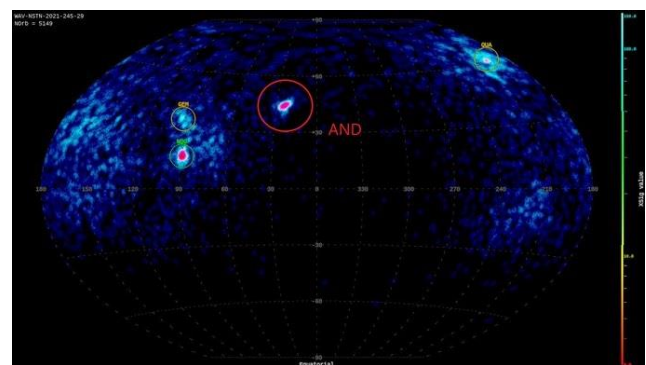*Figure 1* – The Andromedid 2021 outburst recorded by CMOR on November 28.

That night, the CAMS video-based meteoroid orbit surveys in Arizona and California had clear weather and

---

[3] http://cams.seti.org/FDL/
[4] https://globalmeteornetwork.org/data/
[5] https://fireballs.ndc.nasa.gov/cmor-radiants/

[6] Brown (2021). Tweets on topic of Andromedids. November 28, 2021: https://twitter.com/pgbrown

triangulated 122 Andromedids between 1ʰ30ᵐ and 11ʰ55ᵐ UTC (See *Figure 2* and the CAMS-website[7]).
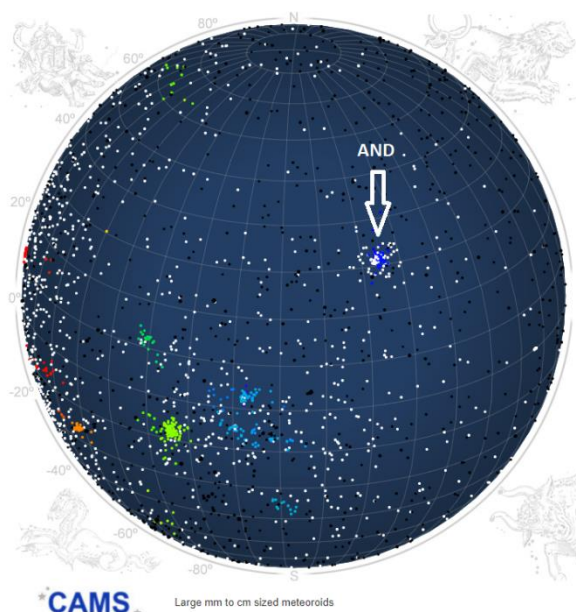

Figure 2 – The high Andromedid activity created a dense cluster of radiant points on the map.

Both CAMS networks detected a spike in rates during the night of November 27–28 over that seen in previous nights. *Figure 3* shows the rate of Andromedids relative to that of sporadic meteors by blue points (on a logarithmic scale). The solid line is a 3-gaussian component fit centered on November 9, 25 and 28.22, respectively, with relative peak activity 0.016, 0.025, and 0.19, and sigma 6.3, 3.2 and 0.087 days.

The graph also shows the raw CMOR counts for each day, which were offset to align with those of CAMS. Note that CMOR followed the CAMS-detected increase of rates after November 20 and also detected the spike in activity. The CMOR-detected spike appears broader, but it probably isn't. The time-dependence of that spike and the actual peak CMOR rate on November 28 are unresolved in the published figures.
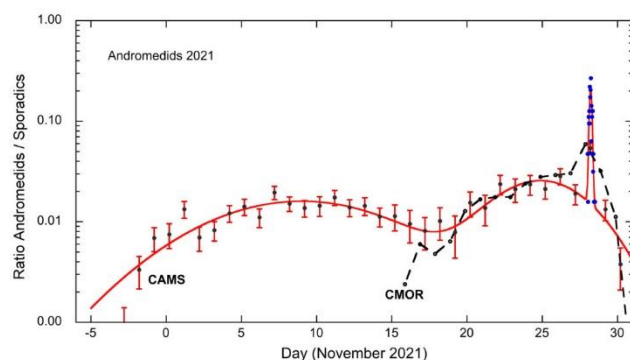

Figure 3 – The Andromedid 2021 rates relative to the sporadic background, recorded by CAMS and CMOR.

The distribution of CAMS-triangulated Andromedids on November 28 is relatively narrow and stands out above previous rates. The distribution is centered on 05ʰ18ᵐ ± 10ᵐ UTC, corresponding to solar longitude 245.887 ± 0.007° (equinox J2000.0) with a full-width-at-half-maximum of only 4.0 ± 0.5 hours. The meteors radiated from a geocentric radiant in the constellation Andromeda at R.A. = 25.8 ± 2.2°, Decl. = +44.7 ± 1.3° (equinox J2000.0) with geocentric velocity v_g = 16.7 ± 3.1 km/s. Median orbital elements were;

- a = 3.8 AU,
- q = 0.858 ± 0.018 AU,
- e = 0.771 ± 0.181,
- i = 13.6 ± 1.9°,
- ω = 225.7 ± 1.9°,
- Ω = 245.87 ± 0.09° (equinox J2000.0).

Most were faint meteors with a steep magnitude distribution index 3.8 ± 0.3. The mean magnitude of the CAMS-detected Andromedids was +1.6. The outburst could be seen also by the naked eye in clear dark skies where the radiant was above the horizon at that time.

Starting on December 1, the CMOR detected Andromedid rate has significantly decreased. CAMS is still seeing some Andromedids. Based on past CAMS-detected outburst activity[8], the shower may remain active until about December 6.

4   Discussion

The cause of the sharp peak and the broad underlaying outburst components are not yet explained. Based on a model that explained the 2011 and 2013 outburst activity with dust trail encounters of the 17ᵗʰ century ejecta prior to the discovery of 3D/Biela (Wiegert et al., 2013), there was no unusual activity expected for 2021. It is possible that the 2021 activity disproves that explanation.

The November 28, 2021, outburst occurred at a solar longitude slightly below that of the 1872 (247.713°) and 1885 (247.336°) meteor storms. The past Andromedid storms were due to the active fragments of 3D/Biela in the 1846 and 1852 returns (Jenniskens and Vaubaillon, 2007), not due to dust generated in the fragmentation of 3D/Biela itself. Perhaps that dust played a role in the activity observed this year. It is also possible that the final breakup of 3D/Biela after the last sightings may be responsible, or even other activity that predates the first sighting of the comet.

Acknowledgements

References

Brown P., Weryk R. J., Wong D. K., Jones J. (2008). "A meteoroid stream survey using the Canadian Meteor

---

[7] http://cams.seti.org/FDL/ for the date of 2021 Nov. 28.

[8] See "Past Data" on http://cams.seti.org/FDL/

Orbit Radar. I. Methodology and radiant catalogue". *Icarus*, **195**, 317–339.

Brown P. (2013). "Andromedid Meteors". CBET 3741, D. W. E. Green (ed.), Central Bureau for Astronomical Telegrams, pp 1–1.

Jenniskens P. (2006). Meteor Showers and their Parent Comets. Cambridge University Press, Cambridge, 790 pp.

Jenniskens P., Vaubaillon J. (2007). "3D/Biela and the Andromedids: Fragmenting versus sublimating comets". *Astron. Journal*, **134**, 1037–1045.

Jenniskens P., Gural P. S., Dynneson, L., Grigsby, B. J., Newman, K. E., Borden, M., Koop, M., Holman D. (2011). "CAMS: Cameras for Allsky Meteor Surveillance to establish minor meteor showers." *Icarus*, **216**, 40–61.

Jenniskens P. (2021a). "Andromedid meteor shower 2021". CBET 5072, D. W. E. Green (ed.), Central Bureau for Astronomical Telegrams, pp 1–1.

Jenniskens P. (2021b). "An outburst of Andromedids (AND#0018) in 2021". *eMetN*, **7**, 1–2.

Vida D., Šegon D., Gural P.S., Brown P. G., McIntyre M. J. M., Dijkema T. J., Pavletić L., Kukić P., Mazur M. J., Eschman P., Roggemans P., Merlak A., Zubrović D. (2021). "The Global Meteor Network – Methodology and First Results". *Monthly Notices of the Royal Astronomical Society*, **506**, 5046–5074.

Wiegert P. A., Brown P. G., Weryk R. J., Wong D. K. (2013). "The return of the Andromedids meteor shower". *Astronomical Journal*, **145**, 70–81.

October zeta Perseids (OZP#1131) - Update

Paul Roggemans[1], Beat Booz[2], Stefano Sposetti[3] and Jochen Richert[4]

[1] **Pijnboomstraat 25, 2800 Mechelen, Belgium**
paul.roggemans@gmail.com

[2] **Department for meteor and fireball calculations, Swiss Fachgruppe Meteorastronomie (FMA), Switzerland**
bbooz@bluewin.ch

[3] **Operator of Station GNO (Gnosca) and LOC (Locarno),**
Swiss Fachgruppe Meteorastronomie (FMA), Switzerland
stefanosposetti@ticino.com

[4] **Operator of Station BOS (Bos-cha), Swiss Fachgruppe Meteorastronomie (FMA), Switzerland**
jochen.richert@gmx.ch

The October zeta Perseids have been reported as a newly discovered meteor shower, now listed in the Working List of meteor showers of the IAU Meteor Data Center. The Swiss FMA video camera network registered one additional orbit during the short activity interval on 2021 October 24. CAMS BeNeLux had finally 4 orbits of this shower, two in common with GMN. A recent stream search on GMN orbit data revealed two more of these peculiar orbits on 2021 October 29, 5 days after the discovery date.

1   Introduction

During the night of 24–25 October 2021, a new long-period meteor shower has been discovered by the Global Meteor Network. The shower experienced a sharp outburst at solar longitude 211.36° (Vida et al., 2021). Meanwhile, the shower has been listed as number 1131 in the IAU MDC shower database[9] (Jenniskens et al., 2020; Jopek and Kaňuchová, 2017; Jopek and Jenniskens, 2011; Neslušan et al., 2020).

Since the first publication about the discovery of this meteor shower, some more information has been collected which is documented in this article.

2   Supporting evidence from FMA

Figure 1 – M20211024_204752 recorded by the FMA video meteor network, image taken with cam no. 5 of station Bos-cha (BOS) by Jochen Richert.

Figure 2 – M20211024_204752 recorded by the FMA video meteor network, image taken from the station GNO by Stefano Sposetti.

The Swiss Fachgruppe Meteorastronomie video meteor network recorded 59 meteors during the night of 2021 October 24–25 within the interval $19^h10^m–22^h13^m$ UT when Global Meteor Network detected 14 October zeta Perseids. A quick check on the multi-station data revealed that one meteor at $20^h47^m52^s$ UT belonged to the newly discovered meteor shower.

This meteor was captured simultaneously by Stefano Sposetti (Locarno and Osservatorio Astronomico di Gnosca) and Jochen Richert (Privatsternwarte Bos-cha). *Figure 1* shows the meteor registered by Jochen Richert and

[9] https://www.ta3.sk/IAUC22DB/MDC2007/Roje/pojedynczy_obiekt.php?kodstrumienia=01131&colecimy=0&kodmin=00001&kodmax=01131&sortowanie=0

Figure 2 the meteor registered by Stefano Sposetti. The following data and orbit have been computed by Beat Booz:

- $\lambda_O = 211.36°$
- $\alpha_g = 59.4°$
- $\delta_g = +32.3°$
- $H_b = 108.5$ km
- $H_e = 90.6$ km
- $v_g = 49.9$ km/s
- $a = 31$ AU
- $q = 0.0827$ AU
- $e = 0.9973$
- $\omega = 326.74°$
- $\Omega = 211.36°$
- $i = 70.1°$
- $\Pi = 178.1°$

This orbit is very similar to the reference orbit listed for the October zeta Perseids (Vida et al., 2021) with discrimination criteria $D_{SH} = 0.086$ (Southworth and Hawkins, 1963) and $D_D = 0.031$ (Drummond, 1981). This contribution by the FMA network is most valuable additional evidence for the meteor shower, obtained by an independent network using a different solver than GMN or CAMS.
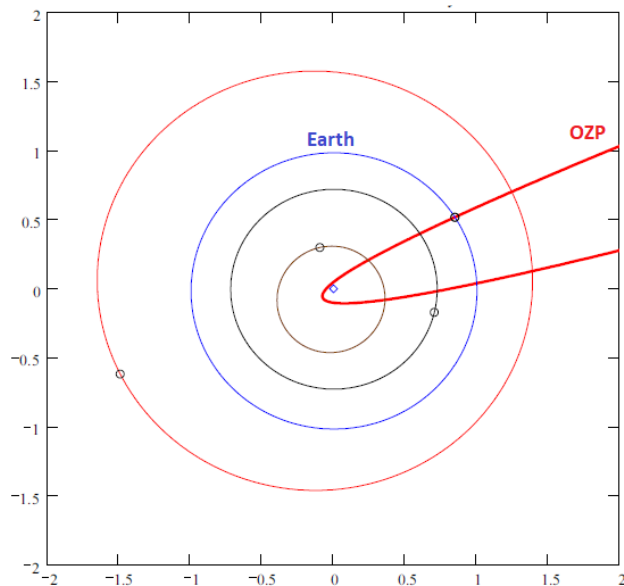

Figure 3 – The October zeta Perseid orbit relative to the Sun and the inner planets (courtesy Beat Booz).
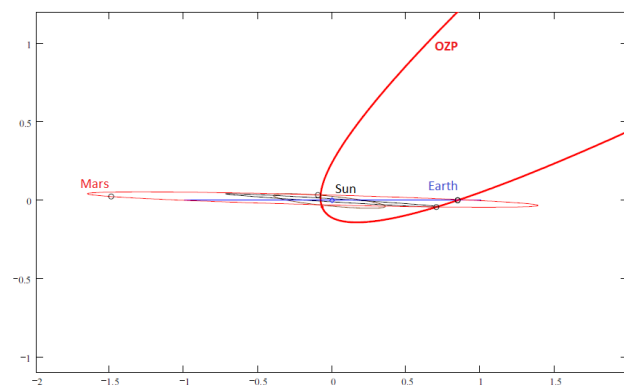

Figure 4 – The October zeta Perseid orbit relative to the Sun the inner planets and the ecliptic plane (courtesy Beat Booz).

3 Four OZP orbits by CAMS-BeNeLux

At the time of the first publication (Vida et al., 2021), a preliminary check on CAMS-BeNeLux data yielded 650 orbits for the night October 24–25, including two October zeta Perseid orbits. When all the data had been collected and could be analyzed, 3621 confirmed meteors were reported of which 2346 were multi-station, good for 715 orbits including four October zeta Perseid orbits. Clouds interfered this night at several stations and reduced the chances to obtain paired meteors.

Figure 5 – The October zeta Perseid meteor registered on 2021, October 24, at $20^h21^m10^s$ UT. CAMS Watec 3900 at Nancy, France (photo Tioga Gulon).

The first OZP meteor was recorded at $20^h21^m10^s$ UT, initially reported double station between Mechelen (Luc Gobin) and Wilderen (Jean-Marie Biets), this meteor was also recorded at Nancy (Tioga Gulon) and at Zoersel (Bart Dessoy). This was a rather faint meteor (see *Figure 5*). A new orbit has been obtained for the combination of these four camera stations.
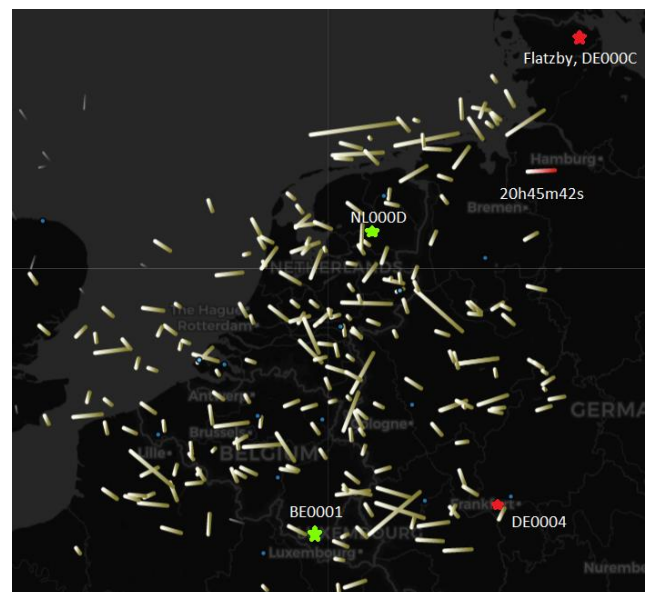

Figure 6 – The meteor map with the trajectory of the OZP meteor on 2021, October 24 at $20^h45^m42^s$ near Hamburg computed by the GMN trajectory solver and the camera locations used by CAMS BeNeLux and GMN.

Figure 7 – The OZP meteor on 2021, October 24 at 20ʰ45ᵐ42ˢ UT recorded at Flatzby by the 6mm RMS camera DE000C (Reinhard Kühn) which was used by both CAMS BeNeLux and GMN.

Figure 8 – The OZP meteor at 20ʰ45ᵐ42ˢ UT recorded at Grapfontaine by the 3.6mm RMS camera BE0001 (Paul Roggemans) which was used by CAMS BeNeLux but rejected by the quality control of the GMN-solver. The meteor appears in the bottom right corner of the FoV.

The second OZP meteor was recorded at 20ʰ40ᵐ18ˢ UT and remained double station between Mechelen (Luc Gobin) and Wilderen (Jean-Marie Biets), without any other camera contributing.

The third OZP meteor is as far as known the most beautiful of all recorded OZP meteors and appeared at 20ʰ45ᵐ43ˢ. This event doesn't increase the total number of OZP orbits as the same meteor appears among the 14 OZP meteors

detected by Global Meteor Network, be it obtained from a different camera combination than within CAMS BeNeLux. The CAMS trajectory solver used the output obtained from three RMS cameras active within the CAMS network: BE0001 (Paul Roggemans) at Grapfontaine, NL000D (Tammo Jan Dijkema) at Dwingeloo and DE000C (Reinhard Kühn) at Flatzby, while GMN based its orbit on the combination of DE000C at Flatzby and RMS DE0004 (Jürgen Dörr) near Frankfurt, a camera which does not

participate in the CAMS network (see *Figure 6*). The orbits obtained by CAMS-BeNeLux and by GMN are compared in *Table 1*.

The reason why the quality control of the trajectory solver of GMN rejected the data from BE0001 and NL000D looks obvious when we look at the images. On the map in *Figure 6* we see that BE0001 in the south-east of Belgium was far away from the meteor and on *Figure 8* we see the

meteor low above the NNE horizon in a corner at the edge of the FoV where the optical distortion is the most problematic. A large distance to the meteor combined with an angular error on the measured position is not ideal. NL000D at Dwingeloo (*Figure 6*) was at a suitable distance from the meteor but got the bright Moon right next to the meteor trail reducing the number of reference stars and therefore limiting the calibration quality (*Figure 9*).

Figure 9 – The OZP meteor at 20ʰ45ᵐ42ˢ UT recorded at Dwingeloo by the 3.6mm RMS camera NL000D (Tammo Jan Dijkema) which was used by CAMS BeNeLux but rejected by the quality control of the GMN-solver. The meteor appears left from the Moon.
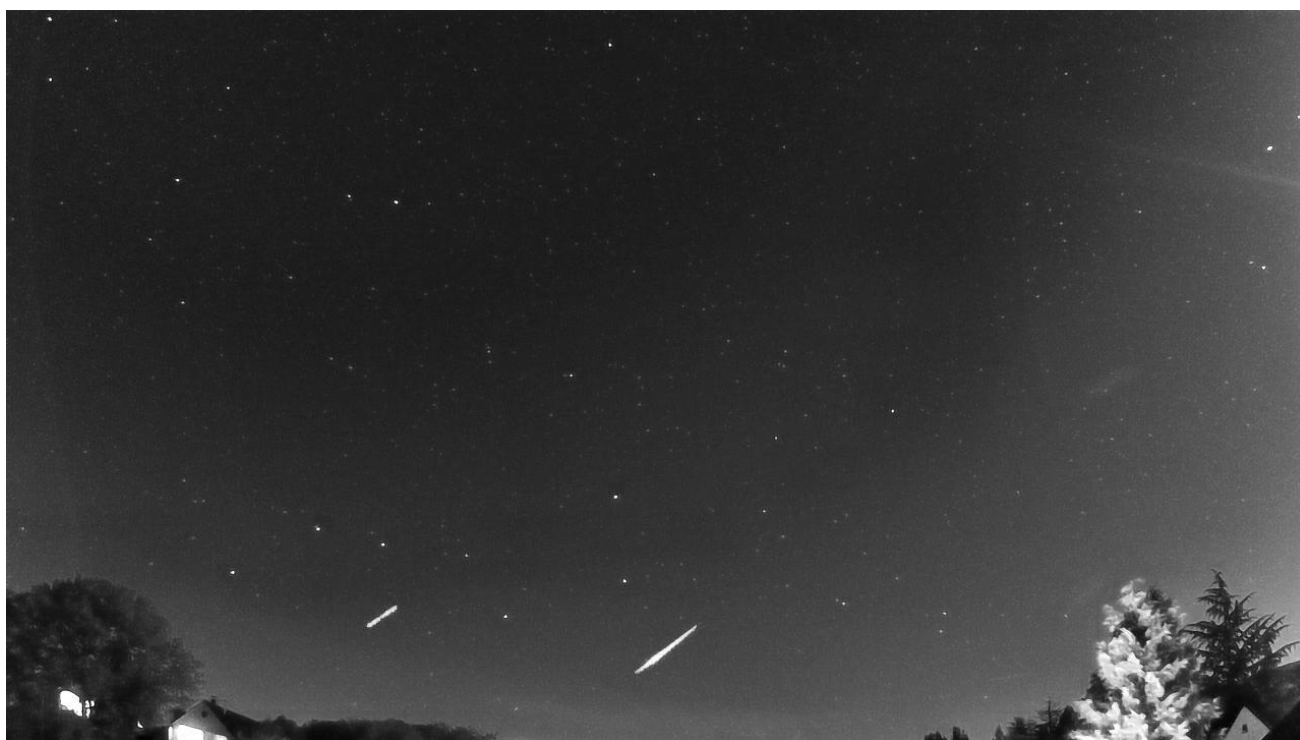

Figure 10 – The OZP meteor at 20ʰ45ᵐ42ˢ UT recorded by the 3.6mm RMS camera DE0004 (Jürgen Dörr) which was used by the GMN trajectory solver but not available for CAMS BeNeLux.

RMS DE000C at Flatzby (*Figure 6*) was at about the same distance from the meteor as NL000D, but with plenty of reference stars and a very good calibration (*Figure 7*). RMS DE0004 near Frankfurt (*Figure 6*) is also far away from the meteor trajectory but registered the meteor trail closer to the center of the FoV with plenty of stars available for a good calibration (*Figure 10*). It is obvious that the best combination was DE000C with DE0004.

Table 1 – Two October zeta Perseid meteors recorded 2021 October 24 by RMS cameras and analyzed independently by CAMS and GMN.

	$20^h45^m43^s$		$20^h53^m16^s$	
	GMN	CAMS	GMN	CAMS
$\lambda_{\odot}$ (°)	211.36	211.36	211.37	211.37
α_g (°)	58.0	58.6	58.7	58.6
δ_g (°)	+33.8	+33.9	+34.3	+34.0
α_o (°)	58.0	58.1	58.7	58.0
δ_o (°)	+34.1	+34.3	+34.7	+34.5
H_b (km)	107.8	110.3	106.0	106.6
H_e (km)	81.1	80.1	95.3	96.0
v_g (km/s)	48.3	50.0	46.9	46.8
m_A	–3.2	–	–0.1	–0.6
$\lambda-\lambda_{\odot}$ (°)	211.76	212.25	212.46	212.30
β (°)	+13.3	+13.3	+13.7	+13.4
a (AU)	–	–	7.58	7.65
q (AU)	0.0834	0.0820	0.0860	0.0835
e	1.0002	1.0087	0.9887	0.9891
ω (°)	326.30	325.82	326.89	327.37
Ω (°)	211.361	211.361	211.367	211.367
i (°)	64.9	70.9	63.7	62.7
Π (°)	177.66	177.18	178.26	178.73

Comparing the output of the trajectory solvers for CAMS and GMN in *Table 1*, the results are not identical but still in good agreement. For CAMS it was the good quality data from Flatzby that saved the solution in combination with the less favorable BE0001 and NL000D camera data. The largest difference between both results is in the absolute magnitude where CAMS suggests $m_A = –13.1$ and GMN $–3.2$, the latter being the most realistic value. Both Denis Vida and Martin Breukers warn that the brightness determination is not reliable. A manual reduction for CAMS by Martin Breukers revealed $m_A = –2.6$. CAMS measured a higher geocentric velocity, 50.0 km/s against 48.3 km/s for GMN, a difference that accounts for the higher inclination i of the orbit. All other orbital parameters are still acceptable in spite of the less favorable combination used by the trajectory solver of CAMS.
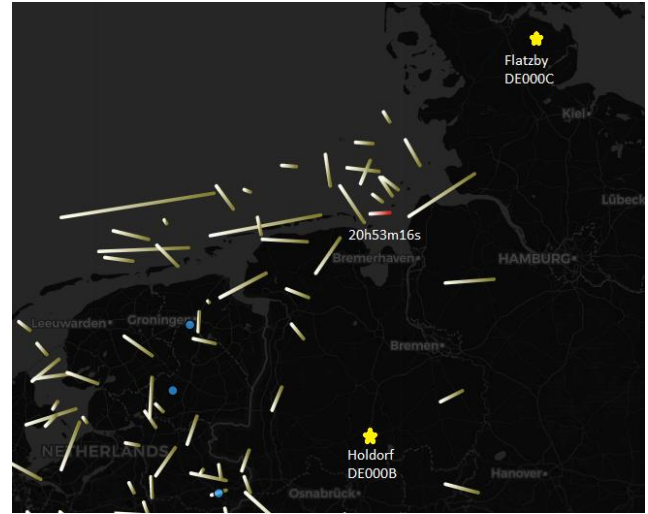

Figure 11 – The meteor map with the trajectory of the OZP meteor on 2021 October 24 at $20^h53^m16^s$ UT, recorded from Flatzby and Holdorf computed by the GMN trajectory solver.

Figure 12 – The OZP meteor at $20^h53^m16^s$ UT recorded by the 6mm RMS camera DE000C at Flatzby (Reinhard Kühn) which was used by both the GMN trajectory solver and the CAMS trajectory solver.

Figure 13 – The OZP meteor at 20ʰ53ᵐ16ˢ UT recorded by the 6mm RMS camera DE000B at Holdorf (Ludger Börgerding) which was used by both the GMN trajectory solver and the CAMS trajectory solver.

The fourth OZP meteor was recorded at 20ʰ53ᵐ16ˢ UT (*Figure 11*) by the two RMS cameras DE000C operated by Reinhard Kühn at Flatzby (*Figure 12*) and DE000B operated by Ludger Börgerding at Holdorf (*Figure 13*) which both participate in the CAMS-BeNeLux network and in the Global Meteor Network. In this case the same DetectInfo positional data was used by both the trajectory solver of CAMS and the trajectory solver of GMN.

Using the exact identical input data for both trajectory solvers does not result in exactly the same numeric output, but the results are in very good agreement (*Table 1*).

Both RMS cameras had plenty of reference stars for calibration and both use a 6mm lens which is recommended within CAMS-BeNeLux because its optical accuracy proved to be significantly better than the 3.6mm lenses. Not only the error margins on the measured positions but also the methodology of the trajectory solver has influence on the differences in the numeric output of orbit computations.

Table 2 – Comparing the mean orbits obtained by Global Meteor Network (14 orbits), CAMS (4 orbits) and FMA (1 orbit).

	GMN	CAMS	FMA
a (AU)	41	45	31
q (AU)	0.0820	0.0808	0.0827
e	0.998	0.9982	0.9973
i (°)	65.2	67.9	70.1
Ω (°)	211.38	211.389	211.36
ω (°)	326.8	326.98	326.74

The four October zeta Perseid orbits obtained by CAMS BeNeLux result in a slightly different mean orbit than the preliminary results based on two orbits. The final result compares better to the GMN than the preliminary published CAMS results in Vida et al. (2021). In *Table 2* we compare the results obtained by GMN, CAMS and FMA.

4   Some late October zeta Perseids?

Running a shower search through the entire GMN meteor orbit dataset with 341249 orbits (version 13 November 2021) to locate the 14 OZP orbits, to our surprise we found 16 instead of 14 OZP orbits. Two more of these peculiar orbits had been recorded on October 29, a first at 04ʰ59ᵐ51ˢ UT in Canada by RMS cameras CA000F, CA000Q and CA000S. The second one appeared at 09ʰ06ᵐ41ˢ UT and was recorded in the USA by RMS cameras US0001, US0004, US0008, US000A, US000C, US000H and US000P.

The orbits of these two events have a close match with the GMN reference orbit of October 24 for the OZP meteoroid stream with $D_D = 0.069$ and $D_D = 0.031$ as discrimination criteria according to Drummond (1981). The parameters for these two orbits are compared in *Table 3*.

Note that a stream search on 1326006 orbits collected by CAMS, EDMOND, SonotaCo and Global Meteor Network before 2021, revealed 20 candidate OZP orbits recorded between 2007 and 2020 on nights before and up to one week later than October 24 (Vida et al., 2021).

A search through the orbit datasets for 2021 of other major video meteor networks would be worthwhile.

Table 3– Two October zeta Perseid meteors recorded 2021 October 29 by RMS cameras in Canada and the USA.

	20211029_045951	20211029_090641
$\lambda_\odot$ (°)	215.693	215.865
α_g (°)	62.8	63.6
δ_g (°)	+35.6	+35.7
v_g (km/s)	47.8	47.8
$\lambda-\lambda_\odot$ (°)	211.7	212.3
β (°)	+14.2	+14.3
a (AU)	30	18
q (AU)	0.09438	0.09269
e	0.9969	0.9948
ω (°)	324.38	324.90
Ω (°)	215.693	215.866
i (°)	64.4	65.9
Π (°)	180.07	180.76
D_D	0.069	0.031

5   Conclusion

Some additional evidence has been found for the recently discovered October zeta Perseids with one more orbit obtained by the Swiss FMA video meteor network. The final results for CAMS-BeNeLux resulted in four OZP orbits. Two of these meteors were used independently by both CAMS-BeNeLux and Global Meteor Network and offered an interesting opportunity to compare the results obtained by two different trajectory solvers. The number of operational RMS cameras in the CAMS-BeNeLux area is still too low to provide a good coverage for the Global Meteor Network. More cameras are required. Another aspect is the size of the network. The GMN covers a much larger part of the atmosphere than CAMS-BeNeLux and therefore has better chances to detect enough meteors to reveal unexpected short-lived activity caused by unknown meteor showers.

Acknowledgment

References

Drummond J. D. (1981). "A test of comet and meteor shower associations". *Icarus*, **45**, 545–553.

Jenniskens P., Jopek T.J., Janches D., Hajduková M., Kokhirova G.I., Rudawska R. (2020). "On removing showers from the IAU Working List of Meteor Showers". *Planetary and Space Science*, **182**, id. 104821.

Jopek T. J. and Kaňuchová Z. (2017). "IAU Meteor Data Center - the shower database: A status report". *Planetary and Space Science*, **143**, 3–6.

Jopek T. J. and Jenniskens P. M. (2011). "The Working Group on Meteor Showers Nomenclature: A History, Current Status and a Call for Contributions". In Meteoroids: The Smallest Solar System Bodies, *Proceedings of the Meteoroids Conference* held in Breckenridge, Colorado, USA, May 24-28, 2010. Edited by W.J. Cooke, D.E. Moser, B.F. Hardin, and D. Janches, NASA/CP-2011-216469, 7–13.

Neslušan L., Poručan V., Svoreň J., Jakubík M. (2020). "On the new design othe IAU MDC portal". *WGN, Journal of the International Meteor Organization*, **48**, 168–169.

Southworth R. R. and Hawkins G. S. (1963). "Statistics of meteor streams". *Smithson. Contrib. Astrophys.*, **7**, 261–286.

Vida D., Šegon D., Roggemans P. (2021). "October zeta Perseid meteor shower (OZP#01131)". *eMetN*, **6**, 536–539.

---

[10] https://tammojan.github.io/meteormap/

October zeta Perseids (OZP#01131), by the Belarusian meteor video network

Yury Harachka

Minsk, Belarus
`astronominsk@gmail.com`

The October zeta Perseids (OZP#01131) meteor shower was discovered during the night of October 24–25, 2021 by the Global Meteor Network. That night, the Belarusian meteor video network also recorded 3 additional orbits from this new shower during the short activity interval on 2021 October 24.

1   Introduction

The end of October is a time when clear skies in Belarus are very rare. However, on the night of 24–25 October 2021 the sky was completely clear, which can be considered as a great luck. The Belarusian meteor video network recorded 218 multi-station meteors that night. Analysis of the data shows that among them three meteors belong to the new October zeta Perseids meteor shower.

2   Chronology of registration of the October zeta Perseids

The first meteor was captured October 24, at $20^h41^m37^s$ UTC by three cameras at the camera stations in Minsk, Derazhnoye and Grodno (*Figure 1*).

The second meteor was also captured by three cameras at the camera stations in Minsk, Derazhnoye and Zaslavl about 8 minutes after the first one October 24, at $20^h49^m56^s$ UTC (*Figure 2*).

The third meteor was captured about 1hour and 12minutes after the second one, October 24, at $22^h02^m15^s$ UTC by two cameras in Derazhnoye and Grodno (*Figure 3*).

The trajectories of meteors belonged to the October zeta Perseids and the camera positions on the ground map are shown in *Figure 4*.

Figure 1 – First meteor captured on October 24, 2021 at $20^h41^m37^s$ UTC. Recorded at Derazhnoye, Belarus.

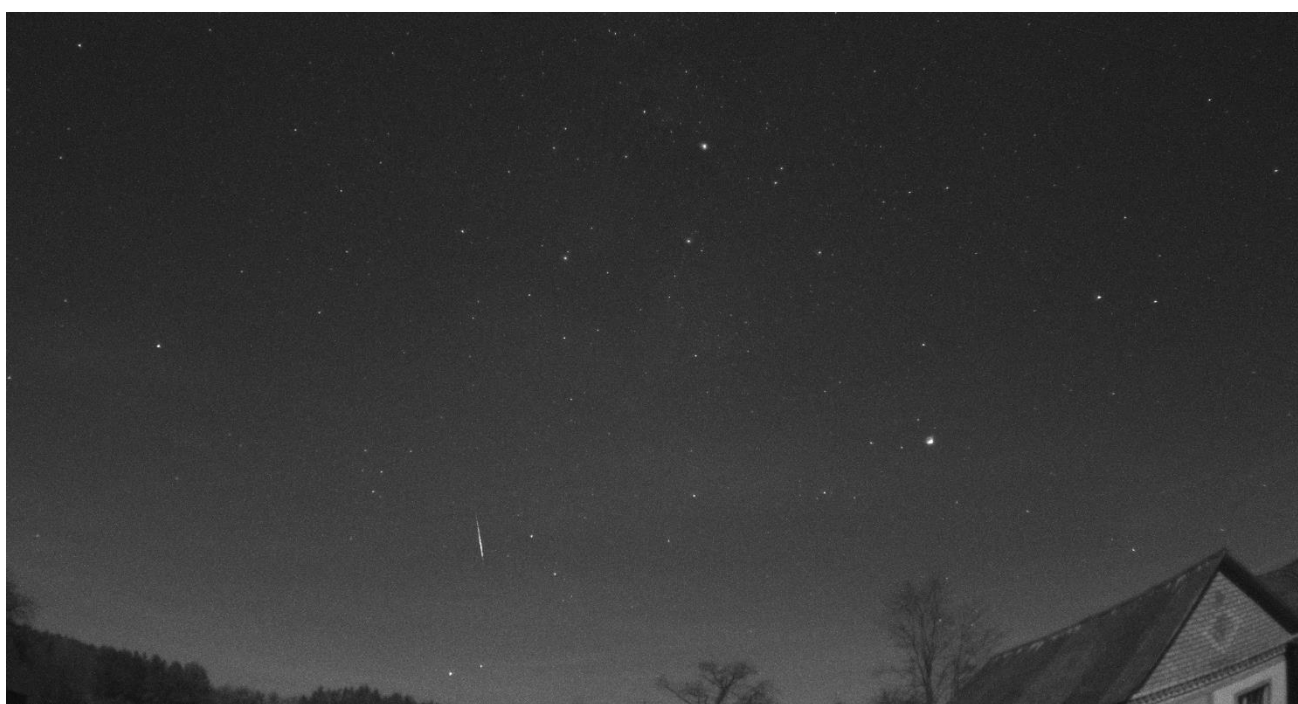*Figure 2* – Second meteor captured on October 24, 2021 at 20^{h}49^{m}56^s UTC. Recorded at Minsk, Belarus.

Figure 3 – Third meteor on October 24, 2021 at 22^{h}02^{m}15^s UTC. Recorded at Derazhnoye, Belarus.

3   Orbital elements

An analysis of the data shows that all 3 meteors coincide well within the October zeta Perseids radiant, the coordinates of which have been added into Meteor Data Center catalog (Vida et al., 2021; Roggemans et al., 2021).

The radiant coordinates for the multi-station meteors and their orbital elements were calculated with UFOOrbit. The quality of the orbits for meteors #1 and #2 is good, it corresponds to Q2 quality in UFOOrbit. The orbit of meteor #3 has Q1 quality. The data obtained are listed in *Table 1* below. The D-criterion according to Drummond (1981) indicates an excellent similarity with the reference orbit.
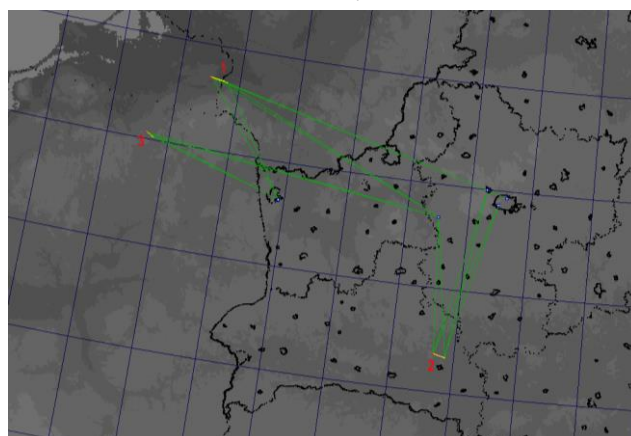

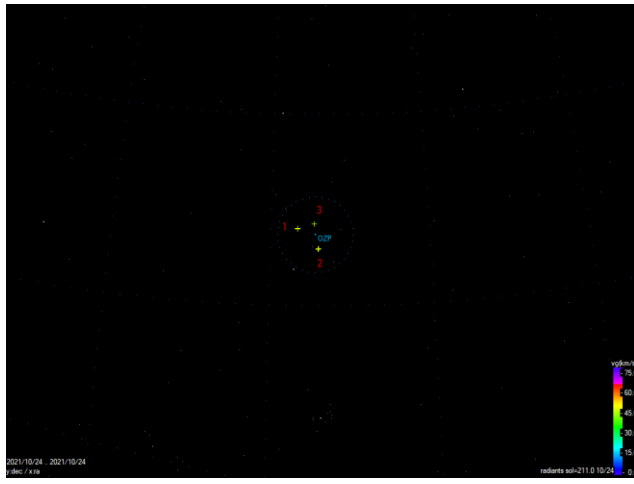*Figure 4* – Trajectories of the multi-station October zeta Perseids plotted on the ground map.

Figure 5 – Radiant positions of three multi-station October zeta Perseids plotted on a star map.

Table 1 – Three October zeta Perseids meteors recorded 2021 October 24 by the Belarusian meteor video network.

	#1 ($20^h41^m37^s$)	#2 ($20^h49^m56^s$)	#3 ($22^h02^m15^s$)
$\lambda_{\odot}$ (°)	211.3585	211.3642	211.4143
α_g (°)	58.315	57.021	57.269
δ_g (°)	+34.025	+32.963	+34.275
H_b (km)	107.3	106.2	98.2
H_e (km)	87.7	88.6	87.9
v_g (km/s)	47.7	47.5	45.5
m_A	–1.0	–1.8	–0.9
a (AU)	18.2	73.0	5.9
q (AU)	0.085	0.082	0.095
e	0.9954	0.9989	0.9839
ω (°)	326.489	326.655	325.417
Ω (°)	211.358	211.364	211.414
i (°)	64.5	59.0	57.2
D_D	0.019	0.039	0.090

4   Conclusion

As previously reported by Denis Vida, October zeta Perseid activity was observed on October 24, 2021 from 19^h10^m UTC to 22^h13^m UTC, with the main peak occurring between 20^h30^m–21^h0^m UTC. The first two meteors (20^h41^m UTC and 20^h49^m UTC), detected by the Belarusian meteor video network, occur exactly at the time near the maximum peak. The 3rd meteor (22^h02^m UTC) appears much later, near the end of the observed shower activity.

Thus, the timing of 3 detected meteors falls within the activity interval indicated by other observers. The radiant positions as well as the orbital elements are in perfect agreement with previously published data. This means that we were lucky enough to catch these amazing meteors, belonging to the recently discovered long-period October zeta Perseid meteor shower.

Acknowledgment

References

Drummond J. D. (1981). "A test of comet and meteor shower associations". *Icarus*, **45**, 545–553.

Roggemans P., Booz B., Sposetti S. and Richert J. (2021). "October zeta Perseids (OZP#1131) – Update". *eMetN*, **7**, 6–12.

Vida D., Šegon D., Roggemans P. (2021). "October zeta Perseid meteor shower (OZP#01131)". *eMetN*, **6**, 536–539.

Figure 6 – The orbits of the October zeta Perseids, top view on the ecliptic.

Aurigid outburst 2021 from Belarus and Ukraine

Yury Harachka

Minsk, Belarus
astronominsk@gmail.com

The predicted outburst of the Aurigid meteor shower (AUR # 00206) occurred during the night of August 31 – September 1, 2021. According to the data from the Belarusian and Ukrainian meteor video networks, the activity profile for this meteor shower during this night could be obtained and it turned out to be twin-peaked. The exact radiant coordinates (RA: 91.06 ± 0.13°, Dec: 39.12 ± 0.07°) and orbital elements of the Aurigids have been calculated for the peak activity of the meteor shower.

1 Introduction

Conditions were quite good in Belarus and Ukraine, despite a low radiant position of about 20° above the horizon (better than in Western Europe). The maximum occurred just after midnight local time. The weather was pretty good for this time of the year. Some cameras did not work due to cloud cover. However, where the sky was clear useful data could be obtained from 18 cameras in Belarus and Ukraine.

2 The activity profile

To determine the activity curve of the Aurigids, all individual meteors that radiated precisely from the radiant were collected for the night of August 31 – September 1, 2021 (*Figure 2*).
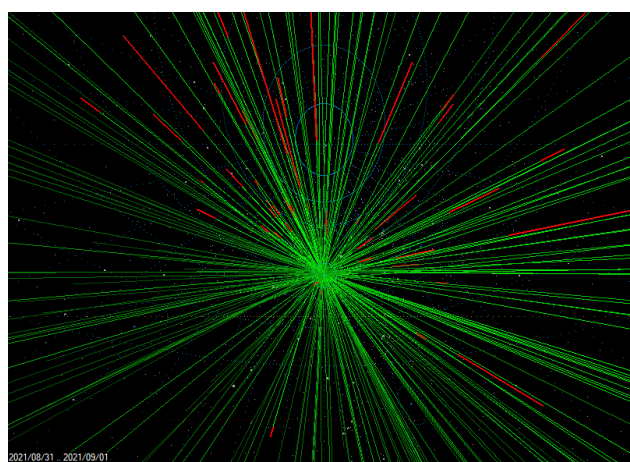

Figure 2 – Individual meteors radiating from the Aurigid radiant.

Figure 1 – Stacked image of registered Aurigids during the night of August 31 – September 1, 2021 from the camera located in Derazhnoye, Belarus.

Duplicates of paired meteors captured by two or more cameras were discarded from this selection. Thus, 79 unique meteors radiating from the Aurigids' radiant were collected. The times of meteor appearances were divided into 5- and 10-minute intervals and the numbers of Aurigids per time interval were then plotted on the timeline shown in *Figure 3*.
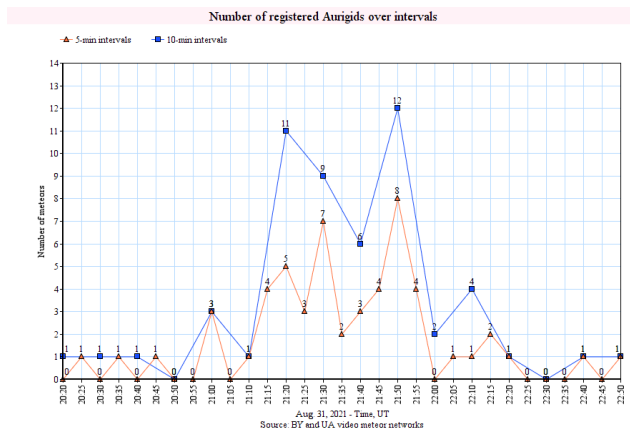

Figure 3 – Using 10-minute intervals results in a smoother profile, while the 5-minute intervals show more scatter with several spikes.

The graph shows that the increased activity lasted for 40 minutes between 21^h15^m–21^h55^m UT. The middle of this interval was at 21^h35^m UT. However, we can also see that the peak had at least two pronounced sub-maxima with a dip in the middle.
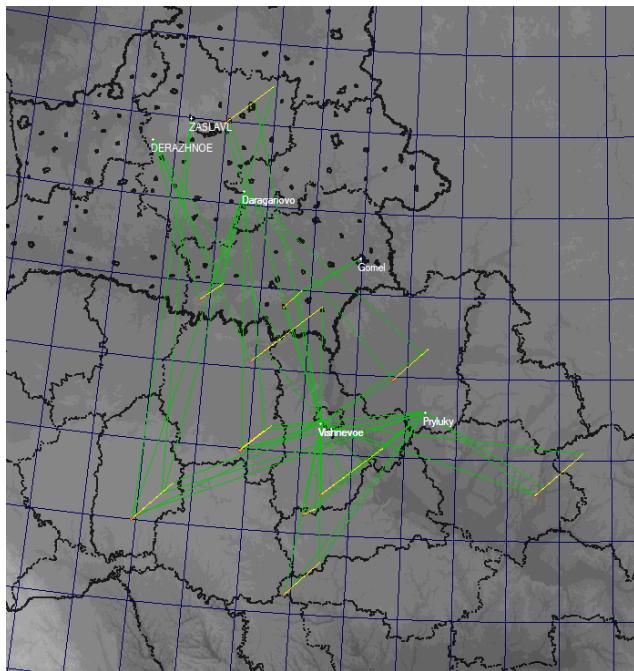
3 Radiant coordinates and orbital elements

Figure 4 – The trajectories of multi-station Aurigids of quality Q2 and Q3 plotted on a ground map.

Radiant coordinates and orbital elements were calculated with UFO-Orbit for multi-station meteors captured by two or more cameras. For greater accuracy, only the best 11 multi-station meteors of quality Q2 and Q3 were used (*Figure 4*). They all fell within the time interval from 21^h22^m UT to 23^h21^m UT.

Figure 5 shows the radiant positions for multi-station Aurigids on the star map. It should be noted that the area of the radiant was remarkably very small, it is smaller than the lunar disk.
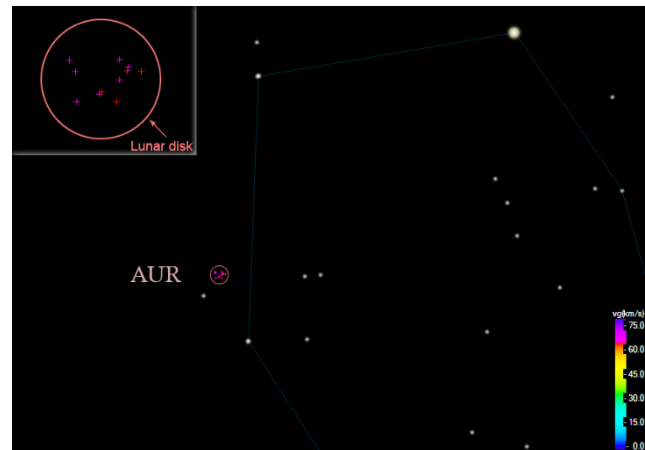

Figure 5 – Radiant positions of 11 multi-station Aurigids with quality Q2 and Q3 plotted on a star map. Note the small size of the radiant area, less than the lunar disk.

After calculations and averaging the data of 11 multi-station meteors, the following radiant coordinates and orbital elements (with standard deviations) were obtained for Solar Longitude 158.406° (*Figure 6*):

- RA: $91.06 \pm 0.13°$
- Dec: $39.12 \pm 0.07°$
- $v_g = 65.3 \pm 0.9$ km/s
- $q = 0.665 \pm 0.014$ AU
- $e = 0.948 \pm 0.052$
- $\omega = 107.4 \pm 2.9°$
- $\Omega = 158.41 \pm 0.02°$
- $i = 148.3 \pm 0.3°$

4 Conclusion

The outburst of the Aurigid meteor shower occurred as previously predicted centered at 21^h35^m UT. The peak turned out to be double with a dip in the middle.

Most Aurigids radiated from a compact radiant with a diameter smaller than the size of the lunar disk.

The results obtained, as well the moment of maximum as the shape of the profile with two maxima and a dip in between, agree well with the results of visual and radio observations obtained by other authors (Miskotte, 2021; Ogawa and Sugimoto, 2021).
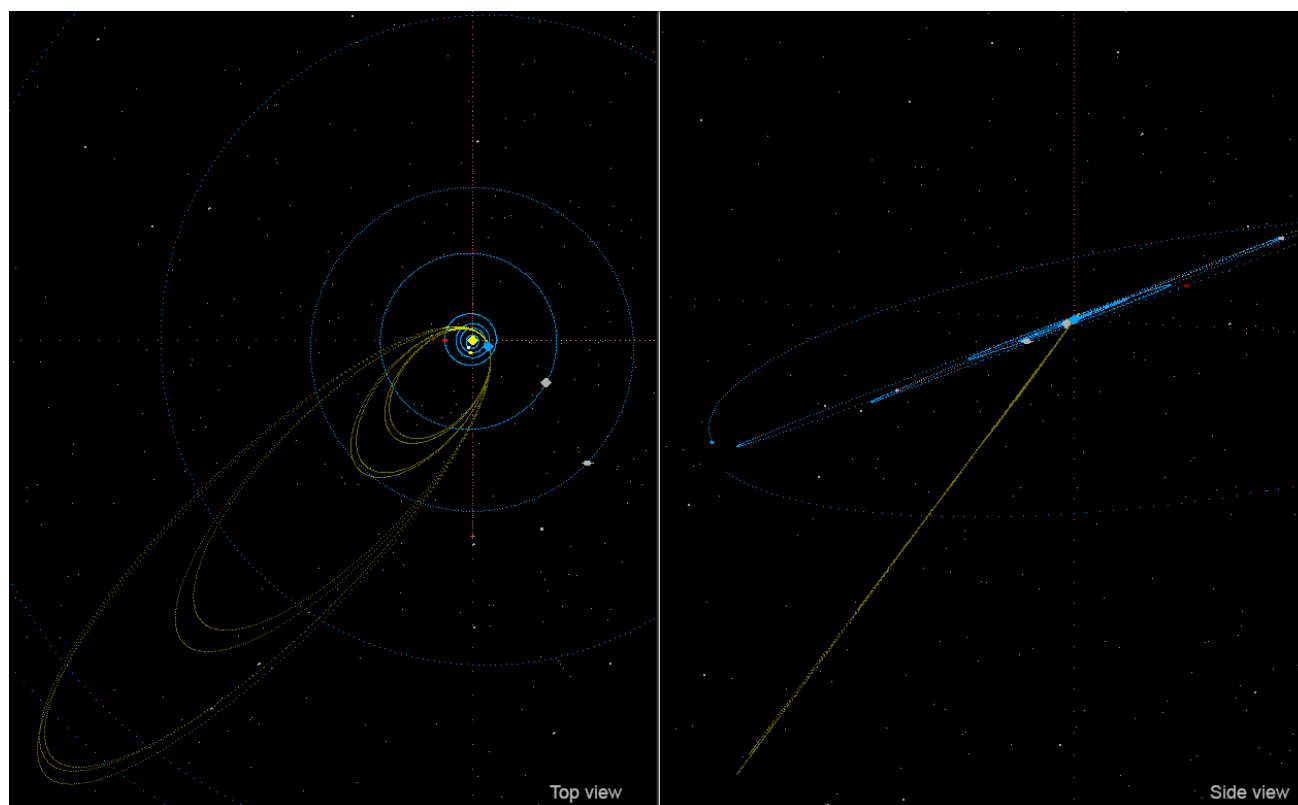
Figure 6 – The orbits of the Aurigids, left top view on the ecliptic, right side view.

Acknowledgments

References

Miskotte K. (2021). "A modest Aurigid outburst in 2021". *eMetN*, **6**, 526–530.

Ogawa H. and Sugimoto H. (2021). "Aurigids (AUR#00206) 2021 using worldwide radio meteor observations". *eMetN*, **6**, 574–577.

The kappa Cygnids (KCG#012) in 2021: analysis of the visual data

Koen Miskotte, Carl Johannink and Hans Betlem

Dutch Meteor Society, the Netherlands
k.miskotte@upcmail.nl, c.johannink@t-online.de

The kappa Cygnids (KCG#012) showed increased activity in 2021 as predicted. This article describes the results of the calculations on the visual observations of the kappa Cygnids. However, during this analysis a number of important and critical questions arose, which the authors have tried to answer by using data from CAMS networks.

1 Introduction

Every year around the Perseid maximum, slow meteors can be seen with sometimes a characteristic (end) flare or multiple flares (see *Figures 1 and 2*). These meteors seem to come from an area roughly between Vega and kappa Cygni, the kappa Cygnids. The meteor shower was first observed by Miklós Konkoly-Thege of the Ó-Gyalla Observatory in Hungary in 1874 (Kronk, 1987). The famous meteor observer William F. Denning gave the name to this meteor shower in September 1893 (Denning, 1893). He noticed that the shower displayed higher activity in some years than in others. In 1954 it was proven that the kappa Cygnids were a real meteor shower: Fred Whipple published orbital elements of 5 kappa Cygnids photographed multi-station (Jenniskens, 2006). The meteors had an orbital period between 7 and 8 years.

2 Recent history

In 1985 Koen Miskotte, together with Robert Haas, Arjen Grinwis and Bauke Rispens (members of team Delphinus from Harderwijk) were able to observe the kappa Cygnids under good conditions from Puimichel, Southern France (Miskotte, 1985). Relatively large numbers of kappa Cygnids were seen there, the hourly counts increased to 8 on the night of August 18–19. Quite a few bright kappa Cygnids were also seen, but only one fireball. In 1986 observations were done again from Puimichel (Miskotte, 1986), but lower numbers of kappa Cygnids were seen, up to 5 in one hour during the night August 14–15. In 1986, most of the time there were more faint kappa Cygnids compared to 1985. In 1993 a major DMS multi-station campaign was organized in the Provence in Southern France to observe the expected Perseid outburst of August 12 (Langbroek, 1993). During these observations, the activity of the kappa Cygnids was also remarkable, for example some kappa Cygnid fireballs of –8 and twice a –6 were observed and photographed, see *Figure 2*. A maximum ZHR of 3 was found from visual data (Jenniskens, 2006, figure 24.8, p. 444). Based on these (photographic) observations, among other things, Peter Jenniskens concluded that the possible parent body of the kappa Cygnids could be the asteroid 2008 ED69 (Jenniskens et al., 2008).

Figure 1 – A beautiful picture from Oostkapelle, Klaas Jobse captured this nice kappa Cygnid in Pegasus on August 16, 2021. The photographic magnitude of the final flare was magnitude –14.

Figure 2 – This beautiful kappa Cygnid was captured during the Perseid outburst of August 12, 1993 from Rognes in southern France. Photo: Team Delphinus, Rognes, South of France.
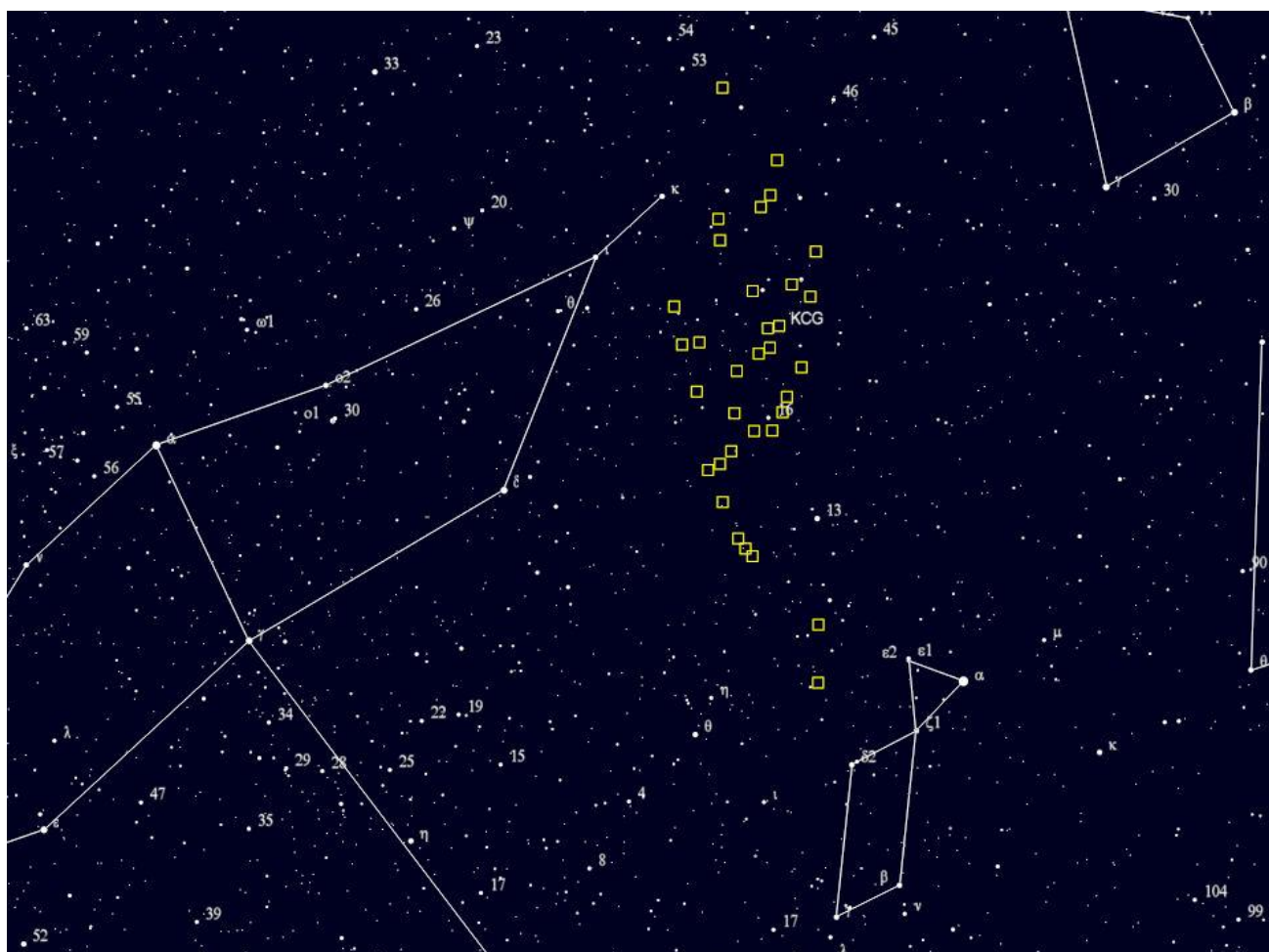

Figure 3 – The radiants (yellow squares) found of paired kappa Cygnids recorded by the CAMS-BeNeLux network on the night of 2021 August 10–11.

In 1999, during the Perseid maximum, a number of kappa Cygnid fireballs were observed and in 2007 again enhanced kappa Cygnid activity has been observed. The activity was very good with a number of fireballs. For example, two kappa Cygnids (–4 and –6) were photographically captured by the authors during a Perseid campaign near the German

town of Grevesmühlen (Johannink, 2007; Jenniskens et al., 2007). Also in 2014, more kappa Cygnids were seen than normal (Rendtel et al., 2015). During the years with normal kappa Cygnid activity, the ZHR is around 1. In years with increased activity, the ZHR varries between 3 and 6.

3   The kappa Cygnids in 2021

As a result of the observations from 1985, 1993 and 2007, it was already expected that the kappa Cygnids would be again more active in 2021. This was confirmed on August 9, 2021 in CBET 5014 by Peter Jenniskens (Jenniskens, 2021a). In a publication on MeteorNews (Jenniskens, 2021b), Peter Jenniskens states that CAMS observations showed that the kappa Cygnids had been active since the end of June. During that time, the radiant moved from the Antihelion position to Lyra around August 8. In addition, the radiant is stretched out up to 15 degrees in declination during each night. See also *Figure 3*.

After the successfully completed chi Cygnid (minor shower) analysis in 2020 (Miskotte, 2020; Miskotte, 2021) the first author decided to make an analysis of the kappa Cygnids in 2021 based on visual observations. However, a number of critical questions arose during the analysis that will be discussed in more detail later.

4   Population index *r*

We could download the visual data from the website of the International Meteor Organization for our analysis. In order to be able to make a ZHR calculation, the population index *r* had to be calculated. To be useful, the observations had to meet the following criteria:

- The minimum limiting magnitude had to be 5.9.
- The difference between the limiting magnitude and the average magnitude of the observed meteors should not exceed 4 magnitudes.
- The population index *r* is determined per night or per range of nights.

Table 1 – Population index *r* on magnitude range [–1;5] for the kappa Cygnids in August 2021. The time mentioned, T_m is the average time of all observation periods used in the calculations of the population index *r*.

Day	T_m (h)	$\lambda_\odot$ (°)	KCG	r[–1:5]
6	23.83	134.425	18	1.9 ± 0.62
8	1.07	135.433	11	2.05 ± 0.84
8	23.60	136.333	24	1.8 ± 0.52
9	23.80	137.301	58	2.72 ± 0.3
10	23.33	138.241	62	3.15 ± 0.29
11	23.60	139.212	137	2.25 ± 0.18
13	1.90	140.264	129	2.76 ± 0.18
14	2.20	141.236	79	2.53 ± 0.25
15	3.30	142.241	30	2.64 ± 0.45
16	3.30	143.202	45	1.76 ± 0.35
24	0.00	150.767	30	2.27 ± 0.45

The period 1 to 6 August had too few kappa Cygnids to determine a reliable population index *r*. The population index *r* could be calculated per night for the period from 6 to 17 August, but again there was too little data for the following period (moonlight!). The result of the calculations on the magnitude range from –1 to +5 shows a very variable population index *r* per night. The results are shown in *Table 1* and *Figure 4*. The *r*-value for August 24 is the result of an *r*-value calculation based on all data from the entire period from August 17 to 31 inclusive. A total of 623 kappa Cygnids were used for the population index *r*.
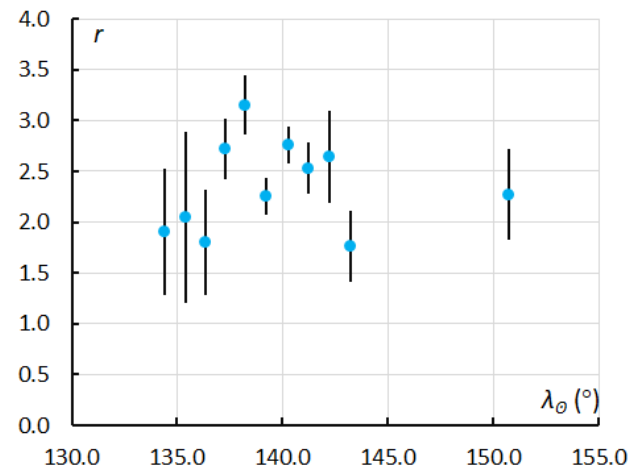

Figure 4 – Population index *r* of the kappa Cygnids in 2021 based on *Table 1*. Some observers reported seeing no kappa Cygnid fireballs in 2021, while others did. The BeNeLux all sky network captured 5 maybe even 7 kappa Cygnids simultaneously with a photographic magnitude of –6 to –14 (Betlem, 2021).

5   Zenital Hourly Rate – ZHR

The following formula was used to determine the ZHR:

$$ ZHR = \frac{n \cdot r^{6.5-lm}}{(\sin h)^\gamma \cdot C_p \cdot T_{eff}} $$

In addition, the radiant height correction was put as $\gamma = 1.0$. To be able to make a good ZHR determination you need to know something about the individual observer. The determination of the perception coefficient C_p was used for this purpose. This is a value that indicates how "perceptive" the observer is. The observed sporadic hourly rate from the end of July and August (observed between 22^h–02^h UT) is compared with that of an assumed sporadic hourly frequency of 10 with a limiting magnitude of 6.5 (a "standard observer"). Naturally, the observed limiting magnitude is corrected to 6.5.

The observations used to determine the ZHR also had to meet certain standards. These are:

- Data with radiant heights below 25 degrees were not used.
- Observations made with a limiting magnitude lower than 5.9 were not used.
- Only intervals of one hour or longer periods of up to 2.5 hours were used. Very short single observation

periods were not used. Short successive periods were merged into longer periods.

- When merging the individual ZHRs, a weighted average was calculated. An observation of 2 hours is obviously more important in the average than an observation of 1 hour.
- The ZHR was determined per night.
- Zero detection observations were also included in the calculations.
- Only data from observers for whom a good C_p has been determined were used. A good C_p could be calculated for a number of relatively new observers.

Table 2 – ZHR of the kappa Cygnids in 2021, based on 820 kappa Cygnids. D = Day, T_m = mean time in hours, P = periods, KCG = number of κ Cygnids, r[–2,+5], O = observers.

| D	T_m	$\lambda_\odot$ (°)	P	KCG	ZHR	r	O
3	4.54	130.781	8	16	1.5 ± 0.4	2.00	5
3	21.92	131.475	1	3	1.3 ± 0.8	2.00	1
4	22.73	132.465	3	15	2.5 ± 0.7	2.00	2
6	5.3	133.685	10	10	1.3 ± 0.4	2.00	4
7	0.11	134.436	8	19	2.3 ± 0.5	2.00	4
8	2.03	135.472	5	13	2.5 ± 0.7	2.05	4
8	23.8	136.341	12	45	3.2 ± 0.5	1.80	6
9	23.12	137.273	16	59	3.2 ± 0.4	2.72	9
10	22.99	138.227	28	106	3.4 ± 0.3	3.15	12
11	23.01	139.188	40	168	3.7 ± 0.3	2.25	16
12	23.37	140.161	44	150	3.3 ± 0.3	2.76	17
14	0.03	141.151	25	100	3.5 ± 0.3	2.53	12
14	22.76	142.059	13	51	4.4 ± 0.6	2.64	6
16	2.83	143.183	7	48	6.0 ± 0.9	1.76	3
17	23.17	144.959	3	4	1.8 ± 0.9	2.27	1
24	20.28	151.582	1	2	2.2 ± 1.5	2.27	1
25	20.33	152.548	1	2	2.6 ± 1.8	2.27	1
30	20.79	157.395	2	4	1.7 ± 0.9	2.27	1
31	21.67	158.398	2	5	1.6 ± 0.7	2.27	1
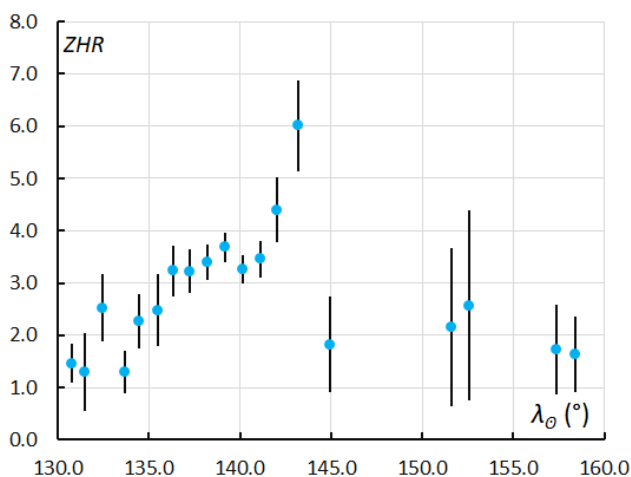
Figure 5 – ZHR Profile of the Kappa Cygnids in 2021 based on Table 2. The "gap" between 145°–151° in $\lambda_\odot$ is caused by the Full Moon.

More than 1600 kappa Cygnids were reported on the IMO website. A large amount of data came from observations from one location by a large group of Czech observers with a lot of overlap among their observations. Therefore, not all data from that group has been used because the final result would be greatly influenced by this large group. A good C_p could be calculated for a number of these observers, so only the data from these specific observers were used. We hope that this group will remain active longer and observe more often so that the C_p coefficients for more people can be determined. Ultimately, 820 kappa Cygnids were used for this analysis. For the period from August 3 to 6, an assumed population index r of 2.00 was used, because it is in line with the population index r on August 6 and 8. The result of all calculations can be seen in *Table 2* and *Figure 5*.

The maximum ZHR was reached on the night of 2021 August 15–16. Several observers got individual ZHRs above 6 and reported relatively many bright kappa Cygnids. This can also be seen in the population index r of that night (*Table 1*). Now this graph alone does not say much about the enhanced activity of the kappa Cygnids. For that we have to compare the activity profile with other years. In this case, 2017 and 2020 were chosen. According to the observations, in 2017 there was certainly no increased kappa Cygnid activity. In 2020 this could also have been the case partly because it was close to the 7-year period of the kappa Cygnids. For this, the observations from 2021 were recalculated again, but now with a fixed population index r. This way, the influence of the population index on the ZHR calculations was the same for all three years. We used a population index $r = 2.2$, the average r-value. The ZHRs from 2017 and 2020 were then also calculated using the same r-value. Furthermore, exactly the same standards also applied to the data used as mentioned above. The result is *Figure 6*.
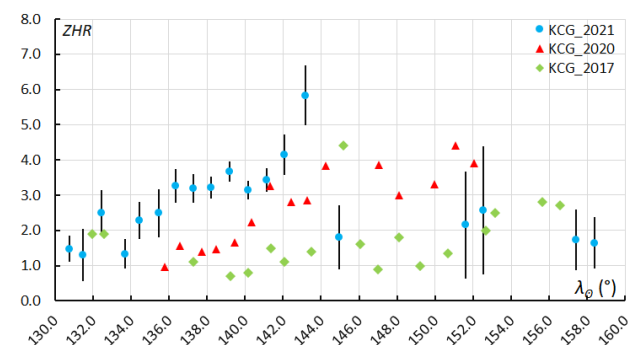

Figure 6 – Combined ZHR profiles based on visual observations of the kappa Cygnids from 2017, 2020 and 2021.

Here we clearly see that the 2021 ZHR profile is the highest with a maximum ZHR of 6 around $\lambda_\odot = 143°$ (August 15–16). The ZHR profile for 2020 remains below that of 2021, while 2017 shows the lowest activity. Based on the 2020 ZHR profile, the kappa Cygnids displayed also some increased activity during that year. Therefore, *Figure 6* seems to give the result of a successful kappa Cygnid analysis with already increased activity in 2020. However, there are also some very critical comments to be made on basis of this analysis, about the observations. We can make

use of the CAMS video network data from 2021 to explain this.

6   Discussion

1 Position and size of the radiant of the kappa Cygnids

In this analysis, the radiant positions from the IMO Meteor Shower Calendar 2021 were used. Problem is that both in right ascension and especially in declination the radiant position of the kappa Cygnids from IMO is very different from the radiant positions according to the CAMS-BeNeLux results. Sometimes the IMO position is more than 15 degrees off. See, for example, *Figures 3 and 7*. The low activity in combination with the radiant, especially in declination, means significant differences in ZHR if you take a higher or lower declination in the calculations. The accompanying text in the Meteor Shower Calendar does mention that a study by Koseki indicates that there is a large radiant complex in Cygnus, Lyra and Draco (Koseki, 2014). It appears to be best to calculate the mean radiant position from CAMS observations. The result is that the ZHRs will be a bit higher, because the IMO radiant position is always higher in the sky than the radiant positions obtained by CAMS-BeNeLux up to the maximum of the kappa Cygnids.
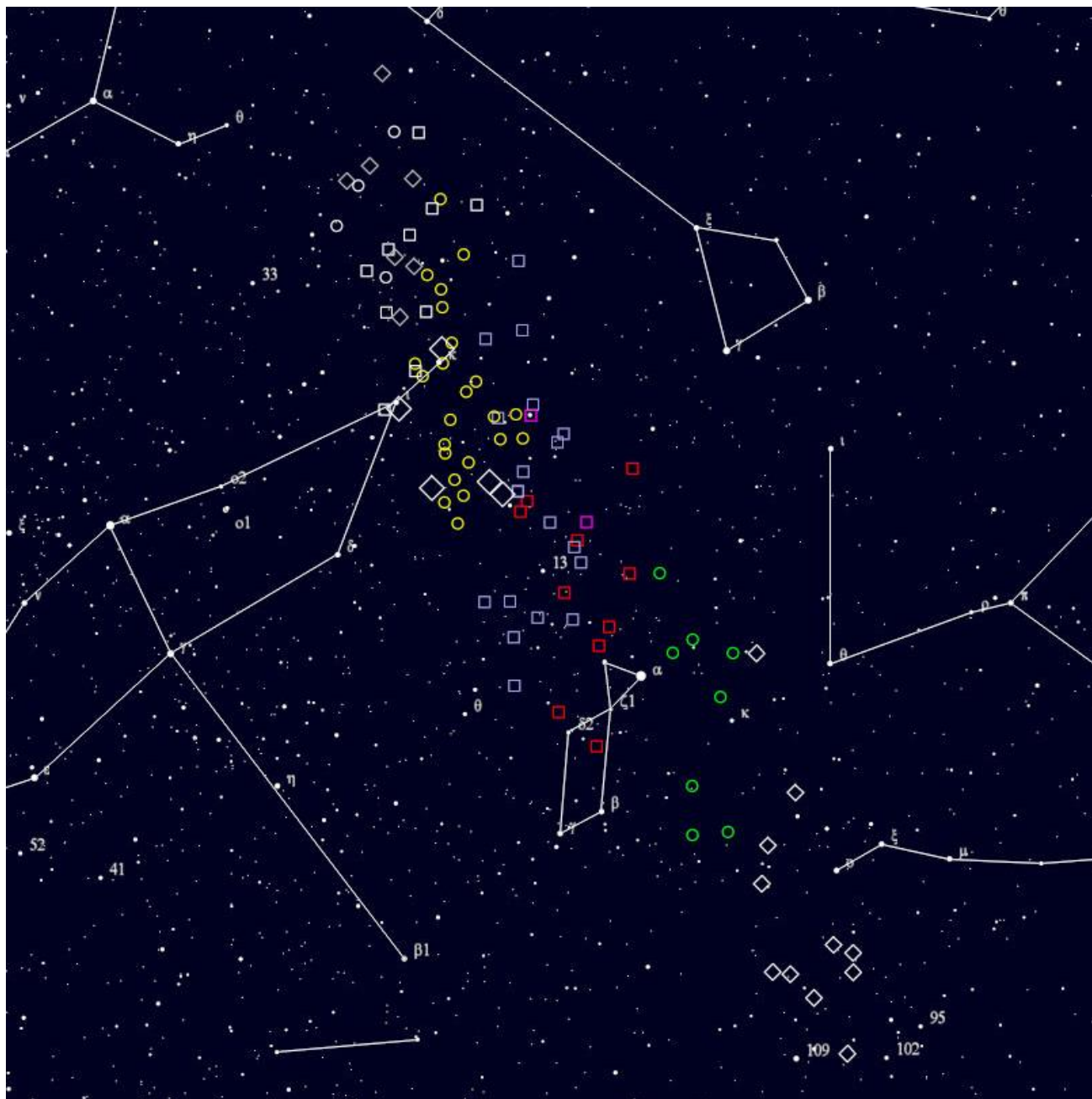
Figure 7 – Radiant drift of the kappa Cygnids between July 19 and August 31, 2021 based on CAMS-BeNeLux data. Legend: White diamonds: period 2021 July 19–25, green circles: 2021 July 25–31, red squares: 2021 August 1–5, lilac squares: 2021 August 5–10, yellow circles: night 2021 August 14–15, white squares: 2021 August 20–21, gray diamonds: 2021 August 24–25 and white circles: 2021 August 28–31. The 5 large white diamonds indicate the radiant positions of the kappa Cygnids captured by the BeNeLux all sky network (Betlem, 2021). See also *Figure 8* for more details. Note: these are not all available radiant positions. A maximum of 100 objects could be entered. When choosing the radiants used, the extreme limits of the radiant positions were mainly taken into account.

2 Visual observer's knowledge of the kappa Cygnid radiant

The above-mentioned point has also a major influence on the observations in the field. Do the observers know the real radiant position? Do the observers know that the radiant is so dispersed in declination? Do they take that into account in the field when classifying? Or do they only use the strict radiant positions in the IMO's Meteor Shower Calendar for that? If an observer focuses solely on the radiant position in the IMO calendar, and is not aware of the size of the radiant of the kappa Cygnids, especially in the declination, some (most!) kappa Cygnids may be incorrectly classified as sporadics. Especially in the second part of the night, when the radiant is lower at the sky, a kappa Cygnid can quickly be misidentified as sporadic if an observer does not know better. This could explain the more than usual decline in observed numbers of kappa Cygnids during an observation night by several observers, as revealed by the visual analyses. See also point 4: Visual observers see 'too few' kappa Cygnids. It is therefore important to adjust the radiant position of the kappa Cygnids in the Meteor Shower Calendar. *Figure 7* shows the radiant positions of the KCG between July 19 and August 31, based on CAMS-BeNeLux data from 2021.
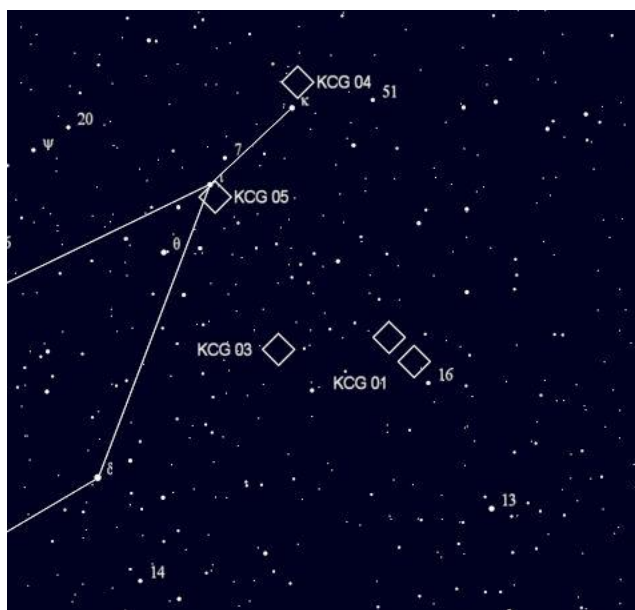
Figure 8 – Overview of the radiant positions of the kappa Cygnids in 2021, found by the BeNeLux all sky network. See also (Betlem, 2021). KCG 01: 2021, August 10, 22^{h}02^{m}36^s UT, KCG 02: 2021, August 11, 22^{h}21^{m}06^s UT, KCG 03: 2021, August 14, 01^{h}40^{m}43^s UT, KCG 04: 2021, August 14, 23^{h}51^{m}47^s UT, KCG 05: 2021, August 17, 01^{h}08^{m}11^s UT.

3. Increased KCG activity in 2020?

Earlier in this article we already showed that visual observers also observed increased kappa Cygnid activity in 2020 compared to 2017, see *Figure 6*. So, it is interesting to take a look at CAMS observations in 2017, 2020 and 2021. Visual and CAMS observations can't be compared one to one. After all, the visual observer only sees part of the activity. The weaker the meteor, the more likely it will be missed. For CAMS we can assume that the largest part will

be recorded. For this study, the percentage of kappa Cygnids was determined relative to sporadic activity. The observed sporadic activity was set to 100% for each night, and then the number of kappa Cygnids each night was reported as a percentage of the sporadic activity for that night. In this way and by using the worldwide CAMS data, an attempt was made to rule out the regional weather and growth of the network. The result is presented in *Table 3* and *Figure 12*.

A different picture emerges from this approach. According to CAMS data, the kappa Cygnids were slightly more active in 2020 than in 2017, but it is very marginal if you compare it with the difference between 2017 and 2021. Because in 2021 it is very clear that the activity had increased considerably. But why are visual observers clearly seeing more kappa Cygnids in 2020 than in 2017? In order to find answers to this question, the following research was carried out. In *Table 3*, the last column activity is the average activity from the Total column multiplied by 1.5. Subsequently, the nights where the average activity was greater than the number in the last column was examined. The higher values are red colored cells. The following conclusions can be drawn from this.

- According to CAMS observations there is not a real maximum during the annual kappa Cygnid activity, such as in 2017.
- The KCG activity in 2020 is only a fraction higher than 2017.
- In 2021, during the increased activity, most activity took place between 11 and 18 August.

Another reason for possible enhanced kappa Cygnid activity in 2020, may be found in another meteor shower, the August Draconids (197#AUD). This meteor shower may also belong to the kappa Cygnid complex (Jenniskens, 2016). These meteors have almost the same speed as the kappa Cygnids and the August Draconids radiant, also extended in declination, lies northeasterly next to the area of the kappa Cygnids radiant. *Figures 8 and 9* display the radiant positions of the kappa Cygnids and August Draconids. Therefore, the activity percentage for the August Draconids was also determined relative to the sporadic activity. (*Table 3*). This calculation shows that the annual activity of the August Draconids is higher than the annual activity of the kappa Cygnids, except when the kappa Cygnids reached their 7-year maximum (see also *Table 3*).

In addition, for most observers the kappa Cygnid and August Draconid radiants are ignored because of the dominant Perseids. It seems quite possible that members of the August Draconid meteor shower are mistaken for kappa Cygnids due to the alignment of the radiants and the same characteristic speed. Of course, this also applies to the other years, so in 2021 there may also be some contamination from the August Draconid meteor shower. This problem for visual observers is well illustrated in *Figures 9, 10 and 11*.

Table 3 – The observed sporadic activity was set to 100% for each night, and then the number of kappa Cygnids each night was reported as a percentage of the sporadic activity for that night. The red cells mark the values that were 1.5× larger than the average value for that year.

| Shower	1	2	3	4	5	6	7	8	9	10	11	12	13	14	15	16	17	18	19	20	21	22	23	24	25	26	27	28	29	30	31	Total	Activity
000#SPO																																	
2017	136	94	88	229	128	364	342	224	146	216	98	267	563	469	424	446	439	312	468	293	210	269	348	151	476	599	404	594	540	227	373	9937	
2018	411	330	446	537	525	644	683	166	335	235	359	509	401	351	207	388	386	792	542	434	484	490	414	189	366	627	410	322	586	356	532	13457	
2019	1015	2172	1450	1070	1401	1172	1075	1780	1214	1520	1605	2399	2246	1960	1114	2161	1588	1780	1543	1777	1843	1889	1337	1730	1818	2230	2135	1812	1948	1461	2088	52333	
2020	1460	1669	1061	1014	1420	1502	1620	1659	1406	1747	1618	1485	1772	1479	1906	1364	1586	1671	1558	1888	1221	1234	1146	1179	1437	1543	1357	1341	1457	1022	682	44504	
2021	1380	1485	1426	1538	1276	1491	1645	1209	1546	1492	1846	1543	1795	1948	2056	1122	1630	1157	1303	1212	1552	1254	1149	1624	1636	1229	1675	1360	1197	954	1455	45185	
197#AUD																																Mean/total	x1,5
2017 (n)	0	0	0	1	1	5	5	2	5	4	1	3	18	7	9	12	12	11	13	12	3	9	9	4	11	13	12	13	4	2	1	202	
2017 (%)	0.00	0.00	0.00	0.44	0.78	1.37	1.46	0.89	3.42	1.85	1.02	1.12	3.20	1.49	2.12	2.69	2.73	3.53	2.78	4.10	1.43	3.35	2.59	2.65	2.31	2.17	2.97	2.19	0.74	0.88	0.27	2.03	3.05
2018 (n)	0	0	2	2	2	5	0	1	2	4	4	9	7	8	3	10	17	19	6	8	13	17	8	4	2	12	7	2	6	8	1	189	
2018 (%)	0.00	0.00	0.45	0.37	0.38	0.78	0.00	0.60	0.60	1.70	1.11	1.77	1.75	2.28	1.45	2.58	4.40	2.40	1.11	1.84	2.69	3.47	1.93	2.12	0.55	1.91	1.71	0.62	1.02	2.25	0.19	1.40	2.11
2019 (n)	0	1	2	1	2	3	4	6	10	15	18	11	23	20	12	23	15	18	29	34	19	25	26	33	27	31	23	19	13	17	19	499	
2019 (%)	0.00	0.05	0.14	0.09	0.14	0.26	0.37	0.34	0.82	0.99	1.12	0.46	1.02	1.02	1.08	1.06	0.94	1.01	1.88	1.91	1.03	1.32	1.94	1.91	1.49	1.39	1.08	1.05	0.67	1.16	0.91	0.95	1.43
2020 (n)	2	5	2	4	6	11	8	14	18	21	27	25	24	28	42	18	24	50	53	27	30	36	24	13	26	19	20	17	14	10	0	618	
2020 (%)	0.14	0.30	0.19	0.39	0.42	0.73	0.49	0.84	1.28	1.20	1.67	1.68	1.35	1.89	2.20	1.32	1.51	2.99	3.40	1.43	2.46	2.92	2.09	1.10	1.81	1.23	1.47	1.27	0.96	0.98	0.00	1.39	2.08
2021 (n)	1	5	5	12	5	10	10	11	19	7	36	26	41	38	46	27	44	37	34	29	32	25	26	45	57	42	43	41	20	7	18	799	
2021 (%)	0.07	0.34	0.35	0.78	0.39	0.67	0.61	0.91	1.23	0.47	1.95	1.69	2.28	1.95	2.24	2.41	2.7	3.2	2.61	2.39	2.06	1.99	2.26	2.77	3.48	3.42	2.57	3.01	1.67	0.73	1.24	1.77	2.65
012#KCG																																Mean	x1,5
2017 (n)	0	1	0	1	0	2	0	1	1	0	0	0	1	4	6	5	1	1	1	0	2	0	4	1	1	0	2	1	4	0	1	41	
2017 (%)	0.00	0.07	0.00	0.07	0.00	0.13	0.00	0.08	0.06	0.00	0.00	0.00	0.06	0.21	0.29	0.45	0.06	0.09	0.08	0.00	0.13	0.00	0.35	0.06	0.06	0.00	0.12	0.07	0.33	0.00	0.07	0.41	0.62
2018 (n)	0	0	2	1	0	0	0	0	1	2	2	2	2	0	0	1	0	3	1	1	1	1	2	0	2	5	0	0	1	0	0	30	
2018 (%)	0.00	0.00	0.14	0.07	0.00	0.00	0.00	0.00	0.06	0.13	0.11	0.13	0.11	0.00	0.00	0.09	0.00	0.26	0.08	0.08	0.06	0.08	0.17	0.00	0.12	0.41	0.00	0.00	0.08	0.00	0.00	0.22	0.33
2019 (n)	3	3	1	2	1	0	3	1	2	2	2	3	5	1	2	4	2	2	10	4	1	2	3	2	2	3	4	1	0	1	2	74	
2019 (%)	0.22	0.20	0.07	0.13	0.08	0.00	0.18	0.08	0.13	0.13	0.11	0.19	0.28	0.05	0.10	0.36	0.12	0.17	0.77	0.33	0.06	0.16	0.26	0.12	0.12	0.24	0.24	0.07	0.00	0.10	0.14	0.14	0.21
2020 (n)	6	3	3	8	8	9	11	11	6	5	7	6	7	4	6	7	4	6	7	3	2	4	3	1	4	1	2	0	2	2	0	148	
2020 (%)	0.43	0.20	0.21	0.52	0.63	0.60	0.67	0.91	0.39	0.34	0.38	0.39	0.39	0.21	0.29	0.62	0.25	0.52	0.54	0.25	0.13	0.32	0.26	0.06	0.24	0.08	0.12	0.00	0.17	0.21	0.00	0.33	0.50
2021 (n)	41	46	70	78	68	105	105	98	140	91	187	215	216	205	214	152	186	126	91	104	107	45	53	88	77	69	75	53	34	12	18	3169	
2021 (%)	2.97	3.10	4.91	5.07	5.33	7.04	6.38	8.11	9.06	6.10	10.13	13.93	12.03	10.52	10.41	13.55	11.41	10.89	6.98	8.58	6.89	3.59	4.61	5.42	4.71	5.61	4.48	3.90	2.84	1.26	1.24	7.01	10.52
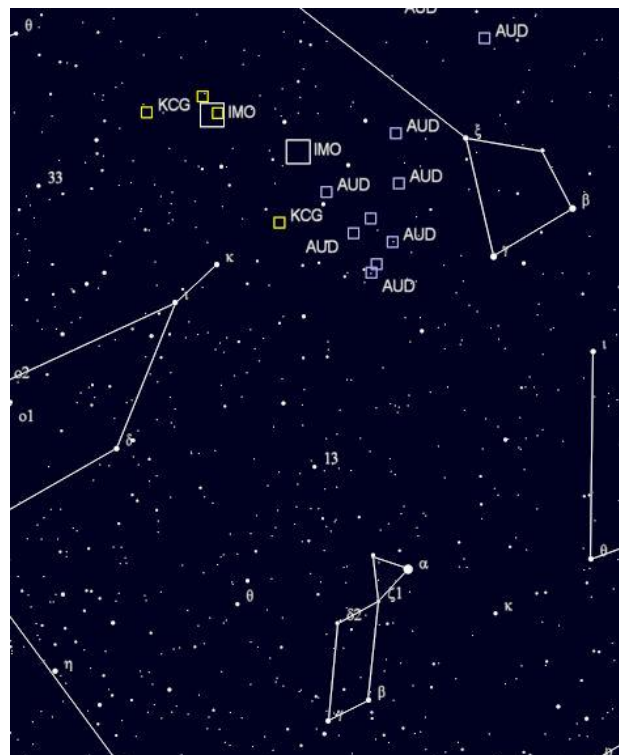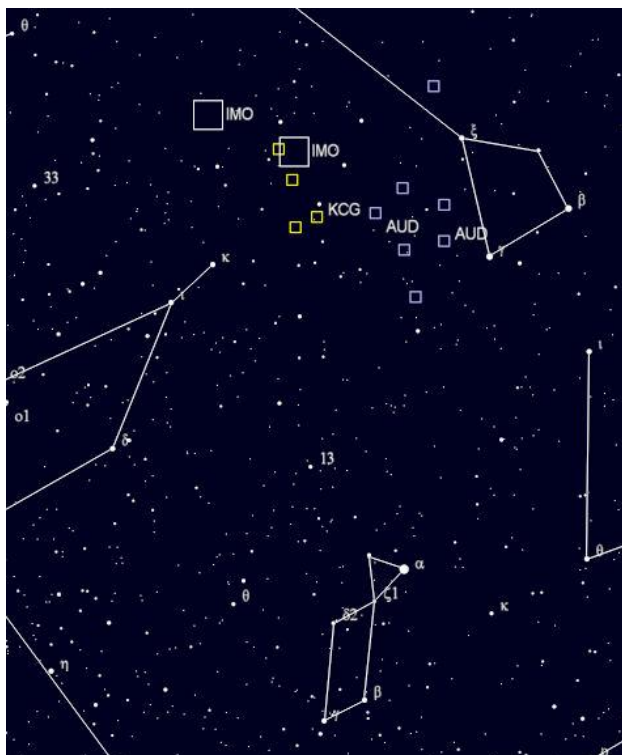
Figure 9 (left) and *Figure 10* (right) – Radiant positions of the kappa Cygnids (yellow squares) and Augustus Draconids (pink squares) on 2020 August 10 (*Figure 9*) and 18–19 (*Figure 10*). The white large squares represent the IMO kappa Cygnids radiant positions on August 1 (lower) and August 30 (upper).
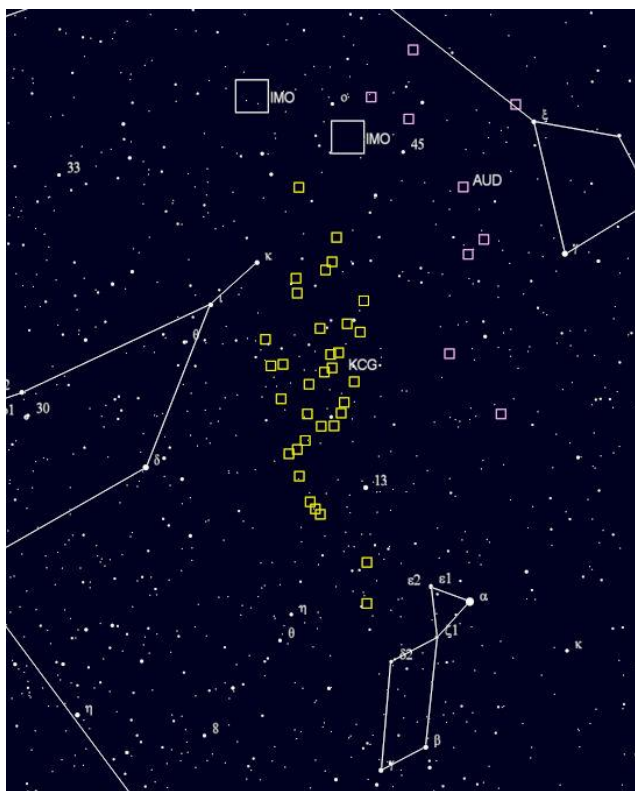

Figure 11 – During the night of 2021, August 10–11, 34 kappa Cygnids and 9 August Draconids were captured by CAMS-BeNeLux. Here are the radiant positions of these meteors shown. Yellow squares are the kappa Cygnids, the lila squares are the August Draconids. It is clear that both meteor showers have an elongated radiant especially in declination. The IMO radiant positions (large white squares) deviate significantly and can lead to problems in the visual classification of kappa Cygnids.

The apparently increased activity in 2020 found from the visual observations is probably caused by a combination of a certain contamination by the August Draconid activity and observations made while using the incorrect radiant positions provided in the IMO's Meteor Shower Calendar, the latter affecting mainly the period outside the maximum. Around the maximum, the radiant positions according to IMO, seem to agree better with the CAMS observations, so more correct kappa Cygnid classifications may be available around that time. That could also be a reason why visual observers found a maximum around solar longitude 145° (18 August). At that time the radiant position of the IMO corresponds nicely with the CAMS-Benelux data (see *Figure 10*).
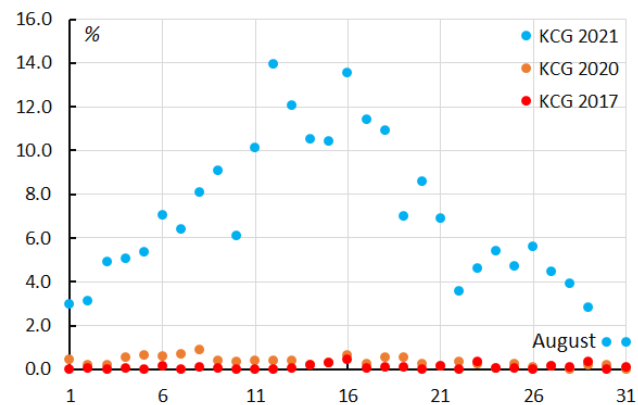
Figure 12 – Percentages of the kappa Cygnids from 2017, 2020 and 2021 plotted for 1–31 August. This graph is based on *Table 3* with all data from CAMS worldwide. SPO = 100%, determined each night. In this graph it is clearly visible that in 2020 there was no increased kappa Cygnid activity.

4. Visual observers see 'too few' kappa Cygnids

While entering the kappa Cygnid observational data we noticed that almost all observers report relatively too few kappa Cygnids in the second half of the night. For example, between 2021 August 10–15, most observers regularly record kappa Cygnids during the first hours, but very few in the second part of the night. That is of course an anomaly. We suspect that this is due to the kappa Cygnid radiant moving lower in the west/northwest over the night (i.e., increasingly out of view for most observers). At the same time the Perseids appear in increasing numbers. Because of these two effects, observers start to pay most attention to the Perseids. In other words, the Perseid activity predominates and draws all attention away from the kappa Cygnids during the night. This effect appears to be even stronger for observers at lower latitudes. The list of simultaneous kappa Cygnids collected by the CAMS-BeNeLux network shows that the radiant height affects the numbers of kappa Cygnids during the night as expected, but the decrease is not as strong as with the visual observers. It therefore appears that the cause may lie in the two effects described above.

5. During which period are the kappa Cygnids active?

CAMS observations worldwide show that the kappa Cygnids are active since June 20: in 2020 the first one was detected on June 20, in 2021 it was June 22. We must of course take into account that this concerns 1 or 2 kappa Cygnids per date through the very large worldwide network of CAMS. The chances for a visual observer seeing a kappa Cygnid during this period are negligible. With the radiant still in or near the Antihelion radiant, these kappa Cygnids will be recorded as Antihelion. The radiant positions appear to move in the same direction through the sky during the annual as well as the enhanced activity years, but the extent of declination appears to be somewhat smaller during the annual years. During the second and third decade of August, visual observers will also have to deal with the August Draconids, which come from an area near the kappa Cygnid radiant (and may be related). Moreover, the August Draconids have the same characteristics as the kappa Cygnids.

In practice, most observers reported their first kappa Cygnids in late July or early August. It is worthwhile to keep an eye out for them in the coming years.

7 Conclusion

The kappa Cygnids showed an increased activity in 2021 as expected. The visual observations from 2021 could be nicely confirmed by the CAMS observations worldwide. Possible enhanced activity in 2020 found from visual observations could not be confirmed by CAMS observations. The problem here is that there is pollution from the August Draconids, especially in the second and third decade of the month. This really presents problems in determining the ordinary annual activity. This analysis may raise questions. In addition, observers need to be made aware of the actual size of the kappa Cygnid radiant as well as its correct position, especially during the years with enhanced activity. Adjustment of the radiant positions in the IMO Meteor Shower Calendar is highly recommended.

References

Betlem H. (2021). Submitted for publication.

Denning W.F. (1893). "The August meteors". *Observatory*, **16**, 317–319.

Jenniskens P. (2006). Meteor Showers and their Parent Comets, Cambridge University Press.

Jenniskens P. (2007). "Kappa Cygnids 2007". CBET 1055, 2007 September 9, editor Daniel W.E. Green.

Jenniskens P., Vaubaillon J. (2008). "Minor planet 2008 ED69 and the kappa Cygnid meteor shower". *Astronomical Journal*, **136**, 725–730.

Jenniskens P., Nénon Q., Albers J., Gural P. S., Haberman B., Holman D., Morales R., Grigsby B., Samuels D., Johannink C. (2016). "The established meteor showers as observed by CAMS". *Icarus*, **266**, 331–354.

Jenniskens P. (2021a). "Kappa Cygnid meteors 2021". CBET 5014, 2021 August 9, editor Daniel W.E. Green.

Jenniskens P. (2021b). "Enhanced κ-Cygnid (KCG#0012) activity in 2021". *eMetN*, **6**, 462–463.

Johannink C. (2007). "Zomeraktie te Gronau". *Radiant, Journal of the DMS*, **29**, 162–167.

Koseki M. (2014). "Various meteor scenes II: Cygnid-Draconid complex (κ-Cygnids)". *WGN, Journal of the IMO*, **42**, 181–197.

Kronk G.W. (1987). Meteor Showers, a Descriptive Catalogue. Hillside, NJ, Enslow.

Langbroek M. (1993). "Vuurwerk boven de Provence!! De aktiviteiten van het 'dreamteam' Rognes". *Radiant, Journal of the DMS*, **15**, 96–106.

Miskotte K. (1985). "Puimichel (2)". *Radiant, Journal of the DMS*, **7**, 103–104.

Miskotte K., Rispens B. (1986). "De Perseiden in Puimichel". *Radiant, Journal of the DMS*, **8**, 80–83.

Miskotte K., ter Kuile C., van Leuteren P., Dijkstra S. (2013). "Perseiden actie vanuit de Provence". *Radiant, Journal of the DMS*, **35**, 63–70.

Miskotte K. (2020). "De χ Cygniden in 2020: een visuele analyse". *Radiant, Journal of the DMS*, **42**, 159–161.

Miskotte K. (2021). "The Chi Cygnids (CCY # 757) in 2020, a visual analysis". *eMetN*, **6**, 540–542.

Rendtel J., Molau S. (2015). "Enhanced kappa-Cygnid activity 2014". *WGN, Journal of the IMO*, **43**, 43–46.

A Perseid campaign at the Cosmos Observatory near Lattrop, the Netherlands

Koen Miskotte and Carl Johannink

Dutch Meteor Society, the Netherlands
k.miskotte@upcmail.nl, c.johannink@t-online.de

A report on a short Perseid campaign at the COSMOS Public Observatory near Lattrop at the Dutch-German border is presented. Three more or less clear nights is a good result to Dutch standards.

1 Introduction

The summer of 2021 treated the Netherlands on very unstable weather. This meant low temperatures, but also a lot of clouds and rain. At the beginning of August, the authors decided to try to observe the Perseid maximum from the COSMOS Public Observatory near Lattrop between August 10 and 13. As this period approached, it seemed that we certainly would experience some clear skies around the Perseid maximum.

2 Pre-maximum observations

In the period before the maximum, Koen was able to observe for a number of nights. The first was July 17–18. 2.00 hours effectively yielded 19 meteors. Besides the sporadic (SPO) meteors, 3 Perseids (PER), 1 Capricornid (CAP) and 1 Antihelion (ANT) were seen. The most beautiful meteor was a very slow –1 SPO moving through Aquila. Afterwards, according to CAMS BeNeLux observations, this turned out to have been a kappa Cygnid (KCG). This night's observations were done from a new spot on the Groevenbeekse Heide near Ermelo. The old site was gradually surrounded by bushes that obstructed the view and this place was also prone to ground fog. The new site is more than 1.5 meters higher and 50 meters to the east. It is located on top of a so-called ice age wall. Debris has accumulated due to ice retention and because of that the landscape is slightly sloping. There was indeed ground fog this night, but it remained below the field of view.

During the evening of July 31, Koen was able to observe at home from the dormer for half an hour before the clouds struck again. Koen counted 6 meteors of which 2 PER and 1 southern delta Aquariid (SDA). The latter was of a fine caliber, this –1 SDA slowly moved up from the horizon near the square of Pegasus. Further observations could be made in the evening of 8 August. During 0.95 hours, 19 meteors were counted. The Perseids were gaining strength, with 6 PER, 1 SDA and 2 KCG being seen despite the low radiant setting. The most beautiful meteor was a nice magnitude 0 KCG in Andromeda. All other nights were cloudy.

3 Observations at the Cosmos Observatory near Lattrop

August 10–11

In the afternoon of August 10, Koen traveled by train to Enschede where he teamed up with Carl. The train was of course delayed again, but Carl was prepared for that in view of previous experiences with people to be picked up at the station in Enschede: he went to have a cappuccino with something delicious in the city center of Enschede and after this short break he went back to the station. That was easier said than done. The city center of Enschede can be reached faster on foot than by car. But in the end, he managed to reach the station via a detour. Koen was already waiting at the exit. It was good to see each other "live" again. After a nice meal there was a little nap before hunting the meteors. Once Carl had started the CAMS systems at home we left for the observatory. We arrived there around half past ten and we met for the first time in a long (due to the covid pandemic) Peter van Leuteren, Sietse Dijkstra and his son Simon. There was not much time to chat, the sky was clear! Not very bright, but with a limiting magnitude of 6.4 we couldn't complain. We were all looking for a spot at the observatory's parking lot.

The observations took place between 21^h08^m and 01^h30^m UT. The Perseids were performing below their usual strength, at least that was the impression. The hourly counts were rather flat and up to a maximum of 21 Perseids an hour. The kappa Cygnids however were clearly active! No fireballs were seen this night, but a couple of KCG of 0 and +1. In addition, the hourly counts were also very nice, up to a maximum of 6 kappa Cygnids per hour. The night was calm, there was some fog hanging over the adjacent meadow. Around 2^h00^m UT, Koen and Carl drove back to Gronau, a 30-minute drive.

August 11–12

During the day there was again the ritual of a late breakfast with tasty brötchen and a walk through Gronau. From a local terrace we pleasantly saw a beautiful blue sky. After

dinner, the observers had another nap in the evening. This way the observations were easy to maintain! This time we drove a different route to the observatory on the Dutch side. The Twente landscape is also beautiful and dark at night. Also present at the observatory were Peter, Sietse, Simon and various employees of the COSMOS observatory, including Arnold Tukkers. This night was a regular public viewing evening at the observatory. So, it was busy the first hour. The parking lot was already fairly full with cars, luckily not yet where we would observe. One option was to observe a kilometer to the north, but we had serious concerns about fog. There were already some patches of fog in the adjacent meadow. We decided to observe at the observatory. Carl parked his car in such a way that we were as little disturbed as possible by the other cars when they drove away. Indeed, until 22^h10^m UT we were occasionally disturbed by departing guests. In addition, we also clearly heard how Arnold Tukkers enthusiastically explained the Perseids to the guests from the roof terrace.

Around 22^h20^m UT we saw the light beams of a car turning into the parking lot. Just around that time Koen saw a nice –5 kappa Cygnid in Pegasus, the other observers saw two flashes of light: one from the meteor and one from the car parked at that moment. For a moment we thought it was still an employee of the observatory, but a little bit later it became clear that they were three students from Almelo, who wanted to view the Perseids. They just were lying down on the floor to enjoy the spectacle. Again, we had the impression that the Perseids hadn't really picked in activity

yet. The hourly counts were between 20 and 28. Things got better in the last hour, but unfortunately the sky got obscured from the west around 00^h15^m UT with thick cirrus. Before that, we had a bit more trouble with mist or fog, so that the limiting magnitude was slightly lower than the previous night. The three students got cold, and the uncomfortable surface was no reason to stay any longer. They left for Almelo again.

The KCGs were again clearly present with hourly frequencies between 4 and 6. In addition to the –5 KCG, a number of 0 and +1 were also seen. The Perseids delivered another set of –2 and –1 meteors. We waited for better skies for a while after 00^h15^m UT, but eventually left for Gronau around 1^h UT. This time we drove back via Germany. Suddenly Carl turned into a small road but then immediately had to hit the brakes heavily! A deer suddenly darted out of the bushes a few meters in front of the car over the road. When asked by Koen why we turned there, Carl told him that we had observed the Taurids of 2005 and the Perseids of 2007 at this location. Koen indeed recognized the location afterwards.

August 12–13
The third night also seemed to be clear for most of the time with in the evening some clouds and perhaps later in the night a cold front. It was the passage of a cold front without rain and accompanied by a small band of cirrus. We therefore left a little later for the observatory. When we
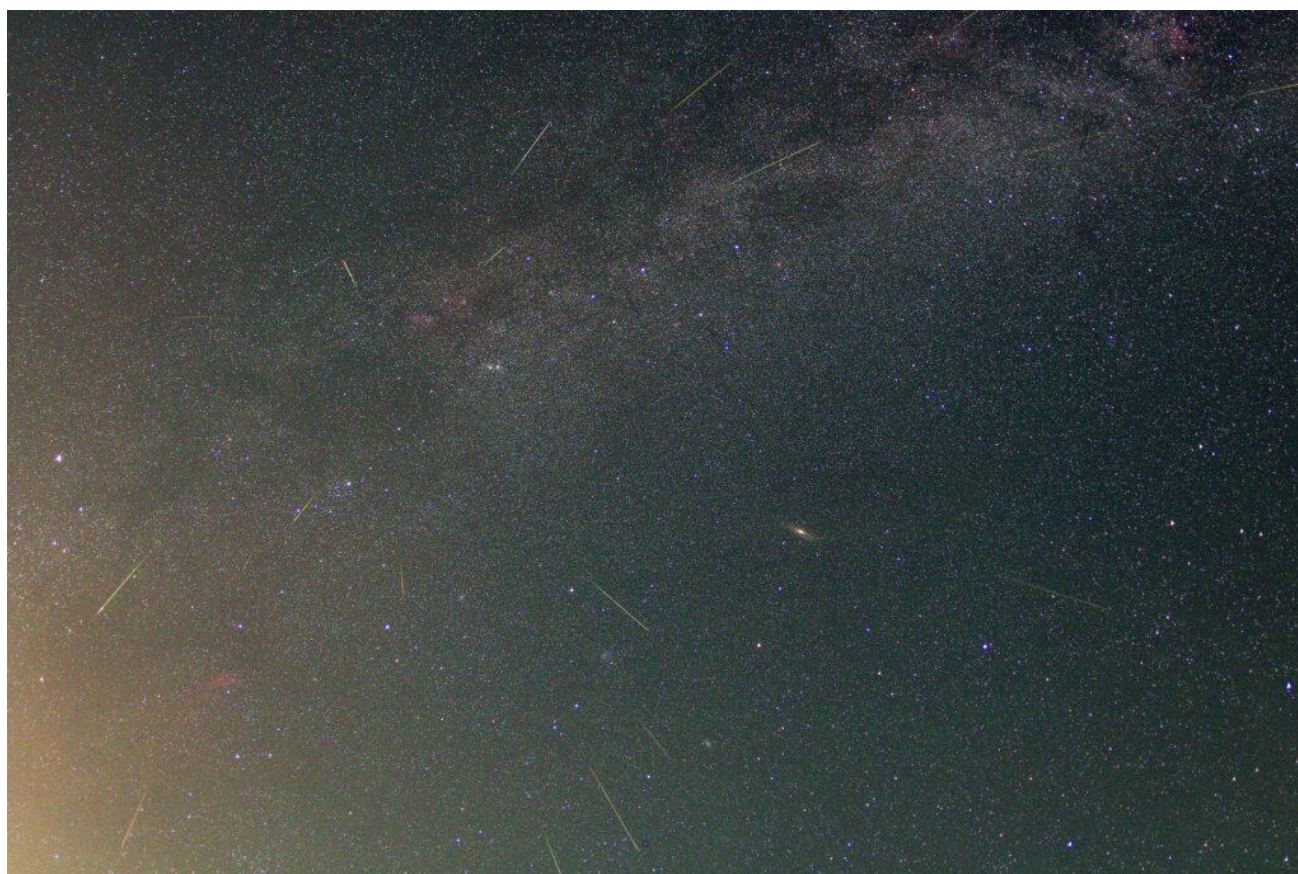
Figure 1 – Perseid meteors captured at the Cosmos Observatory on the night of August 12–13, 2021 | Canon 750D Mod, 15mm F/2.8 Fish-eye lens, exposure time subs 30 seconds, followed with an IOptron CEM60 mount. Courtesy of Peter van Leuteren.

arrived there at 21^h UT sky was mostly cloudy, but the first clear spells were beckoning in the southwest. After a cup of coffee the sky opened completely and Carl, Koen, Peter, Simon and Sietse again started the observations. The starry sky was now almost perfect. With a limiting magnitude of 6.5, it all looked good. Observations started at 21^{h}30^m UT. After a few hours we got again the impression that the Perseids were underperforming. Hourly counts were indeed slowly increasing from 20 to a maximum of 42 per hour. We had seen that much better. Brighter Perseids were seen, up to a pair of magnitude –4.

In the evening, despite the fact that the observatory was closed for the public, we were visited several times by people who wanted to see the Perseids. An amateur photographer who had entered the site, decided to take some pictures. At 23^h UT another car entered the site with bright lights provoking some swearing and yelling among the observers. The photographer now also understood our grumpy reactions at his 'entrance' to the parking lot. The late visitors this time turned out to be two ladies who wanted to see the Perseids. They watched for a couple of hours.

Around 00^h UT the expected cirrus became noticeable low in the west. We could observe until 00^{h}30^m UT, after that there was too much cirrus to observe. We decided to have a drink in the observatory and check for the weather. Clearings would soon follow, as it turned out. From 00^{h}50^m UT the sky was almost cloudless again. The best Perseid hourly counts were reached in the following hour. Incidentally, the kappa Cygnids were also present, but the numbers were a bit lower than the previous two nights. Up to 4 KCG per hour were counted, no fireballs were seen.

This night marked the end of the campaign at Lattrop. For Dutch standards, this one was very successful! Satisfied we stopped the observations at 02^{h}30^m UT. During the day Koen travelled back to Ermelo after another hearty German breakfast!

A strong activity of the Ursids in 2021 by worldwide radio meteor observations

Hiroshi Ogawa[1] and Hirofumi Sugimoto[2]

[1] **The International Project for Radio Meteor Observations**
h-ogawa@amro-net.jp

[2] **The Nippon Meteor Society**
hiro-sugimoto@kbf.biglobe.ne.jp

Worldwide radio meteor observations recorded a strong activity of the Ursids in 2021. The outburst peak time occurred at $\lambda_O = 270.40°$ (December 22, 08^h UT) with an estimated Activity Level Index = 0.8. The estimated ZHR_r was 41 ± 4. The enhanced activity remained for about four hours (December 22, $06^h – 09^h$ UT).

1 Introduction

The Ursid meteor shower is one of the major showers at the end of the year. Although it shows only a weak annual activity level in most years, sometimes outbursts of activity have been recorded such as in 2008, 2009, 2014 and 2016 (Ogawa and Steyaert, 2017). Also in 2020, worldwide radio meteor observers have recorded an activity level twice the usual annual level (Ogawa and Sugimoto, 2020).

For 2021, a dust trail encountering was predicted by Peter Jenniskens (Jenniskens 2006) expected to occur at around $\lambda_O = 270.33°$ (December 22, 06^h47^m UT).

Radio meteor observations make it possible to observe meteor activity continuously even if bad weather interferes or during daytime. Besides, the problem with the radiant elevation is solved by organizing radio observing as a worldwide project. One of the worldwide projects is the International Project for Radio Meteor Observations (IPRMO)[11]. IPRMO uses the Activity Level index for analyzing the meteor shower activity (Ogawa et al., 2001).

2 Method

This research adopted two methods to estimate the Ursid meteor shower activity. One is the Activity Level Index which is used by IPRMO (Ogawa et al., 2001). The second is the estimated ZHR_r (Sugimoto, 2017). This index is estimated by using the Activity Level index and a factor named S_{bas} which translates the activity to the ZHR_r. This method is very useful to compare radio observations with visual observations.

3 Results

3.1 Activity Level Index

Figure 1 shows the result for the Ursids 2021 based on the calculation of the Activity Level Index using 42 observing datasets from 14 countries. The gray line indicates the average for the period 2004–2019. An unusual activity has been detected around December 22, $06^h – 09^h$ UT

($\lambda_O = 270.32°–270.45°$). The activity during this period remained at the same level (see *Table 1*).
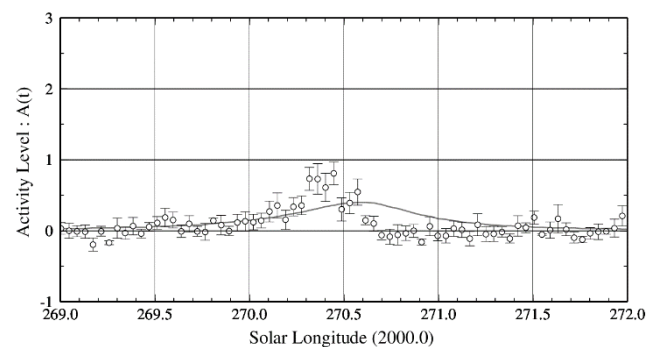
Figure 1 – Activity Level Index of the Ursids 2021. The full line indicates the average for the period of 2004–2019.

Table 1 – Activity Level Index (*AL*) and estimated ZHR_r for the Ursids in 2021.

| Time (UT) | λ_O (°) | Activity Level | | ZHR_r | |
		N	AL	N	ZHR_r
Dec 22 03^h	270.19	25	0.2 ± 0.1	13	19 ± 3
Dec 22 04^h	270.23	26	0.3 ± 0.1	18	16 ± 2
Dec 22 05^h	270.28	25	0.4 ± 0.1	16	20 ± 3
Dec 22 06^h	270.32	27	0.7 ± 0.2	19	26 ± 3
Dec 22 07^h	270.36	28	0.7 ± 0.2	19	37 ± 3
Dec 22 08^h	270.40	21	0.6 ± 0.2	13	41 ± 4
Dec 22 09^h	270.45	17	0.8 ± 0.2	14	38 ± 5
Dec 22 10^h	270.49	17	0.3 ± 0.2	10	24 ± 3
Dec 22 11^h	270.53	14	0.4 ± 0.1	11	22 ± 3
Dec 22 12^h	270.57	18	0.5 ± 0.2	13	23 ± 3
Dec 22 13^h	270.62	20	0.1 ± 0.1	12	15 ± 2
Dec 22 14^h	270.66	24	0.1 ± 0.1	10	6 ± 1

Figure 2 shows the activity components of the Ursids 2021 estimated by using the Lorentz profile (Jenniskens et al., 2000). One component (URS21C01) had a maximum Activity Level = 0.3 at $\lambda_O = 270.36°$ (December 22, 07^h UT) with Full width half maximum (FWHM) = –7.5 / +5.5.

---

[11] https://www.iprmo.org

The other component (URS21C02) had an Activity Level = 0.5 at $\lambda_\mathrm{O} = 270.40°$ (December 22, 08^h UT) with FWHM = –2.0 / +2.5 (see *Table 2*). Although the peak time occurred earlier than during the usual annual activity, it seems that URS21C01 is corresponding to the traditional activity profile. It is possible that URS21C02 represents the outburst activity produced by the dust trail.
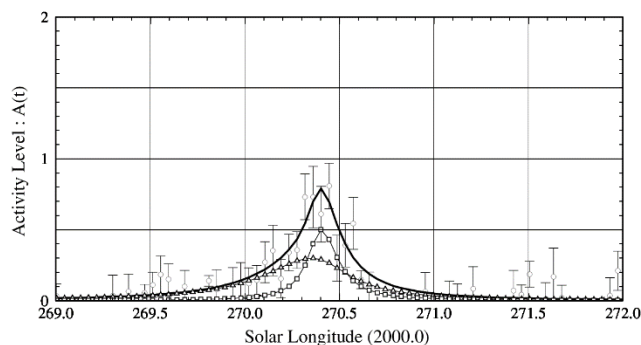

Figure 2 – Estimated Components using the Lorentz Profile. The curve with triangles represents URS21C01, the curve with the circles is URS21C02. The line is URS21C01 and URS21C02 combined. Circles with error bars are the Ursids observed in 2021.

Table 2 – Estimated components of the Ursids activity in 2021.

Component Code	Max. UT	λ_O (°)	Activity Level	FWHM (hours)
URS21C01	Dec 22, 07^h	270.36	0.3	–7.5/+5.5
URS21C02	Dec 22, 08^h	270.40	0.5	–2.0/+2.5

3.2 Estimated *ZHR$_r$*

Figure 3 shows the result for the Ursids in 2021 based on the calculation of the *ZHR$_r$* using 42 datasets worldwide. The estimated *ZHR$_r$* reached 41 ± 4 at $\lambda_\mathrm{O} = 270.40°$ (December 22, 08^h UT). The enhanced activity started at $\lambda_\mathrm{O} = 270.02°$ (December 21, 23^h UT). The unusual increase started at $\lambda_\mathrm{O} = 270.32°$ (December 22, 06^h UT). The activity ended at $\lambda_\mathrm{O} = 270.66°$ (December 22, 14^h UT) (see *Table 1*). The activity level was the same as for the 2020 Ursids when a *ZHR$_r$* = 39 ± 3 at $\lambda_\mathrm{O} = 270.54°$ was recorded.
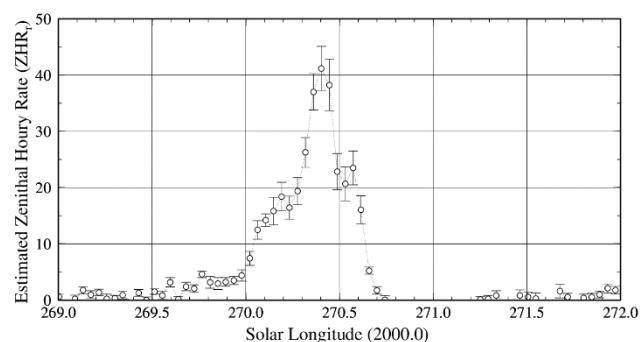
Figure 3 – Estimated *ZHR$_r$* for the Ursids 2021.

Acknowledgment

References

Jenniskens P., Crawford C., Butow S. J., Nugent D., Koop M., Holman D., Houston J., Jobse K., Kronk G., and Beatty K. (2000). "Lorentz shaped comet dust trail cross section from new hybrid visual and video meteor counting technique implications for future Leonid storm encounters". *Earth, Moon and Planets*, **82–83**, 191–208.

Jenniskens P. (2006). Meteor Showers and their Parent Comets. Cambridge University press.

Ogawa H., Toyomasu S., Ohnishi K., and Maegawa K. (2001). "The Global Monitor of Meteor Streams by Radio Meteor Observation all over the world". In, Warmbein Barbara, editor, *Proceeding of the Meteoroids 2001 Conference*, 6-10 August 2001, Swedish Institute of Space Physics, Kiruna, Sweden. ESA Publications Division, European Space Agency, Noordwijk, The Netherlands, 189–191.

Ogawa H. and Steyaert C. (2017). "Major and Daytime Meteor Showers using Global Radio Meteor Observations covering the period 2001-2016". *WGN, the Journal of the IMO*, **45**, 98–106.

Ogawa H. and Sugimoto H. (2021). "Ursids 2020 with Worldwide Radio Meteor Observations". *eMetN*, **6**, 19–21.

Sugimoto H. (2017). "The New Method of Estimating ZHR using Radio Meteor Observations". *eMetN*, **2**, 109–110.

A global network for radio meteor observers

Lorenzo Barbieri and Gaetano Brando

Associazione Astrofili Bolognesi (AAB)
rambometeorgroup@gmail.com

Radio meteor observations have been practiced by few observers in the amateur community using different and sometimes complicated techniques. Based on the experience with RAMBo, the authors have created a device using SDR (Software Defined Radio) technology which measures and records the main physical parameters of the radio meteors by analyzing the meteor radio echoes. The low cost combined with the simplicity of the construction and management makes it suitable for the creation of a global network of receiving stations capable of producing coherent observational data which can be analyzed to study meteor shower activity.

1 Introduction

Almost everything we know about meteors is due to centuries of visual observations. While the ancient observational "reports" date back to the 3rd century BC, it was at the beginning of the 20th century that the observation techniques were based on a standard. This allowed to overcome the subjectivity of the individual observers as well as the difference in observing circumstances, making it possible to put together a large amount of data from all over the world recorded at different times and at different places.

The availability of cameras with wide-field optics which allow video observations resulted in a new observational technique with a number of new standards, such as Metrec, UFO, CAMS, Global Meteor Network as main players which are not entirely compatible with each other but allow to compare observational results.

So far, the observation of meteors by amateurs in the radio field has been characterized by methods and techniques that were often different, depending on the skills and interests of the individual amateur observers.

The project that we introduce here has the ambition to start defining a proposal for a common technique and observational standard applicable in this field.

2 The radio meteors

When a body (meteoroid or debris), after travelling for millennia in interplanetary space, enters the upper layers of the Earth's atmosphere it collides with the upper molecules of the atmosphere it encounters along its path. The speed of these particles moving within the solar system, relative to the Earth, is very high, from a minimum of 12 to a maximum of 72 kilometers per second.

Regardless the small mass of the meteoroid, usually a few grams, its kinetic energy is definitely high. The kinetic energy is defined as:

$$E_c = \frac{mv^2}{2}$$

With the exception of the rare cases in which the meteoroid is of a large mass, after a very rapid increase in temperature the entrance in the atmosphere usually results in its disintegration.

This process causes the emission of light and the disruption of the electrons in the atoms, forming a cylindric tube of free ions and electrons dispersed along the trajectory of the particle in the atmosphere. The first phenomenon is commonly known as a "meteor" or "shooting star".

The cylinder of free ions and electrons can be dense, depending on the kinetic energy of the impact, and more or less persistent, since ions and free electrons tend to recombine immediately.

When free electrons are hit by an oscillating electromagnetic field they are induced to oscillate with the same frequency. This oscillation in turn involves the re-emission of an electromagnetic field and if this oscillation is in phase for a large number of electrons there is a radio electric transmission that can be detected from a distance.

Therefore, if a cylinder of free electrons generated by a meteor phenomenon is hit by a radio electric transmission, then it behaves or at least in a small part of it, as a reflector of this transmission. This reflection lasts until the moment of dissolution due to the recombination of ions and electrons.

The minimum required linear density of a radio meteor is defined by Belkovich (1972, 2006):

$$\propto_o = \frac{U_{eff}}{R_0} \sqrt{\frac{32\pi^2 d_o^2}{\lambda^3 R_i r_e^2 P_T G_T G_R}}$$

Where:

- U_{eff} is the sensitivity threshold of the receiver;

- R_0 is a factor that statistically groups the observability of the radio meteors due to: radius, diffusion and speed of the meteor, also calculated along the direction of the maximum antenna sensitivity;
- d_o is the distance in meter between the receiver and the meteor area along the direction of the maximum antenna sensitivity;
- λ is the wavelength;
- R_i the receiver input impedance (in Ohm);
- r_e is the electron radius;
- P_T is the transmitting power (in Watt);
- G_T and G_R refer to the antenna gains.

It is important to note that the wavelength λ is in the denominator and in the cube.

It is obvious that if the wavelength decreases, the minimum threshold for the detectability of a radio meteor increases, making reception more difficult. This point will be explained further in this article.

If a VHF transmitter is continuously transmitting with an emission pointed upwards and a receiver is tuned at the same frequency at a position on the Earth surface below the horizon for the transmitter, the receiver can detect the transmitted signal when a cylinder of free electrons is generated by a meteor, creating the reflection conditions (*Figure 1*).
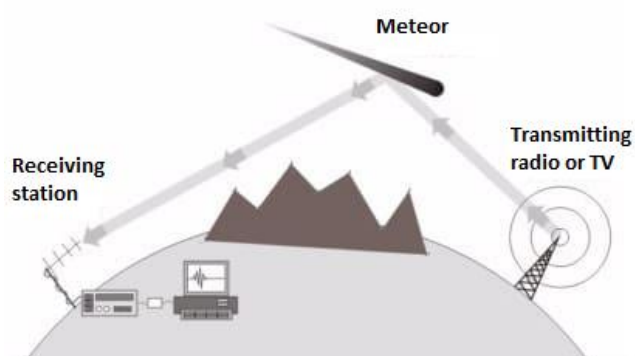
Figure 1 – Radio meteor reflection scheme.

When this signal is being recorded by a receiver, we speak about a "radio meteor".

As already mentioned, a radio meteor is a reflection phenomenon of an electromagnetic signal and is subject to the physical laws that govern these phenomena such as the condition that the entrance angle is equal to the reflection angle. We will consider these characteristics at the end of this article.

3 Receiving radio meteor echoes

Unlike visual meteors which are only visible at night and for which the observability is heavily influenced by lunar illumination, light pollution and weather conditions, radio meteors are continuously detectable. The recording of meteor radio echoes can only be disturbed by echoes caused by airplanes, satellites or by reflection on the sporadic E layer.

Since the second World War, radars have been built to study radio meteors. Generally, there are two types of radars, "forward scatter" and "back scatter", depending on the position of the receiver with respect to the aiming of the transmitter. In the first case the receiver is placed very far from the transmitter, hundreds of kilometers, receiving reflections generated halfway between the receiver and the transmitter. In the second case, the receiver is close to the transmitter and captures the reflections backwards.

Among the many examples of meteor radars, we can mention the one of Vedrana di Budrio (Bologna) owned by the CNR which was in operation in the 1990s or another currently active radar, the Canadian CMOR located in Ontario.

Meteor radars are devices that consists of transmitters that emit pulse signals combined with a set of receivers equipped with directional antennas working as interferometers in order to reconstruct speed, position and the direction of the meteor which indicates the radiant.

Figure 2 – The military radar at Graves, near Dijon, France.

These data allow to know the orbital elements of the meteoroid which make it possible to identify a possible association with known meteoroid streams.

Meteor radars are therefore complex and very expensive devices only available for professional research projects conducted by scientific institutions or universities.

The amateur community, amateur astronomers as well as radio amateurs, has explored this technique with various experiences. For instance, the transmission of communications beyond the Earth's curvature, using the moments when a radio meteor allowed reflection and transmission of the communication.

Obviously, no amateur can afford the purchase and operation of such a powerful transmitting device, therefore the amateur community must make use of other available transmitters such as radio or television transmitters, military radars, amateur radio beacons, etc.

The radio meteor observing is usually done using a normal amateur radio receiver tuned in SSB mode (Single Side Band) about 1000 Hertz separated from the carrier of the broadcast signal.

This technique allows to listen to an audio signal at the output of the receiver at a frequency equal to the difference between the received signal and the frequency tuned on the radio.

In the case with 1000 Hertz, the audio output generated sounds like a whistle that emerges from the noise from time to time, whenever a radio meteor reflection is received. This whistle has intensity and duration proportional to the size of the cylinder with free electrons, and to the ion-electron recombination process duration.

Sometimes dedicated software's are used which graphically represent the audio signal creating the so-called "waterfall", usually in false colors, which is a method that displays the amplitude, frequency, and duration of the audio signal on a video monitor.

Amateur radio meteor observing almost always ends here, just simply listening to the received signals.

4   Counting and measuring radio meteors

Within the Associazione Astrofili Bolognesi we asked ourselves whether it was possible to go further than just listening and to make measurements capable of investigating the activity of meteor showers using an amateur level approach.

Obviously, the kind of tools available to the amateur community impose great limitations.

First, the absence of a pulsed signal transmitter prevents both the measurement of position and direction; in other words, even if there were several receivers arranged in various ways on the Earth surface, and even if they could be connected, triangulation would not be possible.

Once the idea to obtain the orbital elements for the individual meteors had been given up, only the instant of the event, the amplitude of the generated audio signal and the duration of the event of each radio meteor detected remained as possible measurements.

With these data, it is possible to make an analysis of the activity level (hourly rate) and to evaluate the kinetic energy and the mass-distribution of the recorded meteors.

This kind of observation requires to listen continuously, to digitize the signal and to record it in function of the requirements for a physical and statistical analysis.

Given the need for continuous operation for the purposes of digitization and recording, we have discarded the use of personal computers when looking for dedicated hardware.

5   The RAMBo experience

RAMBo (Radar Astrofilo Meteorico Bolognese) uses the signal emitted by the military radar transmitter Graves located in France which continuously transmits in the VHF band at very high power (the frequency is 143.05 MHz) (*Figure 2*).

Figure 3 – Vertically polarized Yagi antenna.

Its transmission is directed upwards and because of the shielding by the Alps, it is not possible to detect it directly from Bologna.

Our receiver has a 10-element Yagi directive antenna (*Figure 3*) pointed in azimuth in the direction of the transmitter and at about 25° elevation, where we calculated that the reflection point with the upper layers of the atmosphere should be. The radio receiver we used is a Yaesu FT 857.

The receiver audio output is amplified with an operational circuit, split into two outputs. One of the two is squared off to measure the frequency, while the other is dedicated for an amplitude measurement.

These two signals are sent to a microprocessor (Arduino) programmed by the authors. The frequency, duration and amplitude are measured by Arduino, the instant of the event is recorded, and the results are written in a log file consisting of records with the data for each meteor event.
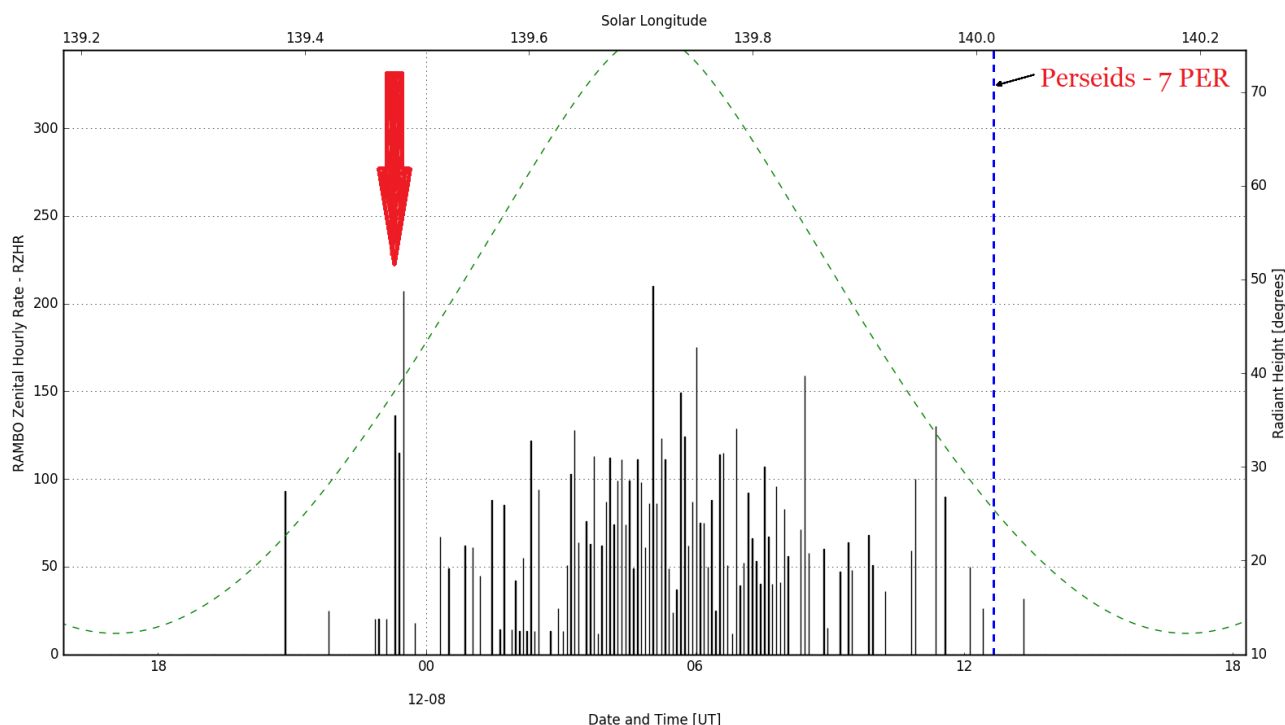
Figure 4 – Perseids 2016.

After a few months of experiments, we were able to improve both the hardware and the software in order eliminate completely the many "false positives" that an AM (amplitude modulation) reception normally creates.

For this purpose, we used the microprocessor as a frequency meter. If several consecutive samples occur in a narrow range around the tuned frequency, we can reasonably assume that it is a meteor.

If the frequencies of consecutive samplings are random, the echo is discarded.

The experience with Rambo was very satisfying. With this project we have recorded and measured almost a million meteors every year since 2014 up to today.

We have calculated the RZHR of many showers and we have detected the filaments of some meteor showers. We have used this data for presentations at two editions of the annual conference of the International Meteor Organization and we published some articles (Barbieri, 2016; Brando, 2016; Barbieri and Brando, 2019).

As evidence for the possibilities of RAMBo, we mention the observations concerning the 2016 Perseid shower: some days before the Earth encounter with this well-known meteor shower an astronomical telegram (CBAT) was issued by P. Jenniskens (2016), analyzing the perturbation on the meteoroid stream by the major planets and predicting the possible presence of a filament a few hours before the shower peak activity at solar longitude 139.5°, or around midnight on August 11–12.

Indeed, as can be seen from the graph in *Figure 4*, the filament was detected by RAMBo on August 11 at 23^h20^m UT. It should be noted that the duration is about three sampling intervals; each sampling interval being 5 minutes long, the total duration of this meteor shower filament was about 15 minutes.

From this data we can roughly extrapolate the dimensions of the filament: since the Earth moves at about 107000 km/h in interplanetary space. From

$$d = v \cdot t$$

we find that the diameter d will be larger than $107000 \times 0.25 = 26750$ km, depending on whether the Earth has intersected the dust filament perfectly in the middle or more or less laterally.

The data collected during a period of time is published dynamically on a page of the website of our Association[13] and archived weekly[14].

6 The limits of the RAMBo experience

Despite the fact that this project has given us a lot of satisfaction, RAMBo also met some limitations.

- First, this project is difficult to reproduce. The sound card is our prototype, its assembly and its use require knowledge of electronics which is not common for all amateur astronomers. The same should be said for the Arduino programming.

---

[13] www.associazioneastrofilibolognesi.it/rambo/

[14] http://www.ramboms.com/

- Another drawback is that the equipment isn't cheap. The radio which we use is extremely expensive and other similar devices are even more expensive.
- Finally, the measurement is taken from an audio signal generated by the radio. We may assume that it could be roughly proportional to the actual radio electric power of the received signal, but we cannot be certain of this at all. If you want to think in terms of radar, you must measure the radio electric power received by the antenna directly.

For these reasons we have tried to develop a receiver that overcomes these three limitations, and to achieve this we have explored the world of SDR.

7 What is SDR (Software Defined Radio)?

A radio device as we know it historically can be defined as a set of analogue components each of which performing a certain function.

For example, if we think of the classical superheterodyne radio, inside of this we find an input amplifier, a local oscillator, a mixer, a band filter, an intermediate frequency amplifier, a double half-wave rectifier and a detector.

All these functions, although performed by analogue devices, are mathematical functions: to remain with the basic functions listed above, these functions are multiplications, divisions, subtractions, application of trigonometric functions, integrations, etc.

As we known, to multiply, to subtract, to divide, to generate sinusoids or to integrate and to derivate, it is much simpler and more efficient today to use a computer rather than an analogue circuitry.

The SDR (Software Defined Radio) in fact performs these functions once the antenna signal has been digitized, it is computer processed by using dedicated algorithms. This way the PC works like a radio.

The first studies on SDR date back to 1970 in the USA and the first SDR transceiver was made in Germany in 1988. Today the SDR devices can be found in every television, digital radios (DAB) and smartphones.
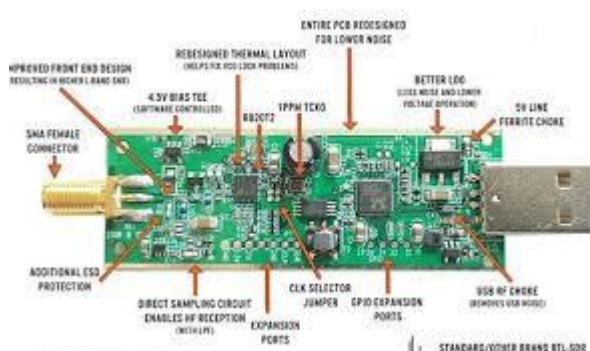
Figure 5 – This chip is commonly implemented in the small circuit called the "dongle" shown here.

In the 2000s, the advent of the RTL2832U integrated circuit made it possible for thousands of amateurs and enthusiasts to access the world of digital radio.

This chip is commonly implemented in the small devices called "dongles" such as shown in *Figure 5*. The connector for the coax cable coming from the antenna is visible on the left side and the USB plug to connect to a computer is on the right side.

We have tested a few and we think that the NooElec NESDR Smart v4 SDR is the best. It costs 32 euro, it is stable, reliable and it is the one with the lowest background noise among those we tested.

With this very cheap device, any enthusiast can make a receiver using a personal computer.

8 Detecting radio meteors with the SDR

Like all software-based applications, not all industry development is industrial and patented. There is also an open-source niche (GNU Radio).

Using this environment, after more than a year of attempts we were not able to build a project that met the expectations we had in mind and this failure led us to give up.

The turning point that led to the resumption of the study and the realization of the project was the discovery of a Python programming language library specially written to operate the integrated circuits RTL2832U and R820T2, which are the heart of the "dongle".

We have therefore written a Python application that performs the work of tuning the dongle to the frequency of the transmitter chosen by the user, setting the gain, sampling the signal, and performing the FFT (Fast Fourier Transform), thus obtaining the frequency and the amplitude of the received signal.

It should be emphasized that this way we obtain the exact measurement not only for the frequency, but also for the radio electric signal power. Unlike all previous experiences based on listening at the audio output, this configuration is comparable to a real radar.

Once these two quantities have been obtained, our application is able to recognize the meteor echo by eliminating false positives both due to satellites or airplanes and to weather transients such as lightning and to anthropogenic transients. The output file allows you to see the shape of the echo profile of the recorded meteor and the frequency of each individual event.

After the first successes obtained using a personal computer, we tried to run this application on a small and cheap microcomputer like the Raspberry. The result was that the execution speed doubled, further improving the application performance.

Figure 6 – Carmelo.

We have thus created an extremely economical device, easy to assemble and to manage: hence the name CARMELO stands of **C**heap **A**mateur **R**adio **M**eteor **E**choes **Lo**gger (*Figure 6*). Carmelo is very reliable. After months and months of uninterrupted operation with three units there has never been any interruption or any failure.

9   First results

The first months of operation showed us Carmelo's potential.

In *Figures 7 and 8* you can see the time on the x-axis and the signal to noise ratio (SNR) on the y-axis.
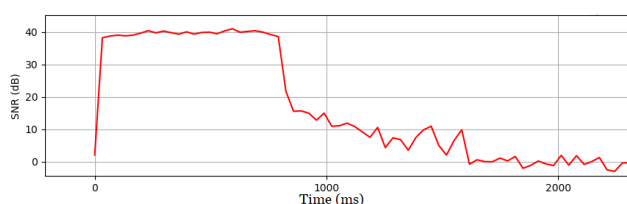
Figure 7 – Typical shape of an overdense meteor.

Figure 7 is a typical example of an "overdense" radio meteor, i.e., an event in which the cylinder of free electrons is sufficiently dense to behave like a solid body. Its reflection shows a very rapid rise, a flat saturation trend and a descent due to the dissolution caused by the ion-free electron recombination.

Another type of reflection is the "underdense" radio meteor, generated by an impact with lower kinetic energy and therefore characterized by a low-density reflecting cylinder (*Figure 8*).
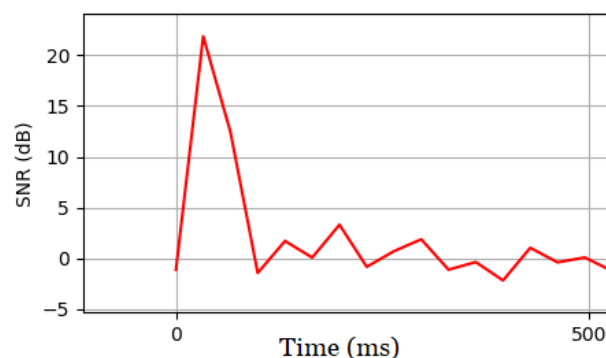
Figure 8 – Shape of an underdense meteor.

Note that the difference between these two cases is not limited to the shape of the profile and duration but also the difference in amplitude is evident which is in these cases 20 dB, a factor of 100 times. *Figure 9* shows the distribution of all the radio meteors recorded in a single week; the x-axis displays the time, the y-axis the SNR while the size of each single dot is proportional to the duration.

The page shows in real time the individual recordings sent by each receiver wherever it is located. The only required condition is that the receiver is connected to the internet.

Figure 9 – Radio meteor echo events recorded by three Carmelos in one week. The three receivers can be identified by the different symbols that identify each of them. This image is taken from the web page[15].

---

[15] http://www.astrofiliabologna.it/graficocarmelo
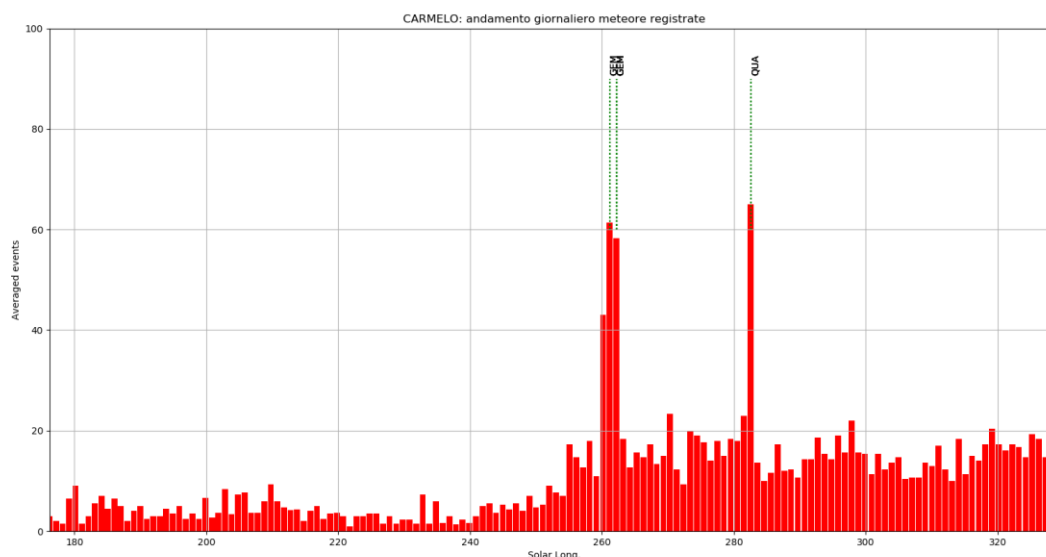
Figure 10°– RHR (Radio Hourly Rate) made with only three observing systems.
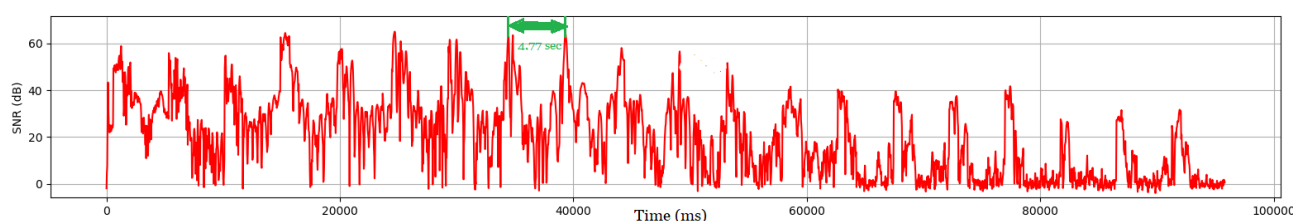
Figure 11 – Radio echo profile with an exceptional long duration.

Hovering the mouse over an event on the webpage, you can read the data related to the recorded radio meteor (date and time, location, amplitude and duration of the echo), clicking on an event displays its reflection profile.

Despite the small number of receivers built and put into operation so far, it is already possible to understand the potential of a recording made with a large number of receivers located throughout a large area. To show this potential we have created *Figure 10* which shows the computed RHR (Radio Hourly Ratio) covering the time span autumn–winter 2020. The Geminid and the Quadrantid meteor showers are very evident.

The three receivers used so far are all tuned at the frequency of the military transmitter Graves, located near Dijon, France.

This transmitter has an advantage and at least two disadvantages:

- the advantage is that it transmits at very high power and this makes it suitable to be used by receivers located hundreds of km away;
- the first disadvantage is that its frequency (143 MHz) is much higher, at least three times, than the optimal frequencies for receiving meteor radio echoes and this decreases the efficiency of the system, as we have seen in the introduction;

- the second significant disadvantage is the fact that, as a radar, its beam scans the sky with a fixed periodicity thus generating an alternation of intervals during which the signal is receivable and intervals when the signal is totally absent.

Symbolic of this situation is the echo caused by a huge meteor event on 2021, April 2 with a duration exceeding half a minute (*Figure 11*). The profile of this long persistent echo shows the intervals in which the radio meteor reflects the signal and the intervals during which it reflects no signal. As you can see, the transmitting radar sweep period is approximately 4.8 seconds (marked in green on *Figure 11*).

This means that if a meteor appears in an interval during which Graves does not transmit a signal towards the area of the meteor, it will not be detected. Moreover, the shapes of the echo profiles we measure, the amplitudes we calculate and also the recorded durations are strongly influenced by the oscillating behavior of the transmission.

In this regard, there are two considerations to be made:

- The first is that only with a reception like that of Carmelo, which is defined by the measurement of the radio electric power received instead of the audio of the radio receiver, it was possible to notice this characteristic of Graves. Years of experience with

RAMBo did not provide this insight which is so obvious in a single echo profile generated by Carmelo.

- The second consideration is that a transmitter dedicated to the purpose of meteor observing, operating at lower power but with a suitable frequency and continuous emission, could lead to excellent results for hundreds of receiving stations. The progress in electronics makes this idea much more affordable than in the past.

A next test that should be carried out in north-western Europe, could be to receive the signal from the Belgian meteor transmitter BRAMS (**B**elgian **RA**dio **M**eteor **S**tations). BRAMS is transmitting at 49.97 MHz.

10 A global Carmelo network

There are at least three considerations that lead us to suggest the creation of a network of receiving stations based on a standard registration on a global scale.

The first consideration is that the sensitivity of a SDR dongle is lower than that of an amateur radio receiver. The data in our possession does not allow us to quantify this difference at the moment, but we can assume that it could be considerable.

Furthermore, the sampling frequency carried out with the mini computer is not particularly high with one sampling every 33 ms, which is longer than the duration of short underdense meteors.

Therefore, we do not expect a quantity of received radio echoes equal to those recorded with the RAMBo equipment with about one million radio meteors every year.

While with RAMBo the underdense radio meteors were the majority (90%), with Carmelo these are significantly less present, while the overdense ones prevail.
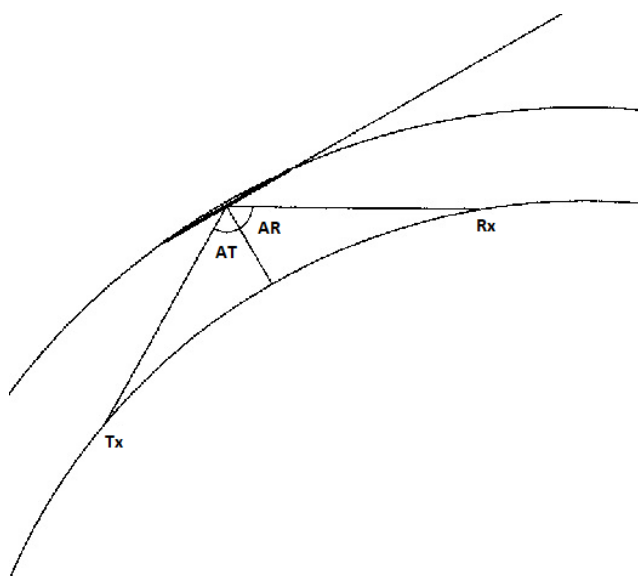
Figure 12 – Reflection geometry.

The result is a lower presence of sporadic meteors and a greater portion of those with larger mass and therefore presumably related to meteor showers.

More receivers placed at different distances from the transmitter can guarantee better coverage and a high number of received echoes.

A second consideration, as already mentioned in the introduction, unlike visual meteors that can be seen from any position on the surface as long as the light emission is sufficient to be detected, the same condition does not apply to radio meteors.

As a radio meteor is a phenomenon due to the reflection of an electromagnetic emission, the reflected ray must have the same angle *AR* as the transmitted one *AT* (see *Figure 12*). Therefore, the echo from a radio meteor can be received only if the receiver is located at a position that complies with this condition. In another configuration the reception cannot take place.

Consequently, receiver stations located at different positions will detect different radio meteors and therefore only a network of observers spread over a large area can aspire to collect a considerable share of the radio electric echoes that can be received within that region.

Another consideration could be added. The cylindric shape of the reflecting tube let us assume that the reflected signal with the angle equal to that of the transmitted signal can be considered on a plane.

The line joining the points *Tx* and *Rx* on the Earth's surface is orthogonal to the direction of the origin of the meteor, which is the direction or azimuth of the radiant (Barbieri, 2016). If two receivers detect the same echo simultaneously, they would then identify this line. In this case, we would obtain important information because knowing the position of the transmitter, we might be able to derive the trajectory of the meteor, a fundamental information for the association with a meteor shower.

Similarly, but in another way, Jean Marc Wislez (2006) describes the ellipsoid in which the transmitter and receiver are in the foci and the meteor's trajectory is tangent at the point *p*. In the case of reception at two different locations there will be two ellipsoids intersecting with the point *p* in common.

Sasa Nedeljkovic (2006) tackled the geometry of this particular case with the aim to derive the trajectory of the meteor that produced the radio echo. These considerations let us assume that with a large network of receiving stations distributed over a large area, the challenge to obtain the trajectory of radio meteors that we had initially excluded from the possibilities of amateur radio meteor observing will once again become an intriguing subject of investigation.

These considerations are true only if we assume that the shape of the meteor ionized cylinder does not change over time.

But the shape of the cylinder could be distorted by the high-altitude winds. This could create multiple echoes,

consequently the same meteor could be seen by multiple receivers.

A third and final consideration, as mentioned in the introduction, observing radio meteors has an undeniable advantage because it is always possible uninterruptedly, regardless of weather conditions and light pollution.

The only limitation, as for all astronomical observations carried out from the ground, is imposed by the horizon. Any observer can only observe visual meteors or radio meteors when the radiant is above or near the horizon.

Therefore, some meteor showers are observable from one hemisphere but not from the other or vice versa. Also, the observability conditions for the same meteor shower change, for a given receiving station, from year to year depending on the time when the activity peak occurs.

A global network of receiving stations all over the world capable to observe continuously with the same standard is able to overcome these limitations by ideally performing as a global terrestrial receiving station travelling in the interplanetary space with a 360 degrees field of view.

For the three conditions listed above, a global network of receiving stations based on a common standard is therefore highly desirable. Using Carmelo, this is also easily achievable. The data produced today is collected, processed and displayed on the website[16] and is publicly available to the meteor observing community. Its eventual realization is based on the availability of individual amateurs, radio amateurs, educational institutions, research institutions or simple curious citizens to host a simple, economical, robust and reliable receiver.

11 What is needed to build a receiving station for radio meteors in the global network?

First of all, it is necessary to identify a known transmitter which is in continuous operation on the VHF (Very High Frequency) radio band. This transmitter must emit on a known frequency and must be tens or hundreds of km away from the receiving station and preferably be below the horizon.

Therefore, it is necessary to have an observation site as free from obstacles as possible. Most obstacles are man-made artificial objects but natural steep mountains in the immediate proximity can also obscure the observation horizon.

The best location can be the roof of a building, but it can also be a large garden if there are no buildings close to it. Otherwise, if the receiver is installed at some of the lower floors of a high building, this will undo the global coverage (360°).

The choice of the antenna and its correct installation should in no way be underestimated. This is where the effectiveness of the radio meteor detection is determined. There are two types of antennas: directional and omnidirectional ones.

In the first category we mention the Yagi type antennas (see *Figure 3*), in the second the collinear antennas (*Figure 13*).

Figure 13 – Collinear antenna.

For those who are completely uninformed about antennas we can say that if we listen with an omnidirectional antenna, it is as if we were looking at the starry sky with the naked eye, seeing many stars in a very wide field of the sky. If we listen with a directional antenna, it is as if we were looking at the sky with binoculars or a telescope, seeing a much smaller portion of the sky but with fainter stars than those visible to the naked eye.

Out of the metaphor: an omnidirectional antenna has a low and fixed gain, while a directive antenna has a higher gain but only towards a certain direction. The characteristic of the construction of the directional antennas determines the higher the gain, the smaller the area at the sky covered.

---

[16] http://www.astrofiliabologna.it/carmelo

Figure 14 – "Discone" antenna.

Figure 15 – Self-built ground plane antenna "Carmelina_143".

Although most of the radio meteor observations are commonly made with directional antennas generally pointed in the direction of the transmitter and at a certain angle to the vertical, we suggest to use the vertically polarized omnidirectional antennas for the following reasons.

- First of all, this type of antenna is easier to assemble, less bulky and less critical in windy areas.
- Furthermore, omnidirectional antennas, in the case of a network distributed over a large area, allow a better comparison between individual receiving stations because it is independent of the gain in the antenna and it provides more comparable results for any possible triangulation.
- A third reason is the cheapness of the antenna. The omnidirectional antennas available on the market can be of various types, ranging from "discone" antennas,

which cost is around 80 euro, up to balcony antennas that cost less than 30 euro.

Self-construction should not be underestimated at all. The self-construction of a "ground plane" type antenna has two advantages. First of all, it is very cheap, since it can be built for a few euros (*Figure 15*).

Moreover, it seems absurd but it is not, its efficiency is better than the commercial ones. The explanation for this apparent contradiction can be justified as the commercial antennas are almost never designed to operate on a single frequency but are produced and sold to allow radio amateurs to receive (and transmit) on many channels.
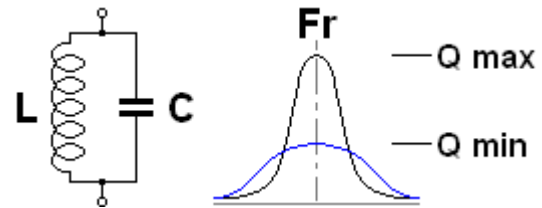
Figure 16 – LC circuit and merit factor Q (gain).

An antenna is equivalent to an LC circuit which electrical characteristics determine the frequency on which it resonates.

$$f_o = \frac{1}{2\pi\sqrt{LC}}$$

- f_o is the resonant frequency (in Hz);
- L is the inductance (in H);
- C the capacitance (in F).

A "pure" LC circuit has a narrow and high Gaussian curve of the Q factor (similar to gain) on the main frequency (*Figure 16*).

$$Q = \frac{f_o}{\Delta f}$$

Q is the merit factor, comparable to the antenna gain and Δf is the bandwidth.

A "loaded" LC circuit distributes the gain on a larger basis, the Gaussian is much wider, thus allowing us also to tune effectively on the adjacent frequencies, but the Gaussian is also lower and therefore loses gain at the main frequency.

Commercial antennas are also designed to transmit and this is the feature that affects most of their price due to the required construction accuracy, for simple reception no sophisticated antennas are required. To confirm the aforementioned reasons, a homemade ground plane like the "Carmelina_143" (*Figure 15*) proved to be more performant than all the other commercial omnidirectional systems that we have tested.

Once the antenna is mounted, a coaxial cable is required to connect the receiver to it. This should be a normal coaxial cable rg58 type or similar, suitable for VHF. We advise to use a cable as short as possible, both to save money, to

minimize losses and to keep the signal to noise ratio (snr) as high as possible. The connectors at its ends must be on one side a male "SMA" to connect to the dongle and on the other side a connector suitable for the chosen antenna, in most cases this is a male "pls". These can be purchased at specialized shops and via the internet, including adapter, for a few euro.

Figure 17 – Testing of the self-built ground plane antenna.

The dongle must be based on the integrated RTL2832U. We have tested a few models and the one we recommend is the NooElec NESDR Smart v4 SDR, it costs 32 euro, it is stable, reliable and it is the one with the lowest noise among those we tested.

As mentioned, the minicomputer adopted is the famous Raspberry Pi 4B, 2GB. This works fine. A SD card must be placed in the RPi. The available volume does not matter, the software (operating system, program and libraries) takes up only 3 Gigabytes.

The Raspberry Pi must be powered with a 5V power supply with USBc socket (i.e., the one for second-generation smartphones). Carmelo absorbs about 75 milliamps which at 5 v means a power of less than 400 mW. This is comparable to some small LED flash light.

Then, you need a LAN network cable that connects the RPi microcomputer with a router that allows access to the Internet. This cable can also be particularly long, indeed the advice we give is to place Carmelo as close as possible to

the antenna and to reach the router with a network cable of the required length.

We have not enabled the wireless function on the Raspberry. After all, Carmelo is still a radio receiver and the fewer transmissions there are in the immediate vicinity, the better.

The total cost of these purchases is about 200 euro.

12 The software

The hardware is simple, cheap and common. What transforms this hardware into a real miniature meteor radar is the software.

Carmelo requires the following:

- The installation of the operating system, the simple and light version of Raspbian is fine.
- The Python libraries and our program, of course free available.
- A small csv file containing the data of the receiver radio station such as the location, geographic coordinates, frequency on which the receiver works, the type of antenna used, the symbol and the color to identify the observations from this receiver in the overall data visible on the appropriate page of the website.

13 Interested to join this project?

Visit our website[17] and we'll be happy to answer any questions you may have.

References

Barbieri L. (2016). "An antenna, a radio and a microprocessor: which kind of observations are possible in meteor radio astronomy?". In Roggemans A. and Roggemans P., editors, *Proceedings of the International Meteor Conference,* Edmond, the Netherlands, 2-5 June 2016. IMO, pages 26–30.

Barbieri L. and Brando G. (2019). "Concerning the height of meteors". *WGN Journal of the IMO*, **47**, 108–115.

Belkovich O. I. (1971). Statistical theory of meteor radar observation. Kazan University, Russia.

Belkovich O. I. (2006). "Processing of radar observation 1: Sporadic background, detection threshold, radar sensitivity". In, Juan Martine Semegone, Pavol Zigo, and Cis Verbeeck, editors, *Proceedings of the Radio Meteor School*, Oostmalle Belgium 10–14 September 2005. IMO, International Meteor Organization, pages 34–47.

---

[17] http://www.astrofiliabologna.it/about_carmelo_en

Brando G. (2016). "The 2016 Quadrantids". In Roggemans A. and Roggemans P., editors, *Proceedings of the International Meteor Conference,* Edmond, the Netherlands, 2-5 June 2016. IMO, pages 39–41.

Jenniskens P. (2016). "2016 Perseid meteors". CBET, 4293.

Nedeljkovic S. (2006). "Meteor forward scattering at multiple frequencies". In Verbeeck C. and Wislez J. M., editors, *Proceedings of the Radio Meteor School*, Oostmalle, Belgium 10-14 September 2005. IMO (International Meteor Organization), pages 108–118.

Wislez J. M. (2006). "Meteor astronomy using a forward scatter set up". In Verbeeck C. and Wislez J. M., editors, *Proceedings of the Radio Meteor School*, Oostmalle, Belgium 10-14 September 2005. IMO (International Meteor Organization), pages 85–107.

Radio Observations in October and November 2021

Ivan Sergei

Mira Str.40-2, 222307, Molodechno, Belarus
seriv76@tut.by

This article presents the results of radio observations made in October and November 2021. The results of the radio observations are compared with the CAMS video network summaries.

1 Introduction

The observations were carried out at a private astronomical observatory near the town of Molodechno (Belarus) at the place of Polyani. A 5 element-antenna directed to the west was used, a car FM-receiver was connected to a laptop with as processor an Intel Atom CPU N2600 (1.6 GHz). The software to detect signals is Metan (author – Carol from Poland). Observations are made on the operating frequency 88.6 MHz (the FM radio station near Paris broadcasts on this frequency). The "France Culture" radio broadcast transmitter (100 kW) I use is at about 1550 km from my observatory which has been renewed in 1997.

2 Automatic observations

October is a fairly quiet month with an average number of about 30 signals per hours. A very weak peak around October 10 may be related to STA activity (#0002). Some enhanced activity was detected in the period of October 20–22 due to the Orionid maximum (#0008). Another period with higher activity appeared around October 29–30 and may be explained by some increased activity produced by a number of minor showers, as well as an increase in the number of observed meteor showers themselves (see the CAMS data section). According to the IMO meteor calendar, the OCT (#0281) and DRA (#0009) meteor have their maxima on October 5 and October 8. However, no trace of any peak activity can be seen in the graph. No peak activity for these showers occurred, or it remained hidden in the sporadic background of meteor signals.

The first half of November showed a very quiet meteor activity at about 15–18 signals per hour on average. The second half of the month was more active when the average number of signals increased to 30 per hour. The graph shows three periods of activity: November 1–13, November 14–22, November 23–30. The blurred Leonids maximum happened during the second period and is not very pronounced. The maxima of NTA (0017), November 12, AMO (#0246), November 21, NOO (#0250), November 28 were not resolved due to the weak activity of these showers, hidden in the sporadic background.

Figure 1 shows the hourly rates of radio meteors in October 2021 recorded at 88.6 MHz. *Figure 2* shows the hourly rates of radio meteors in November 2021 at 88.6 MHz. *Figures 3 and 4* show the corresponding heat maps.
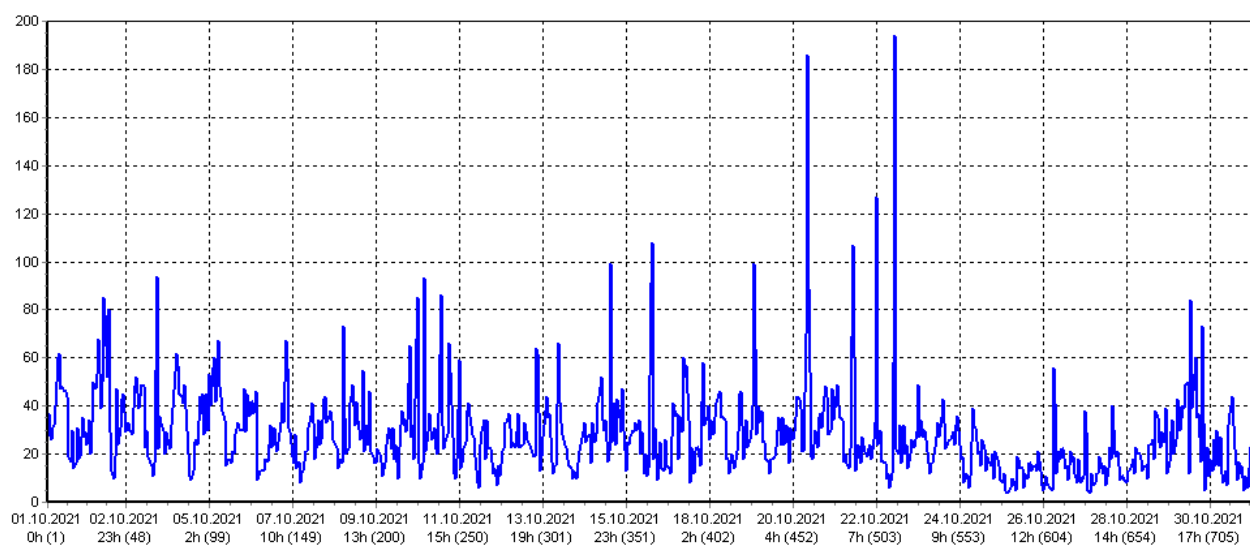
Figure 1 – Radio meteor echo counts recorded at 88.6 MHz during October 2021.
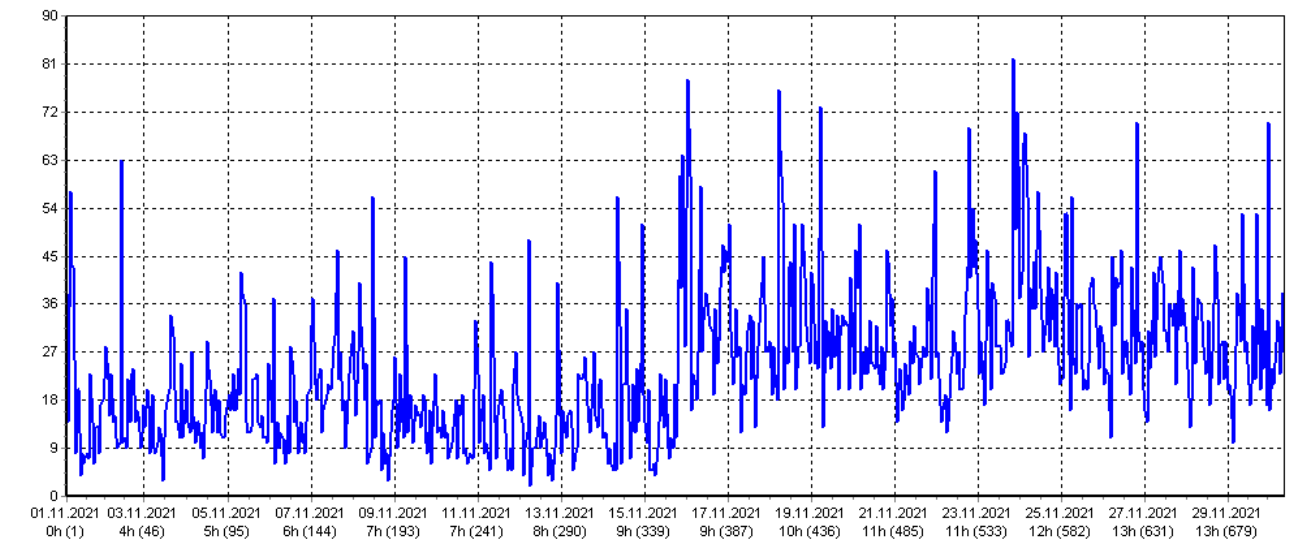
Figure 2 – Radio meteor echo counts recorded at 88.6 MHz during November 2021.
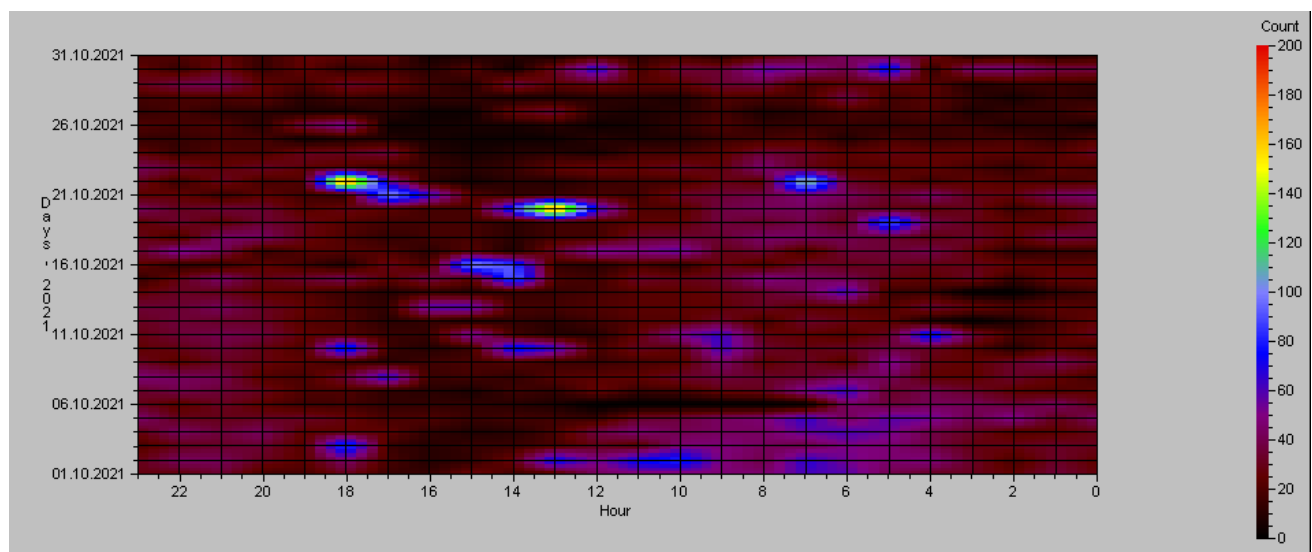
Figure 3 – Heatmap for radio meteor echo counts recorded at 88.6 MHz during October 2021.
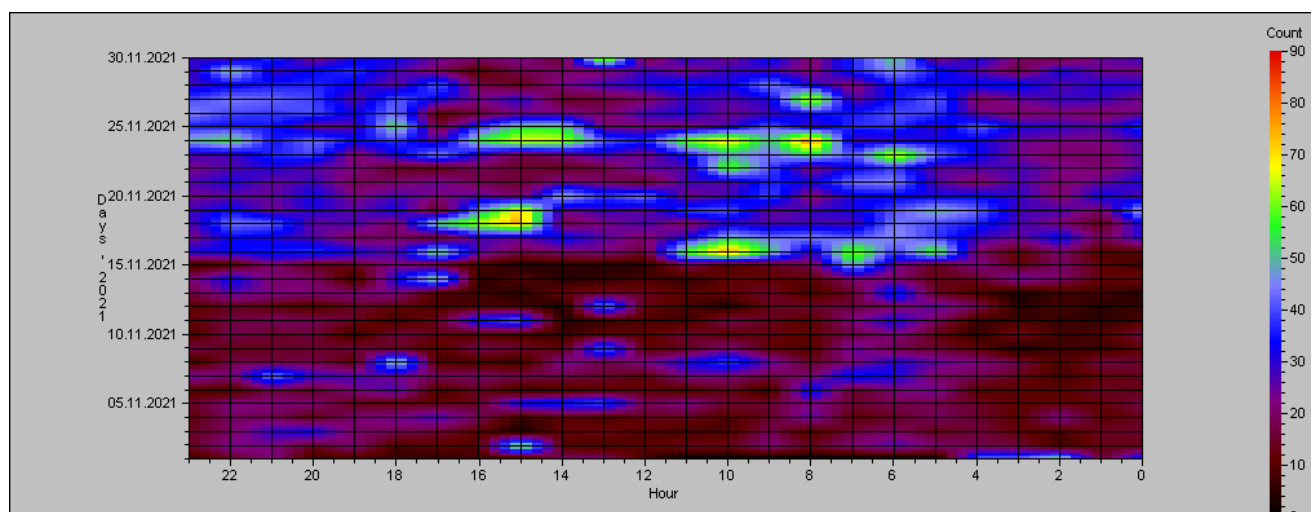
Figure 4 – Heatmap for radio meteor echo counts at 88.6 MHz during November 2021.
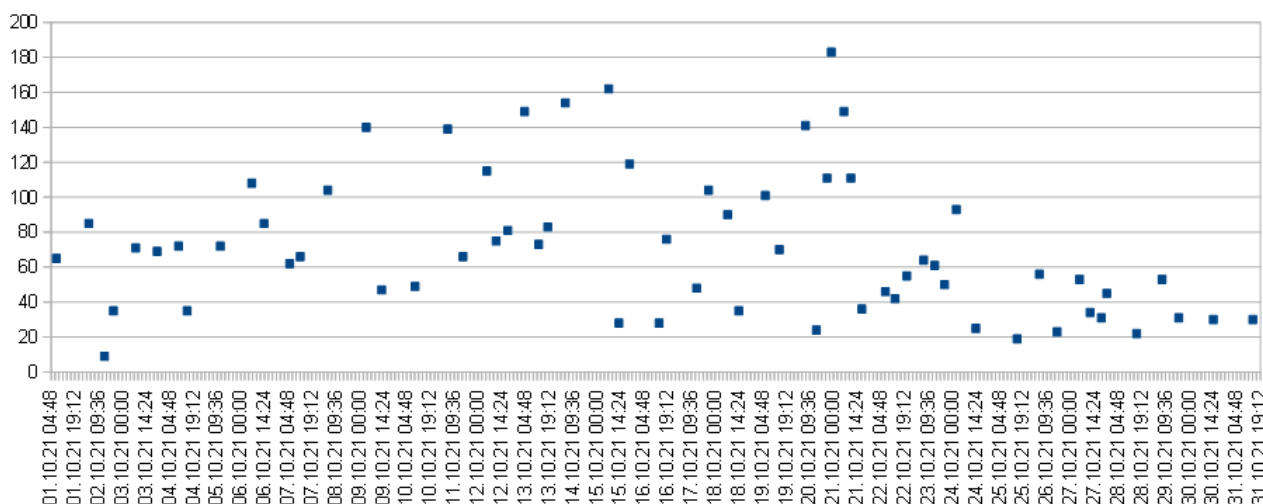
Figure 5 – The calculated hourly numbers of meteor echoes obtained by listening to the radio signals during October 2021.
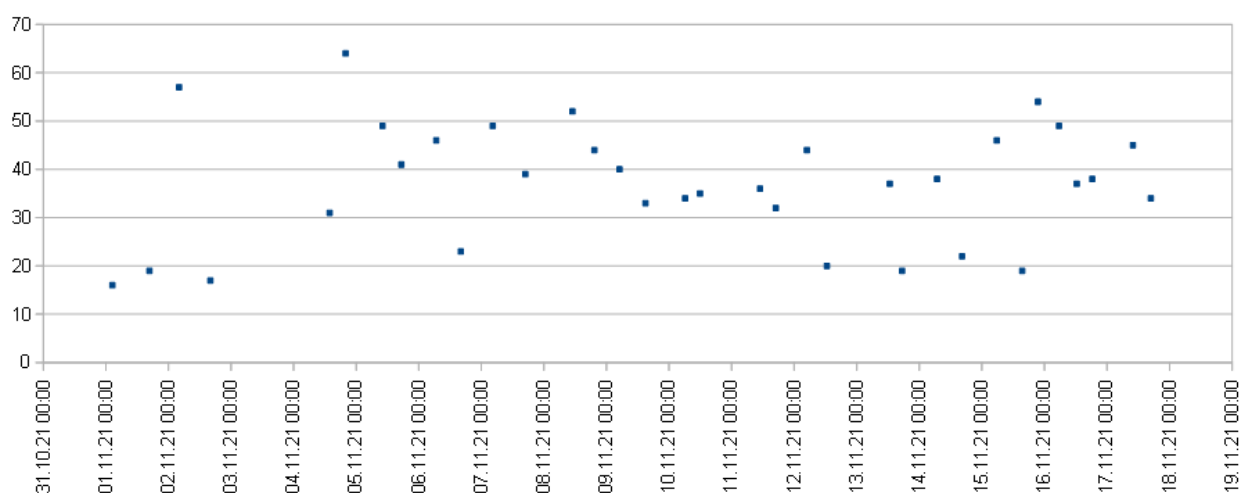
Figure 6 – The calculated hourly numbers of meteor echoes obtained by listening to the radio signals during November 2021.

3   Listening to radio echoes on 88.6 MHz

Listening to the radio signals 1 to 3 times a day for one hour was done in order to control the level of the hourly rates, as well as to distinguish between periods of tropospheric passage and other natural radio interference. The total effective listening time was 64 hours in October and 34 hours in November.

The October activity graph shows an increase in signal activity around the middle of the month. The peak around October 21 is associated with the Orionid (#0008) maximum, a weaker peak around October 23–24 may be associated with a secondary Orionid peak, perhaps on top of the LMI (#0022) minor shower maximum.

The activity of the new OZP (#1131) shower could not be detected because its activity period was limited to only few hours and the total number of OZP orbits was very low. In the morning of October 24, from 05ʰ02ᵐ to 06ʰ02ᵐ local time I heard 93 music or speech signals reflected by

meteors, whereas in the morning of October 23 the activity was less with 64 signals per hour, and earlier on October 22 with 46 signals in the morning. There are no morning data for October 25, only evening data. On October 26 in the morning, I heard 56 signals per hour, and on October 27, 53 signals per hour. The enhanced activity in the morning of October 24 may have been caused by a late sub-maximum of the Orionids.

For November, there is some weak peak of activity around November 16, probably related to the Leonids (#0013).

4   Preliminary CAMS Data

Figures 7 and 8 show the total daily activity of meteors obtained by the CAMS video networks data (Jenniskens et al., 2011). For October and November, there is a noticeable correlation between the activity level of sporadic meteors and the activity level of shower meteors. I used the preliminary CAMS data as available on the website[18] on December 20, 2021.

---

[18] http://cams.seti.org/FDL/
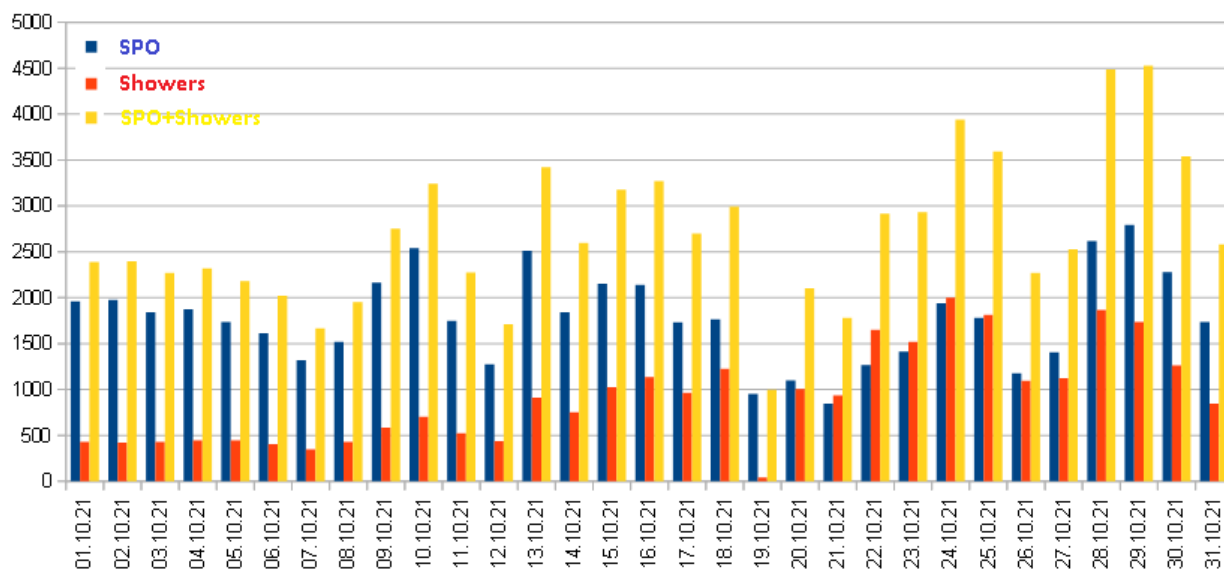
Figure 7 – Daily number of orbits recorded by CAMS video networks in October 2021, yellow bars are the total number of orbits.
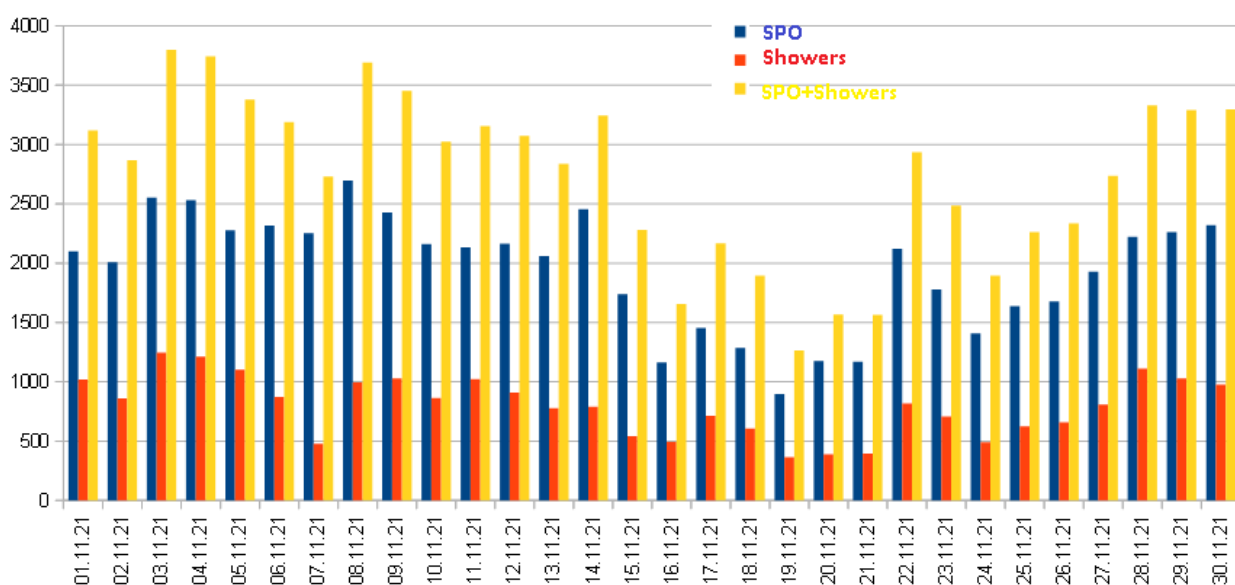
Figure 8 – Daily number of orbits recorded by CAMS video networks in November 2021, yellow bars are the total number of orbits.
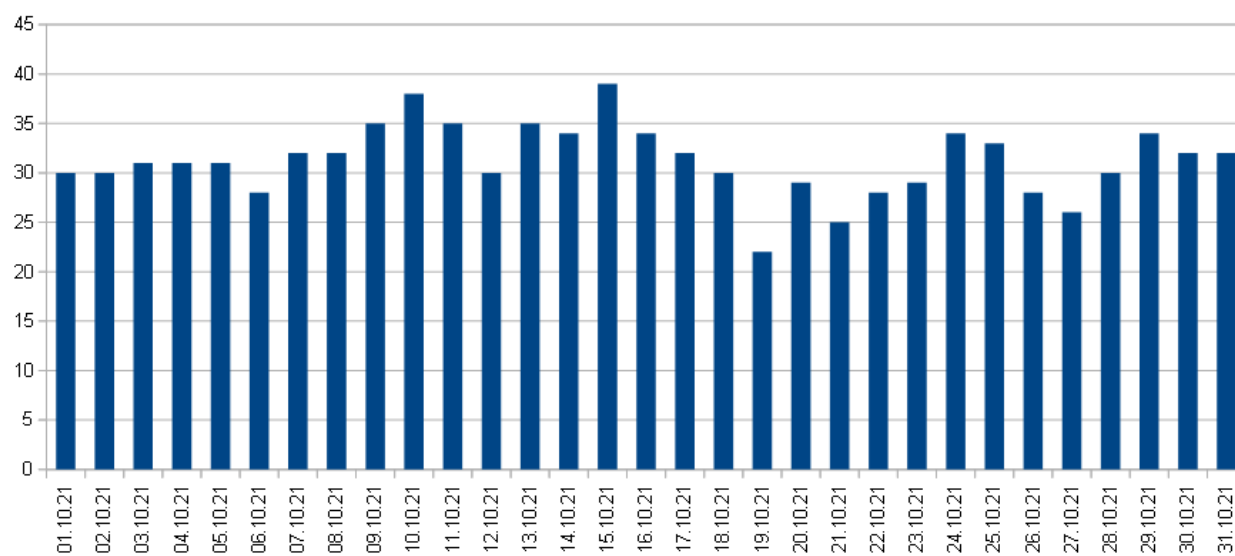
Figure 9 – Numbers of meteor showers detected by CAMS video networks in October 2021.
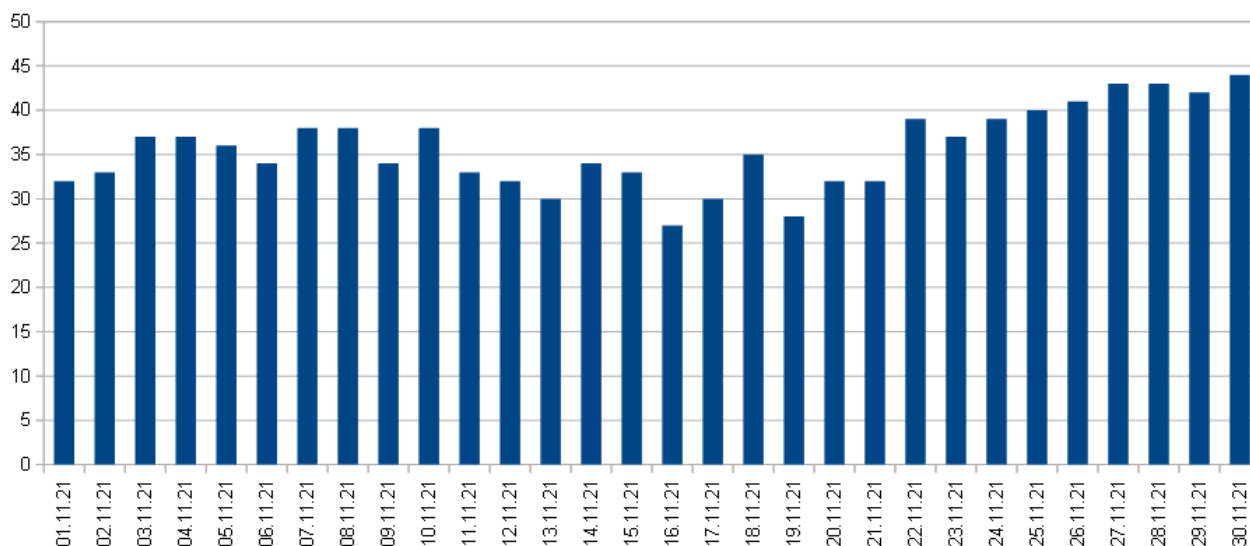
Figure 10 – Numbers of meteor showers detected by CAMS video networks in November 2021.

CAMS data had several dates with enhanced activity for instance October 10, 13, 16, 18, 22, 24 and 28. October 10 had 204 STA (#0002) orbits, as well as an increase in the number of detected showers. On October 13, there was a peak of minor shower XAR (#0624) with 210 orbits and a secondary peak with 188 STA (#0002) orbits. Peaks between October 16 and 22 were due to a marked increase in Orionid activity. The peak on 24 October is the main Orionid maximum with 1557 orbits, which is in disagreement with the IMO shower calendar that lists the peak on 21 October. The peak on October 28 can be explained by some increase in the activity of the sporadic background, ORI (#0008), NUE (#0337), LUM (#0524), TAR (#0630) and, to less extent, the activity by some other minor showers.

CAMS data for November had November 3, 8–9, 11, 17, 22, 28 with peaks in the activity of some meteor showers. The peak on November 3 is associated with some increase in activity of various meteor showers like STA (#0002), NTA (#0017), NUE (#0337), CTA (#0388), NET (#0632), STS (#0628). On November 8–9, different radiants of the Taurid complex displayed enhanced activity. On November 11, there was a maximum of ATS (#0629) radiant with 212 orbits detected. On November 17, there was a maximum of LEO (#0013) activity with 308 orbits detected. On November 22 the video networks registered some increase of activity of LEO, NTA, NOO, and also there was a burst of AND (#0018) activity. On November 28, there was unusual activity from the Andromedids AND (#0018) with 235 orbits detected and further some enhanced activity for the meteor showers NOO (#0250) and HYD (#0016).

Figures 9 and 10 show the total numbers of meteor showers detected by CAMS on a daily basis.

5 Conclusion

The generalized data of radio observations obtained by automatic detection of meteor echoes and by listening for meteor echoes show a satisfactory correlation between them and the CAMS video network data. The reason for a less good correlation of the data may be the difference in the masses of meteoroids, since the radio method registers smaller particles, while the video networks record larger meteoroid particles. The second reason is that radio methods do not depend on weather conditions and allow to obtain a continuous time coverage with observational series, whereas video methods strongly depend on weather conditions interfering with meteor statics. If each night at all CAMS observing sites were clear, the correlation between radio and video methods would be excellent.

Acknowledgment

References

Jenniskens P., Gural P. S., Dynneson L., Grigsby B. J., Newman K. E., Borden M., Koop M., Holman D. (2011). "CAMS: Cameras for Allsky Meteor Surveillance to establish minor meteor showers". *Icarus*, **216**, 40–61.

Rendtel J. (2020). "Meteor Shower Calendar". IMO.

Radio meteors October 2021

Felix Verbelen

Vereniging voor Sterrenkunde & Volkssterrenwacht MIRA, Grimbergen, Belgium
felix.verbelen@skynet.be

An overview of the radio observations during October 2021 is given.

1   Introduction

The graphs show both the daily totals (*Figure 1 and 2*) and the hourly numbers (*Figure 3 and 4*) of "all" reflections counted automatically, and of manually counted "overdense" reflections, overdense reflections longer than 10 seconds and longer than 1 minute, as observed here at Kampenhout (BE) on the frequency of our VVS-beacon (49.99 MHz) during the month of October 2021.

The hourly numbers, for echoes shorter than 1 minute, are weighted averages derived from:

$$N(h) = \frac{n(h-1)}{4} + \frac{n(h)}{2} + \frac{n(h+1)}{4}$$

Local interference and unidentified noise remained moderate during most of the month and only on 3 days lightning activity was detected.

While not spectacular, the Orionids remained the most eye-catching shower of the month, culminating on October 22nd. Several minor showers also produced some long-lasting reflections, i.e. around October 15th.

This month 16 reflections longer than 1 minute were observed here. A selection of these, together with some other interesting reflections are shown in *Figures 5 to 13*.

If you are interested in the actual figures, or in plots showing the observations as related to the solar longitude (J2000) rather than to the calendar date. I can send you the underlying Excel files and/or plots, please send me an e-mail.
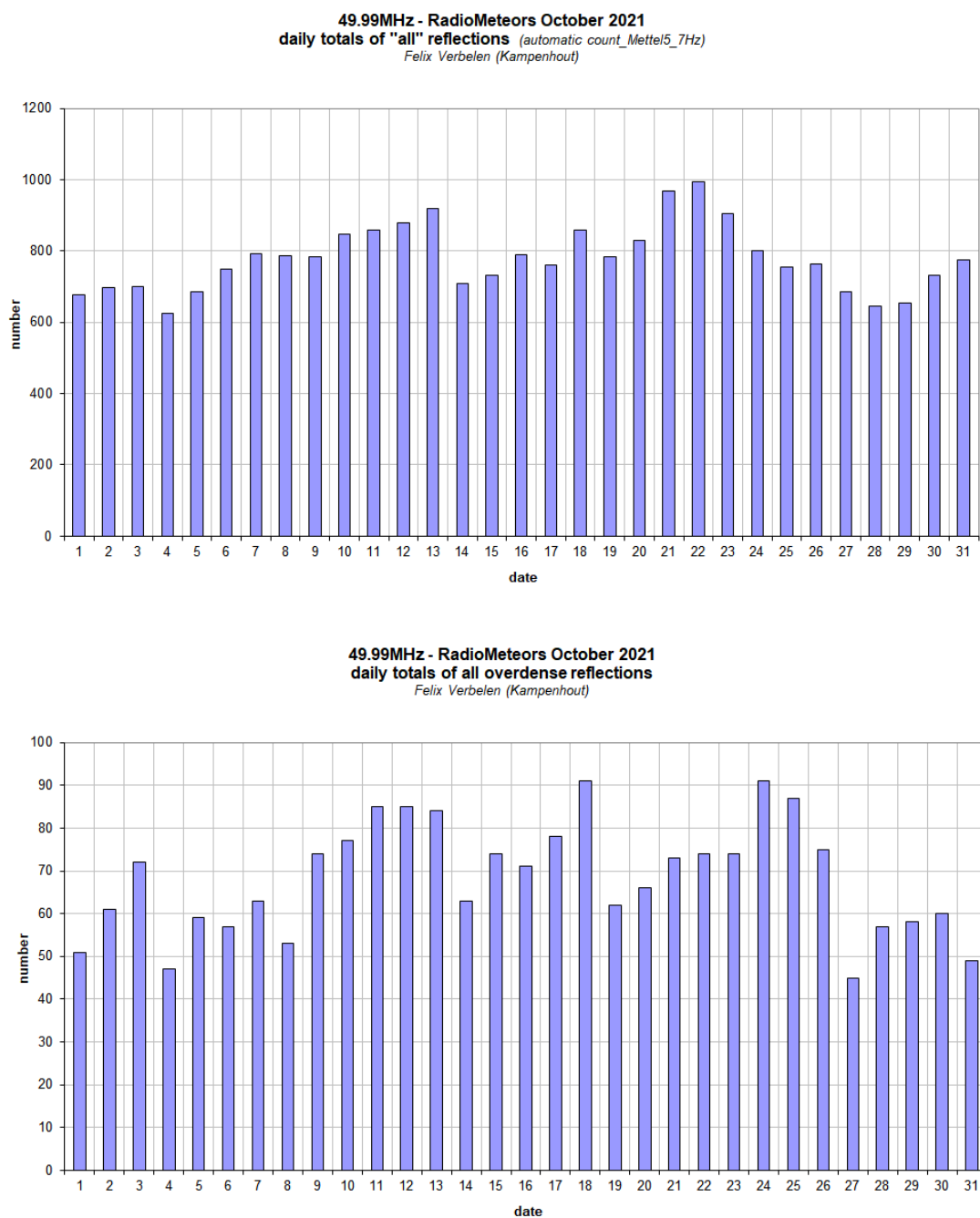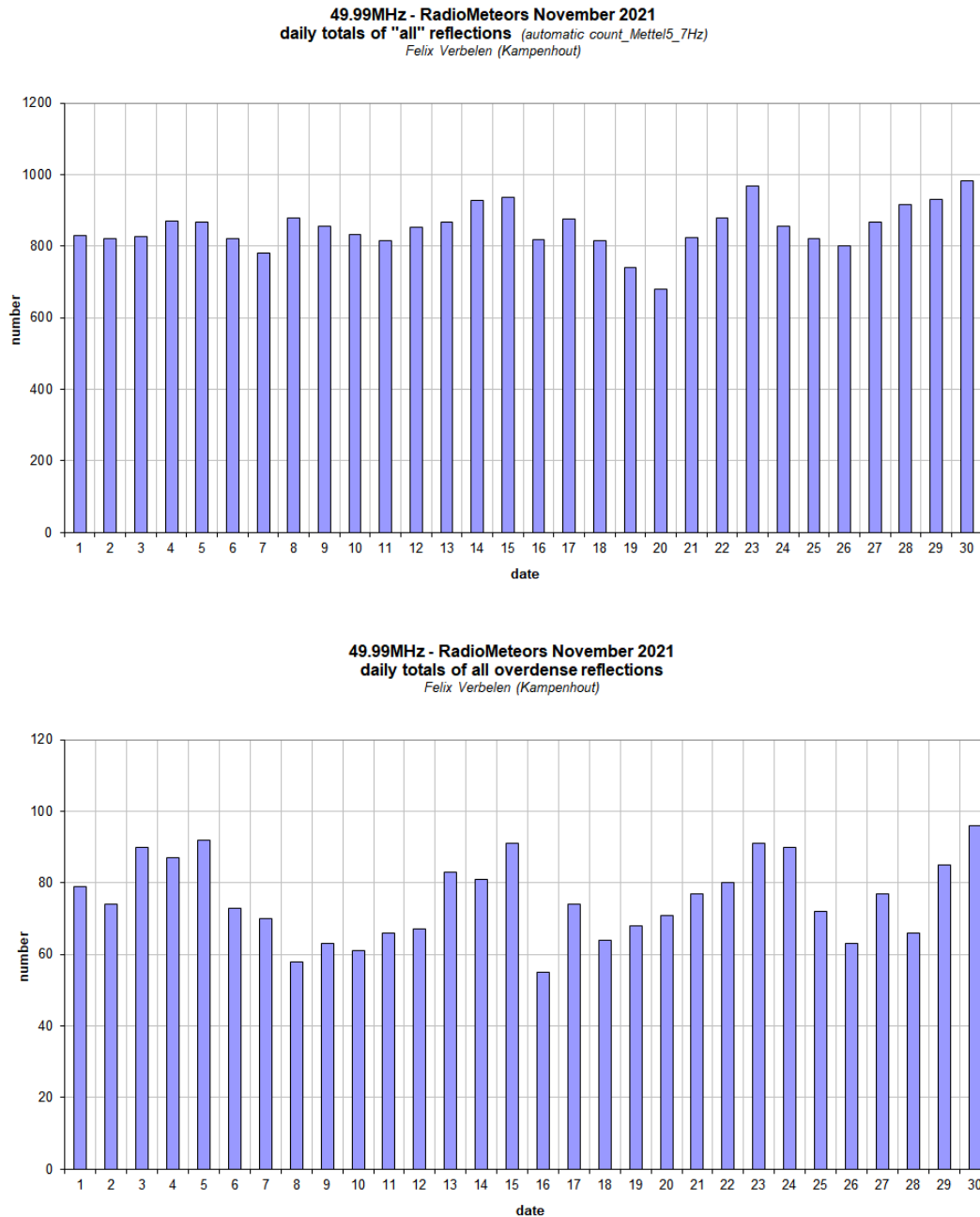
Figure 1 – The daily totals of "all" reflections counted automatically, and of manually counted "overdense" reflections, as observed here at Kampenhout (BE) on the frequency of our VVS-beacon (49.99 MHz) during October 2021.
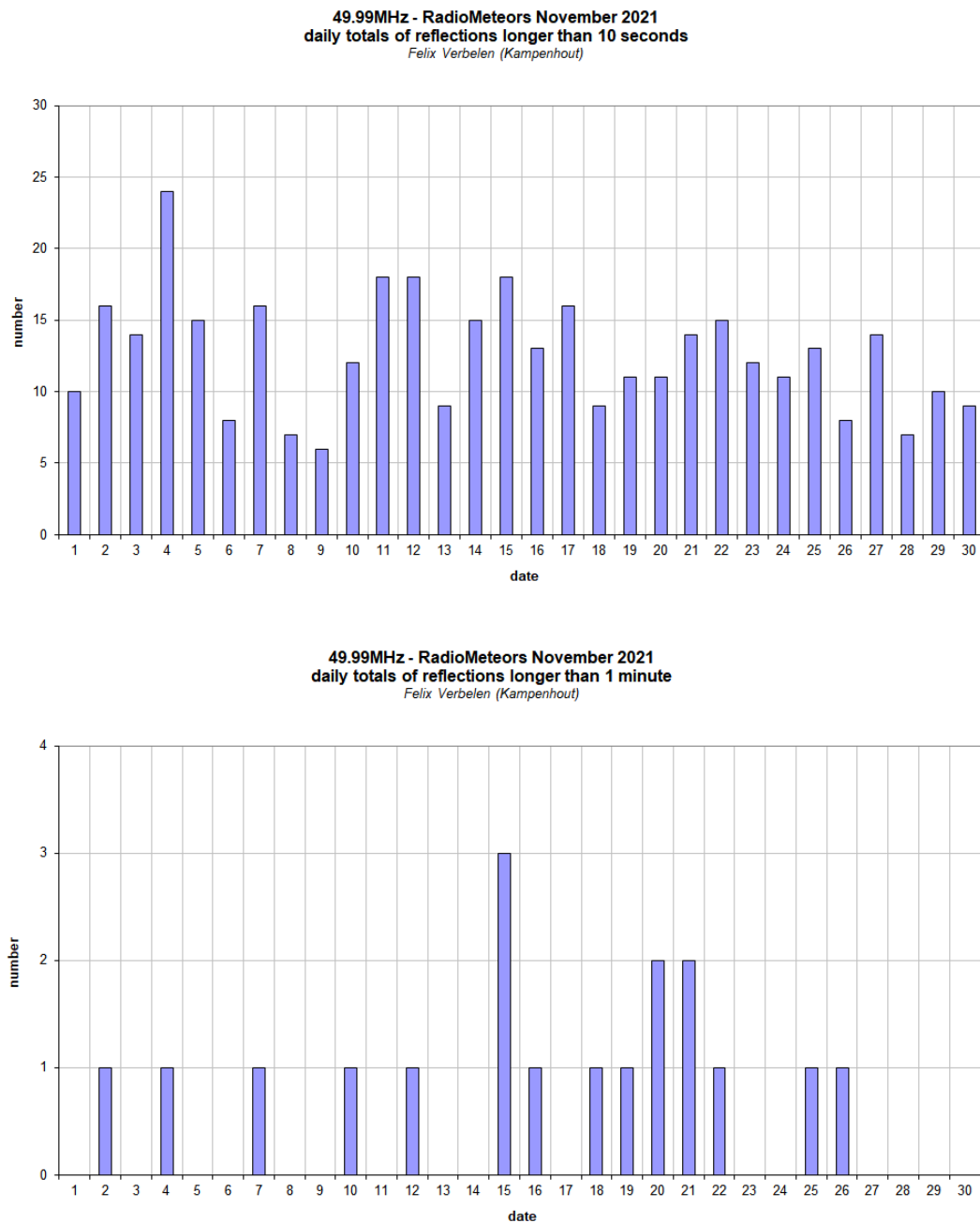
Figure 2 – The daily totals of overdense reflections longer than 10 seconds and longer than 1 minute, as observed here at Kampenhout (BE) on the frequency of our VVS-beacon (49.99 MHz) during October 2021.
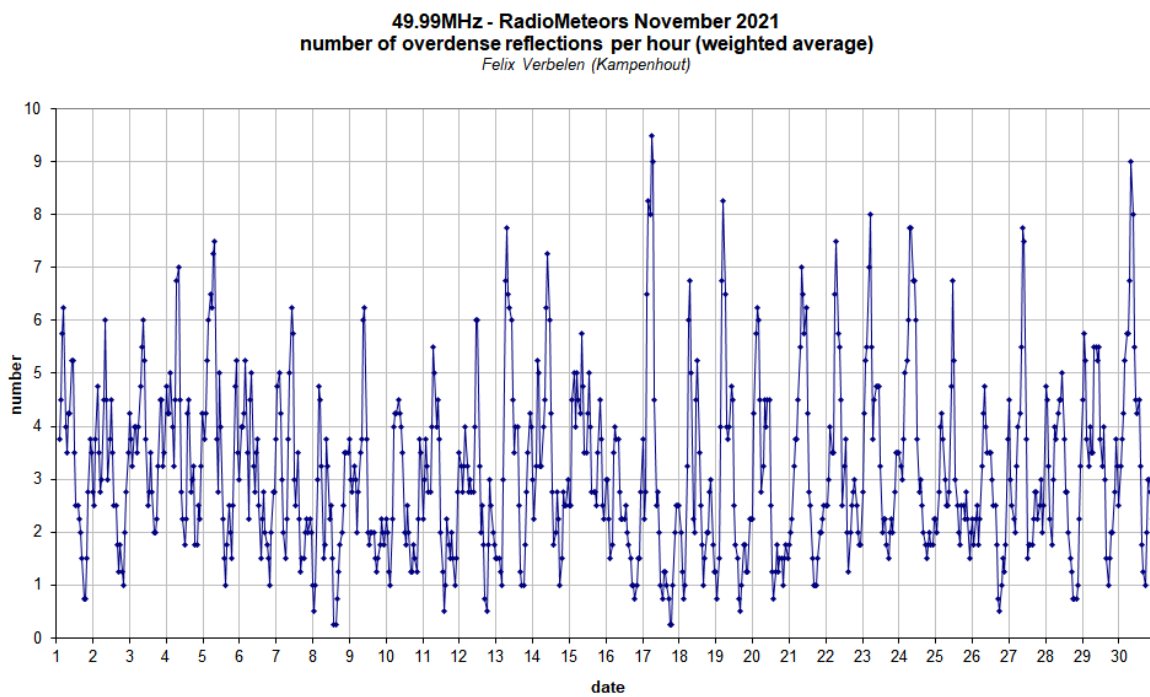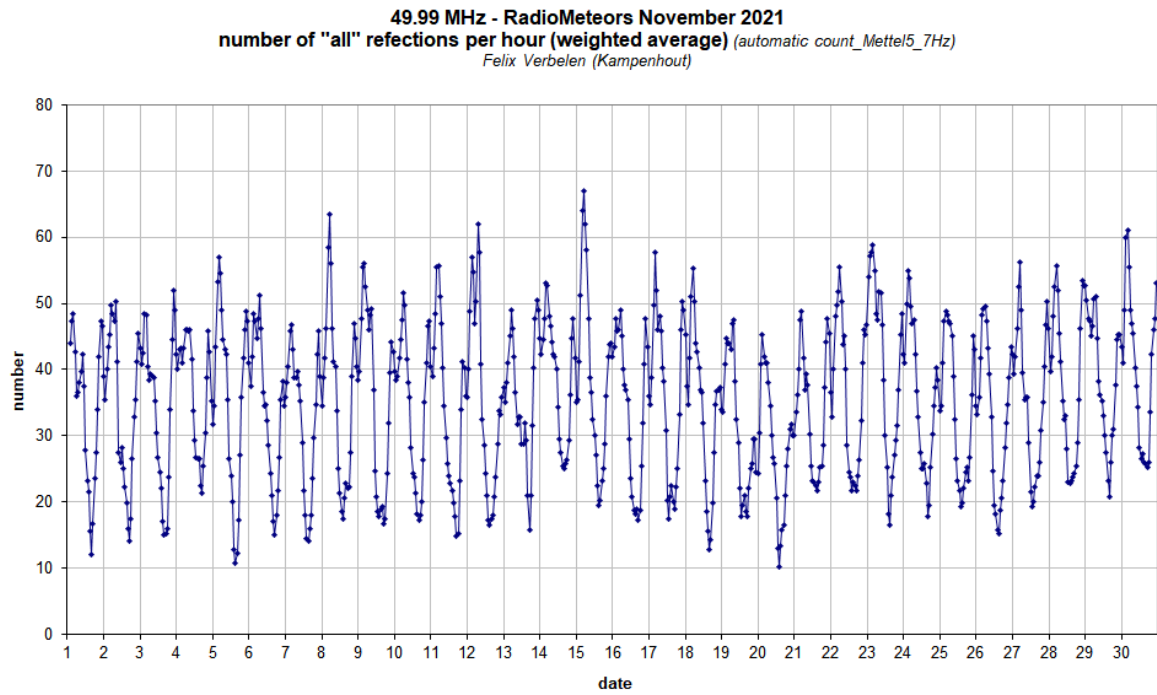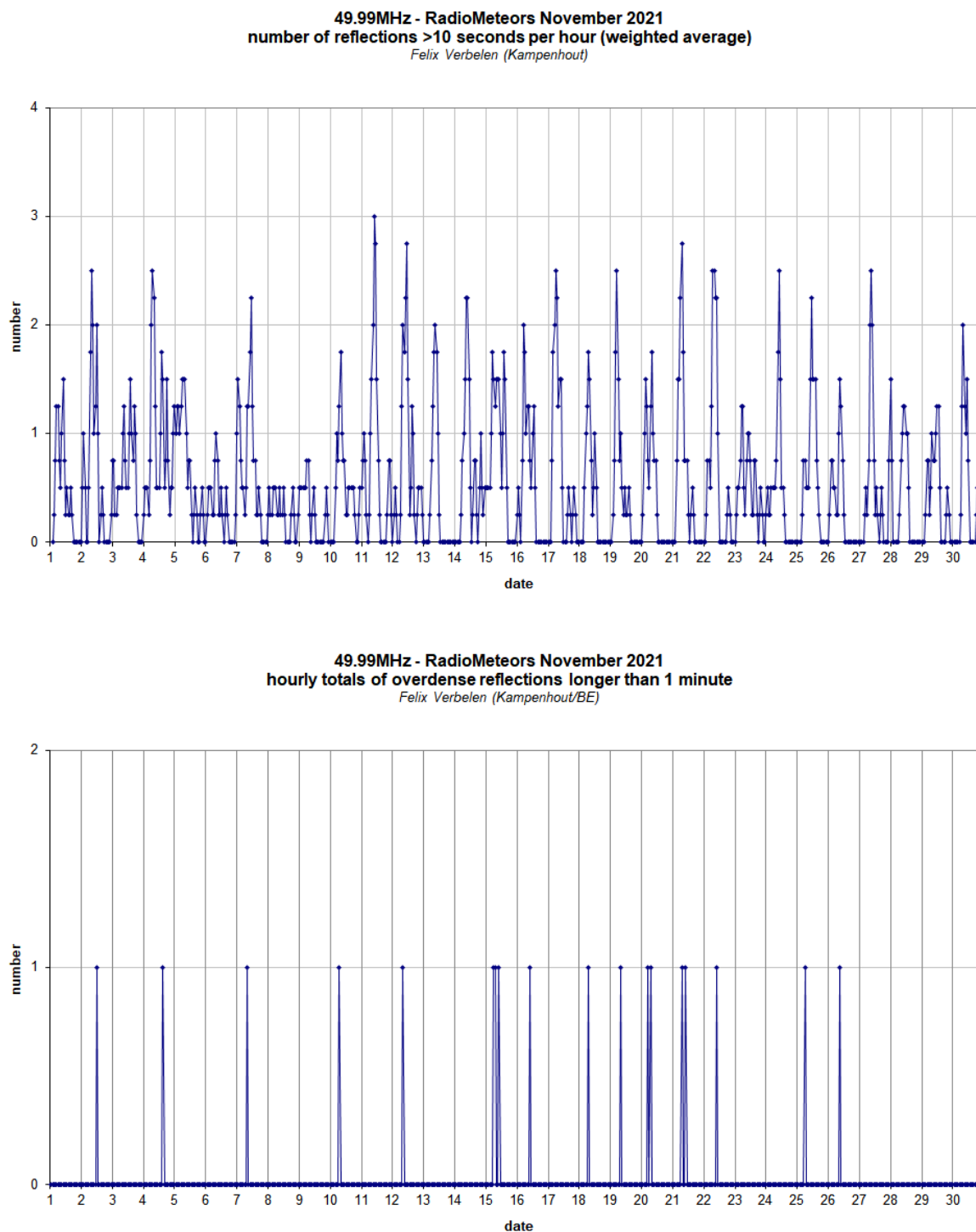
49.99 MHz - RadioMeteors October 2021
number of "all" refections per hour (weighted average) *(automatic count_Mettel5_7Hz)*
Felix Verbelen (Kampenhout)

49.99MHz - RadioMeteors October 2021
number of overdense reflections per hour (weighted average)
Felix Verbelen (Kampenhout)

Figure 3 – The hourly numbers of "all" reflections counted automatically, and of manually counted "overdense" reflections, as observed here at Kampenhout (BE) on the frequency of our VVS-beacon (49.99 MHz) during October 2021.

49.99MHz - RadioMeteors October 2021
number of reflections >10 seconds per hour (weighted average)
Felix Verbelen (Kampenhout)

49.99MHz - RadioMeteors October 2021
hourly totals of overdense reflections longer than 1 minute
Felix Verbelen (Kampenhout/BE)

Figure 4 – The hourly numbers of overdense reflections longer than 10 seconds and longer than 1 minute, as observed here at Kampenhout (BE) on the frequency of our VVS-beacon (49.99 MHz) during October 2021.
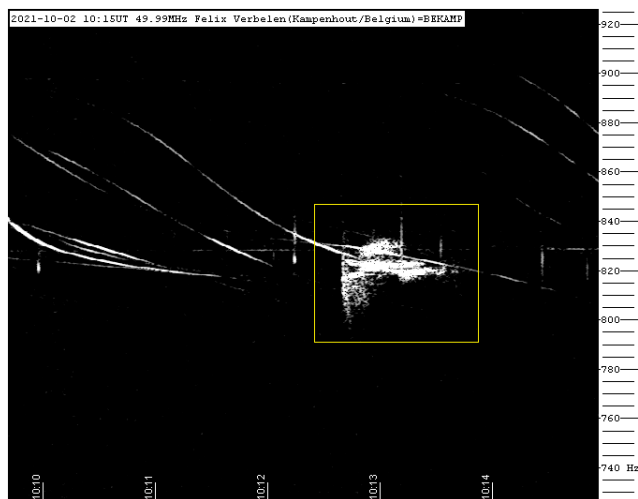
Figure 5 – Meteor reflection 2 October 2021, 10ʰ15ᵐ UT.
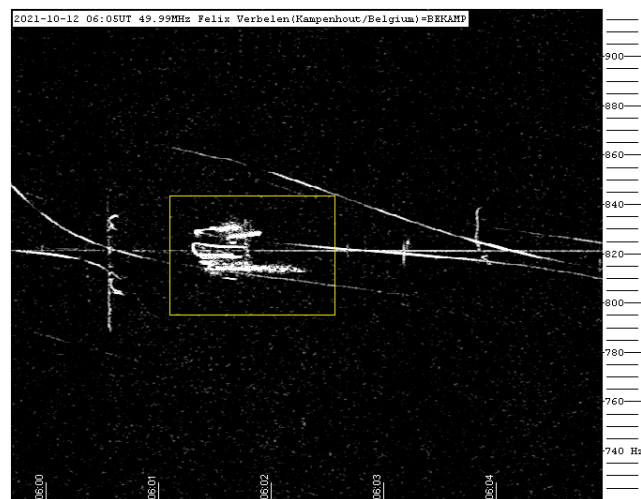
Figure 8 – Meteor reflection 12 October 2021, 06ʰ05ᵐ UT.
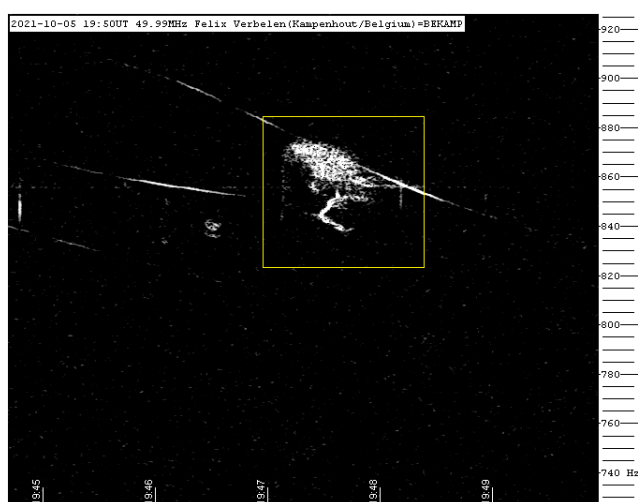
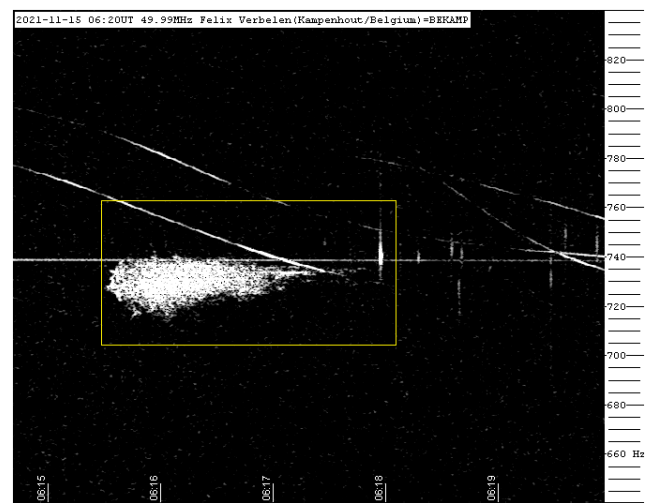*Figure 6* – Meteor reflection 5 October 2021, 19ʰ50ᵐ UT.
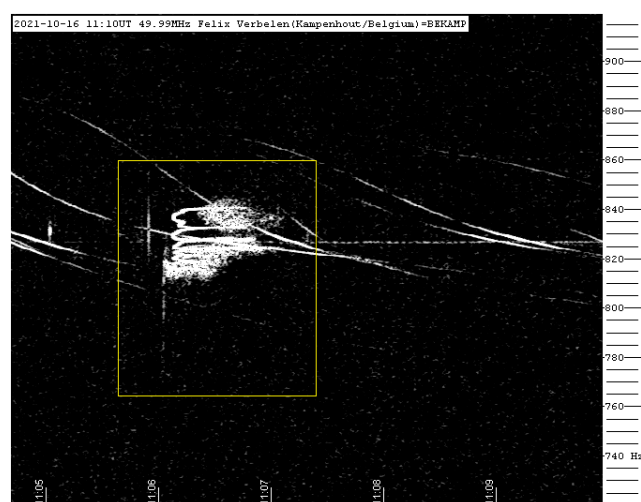
Figure 9 – Meteor reflection 16 October 2021, 11ʰ10ᵐ UT.
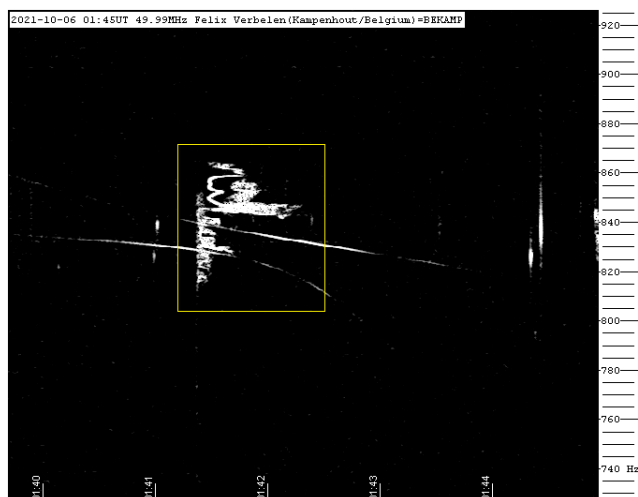
Figure 7 – Meteor reflection 6 October 2021, 01ʰ45ᵐ UT.
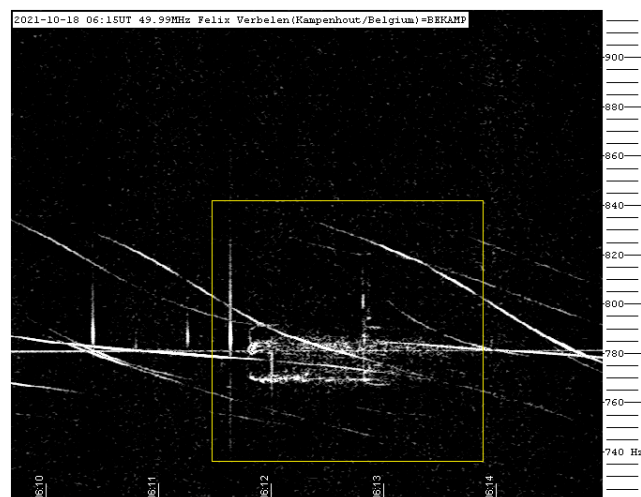
Figure 10 – Meteor reflection 18 October 2021, 06ʰ15ᵐ UT.
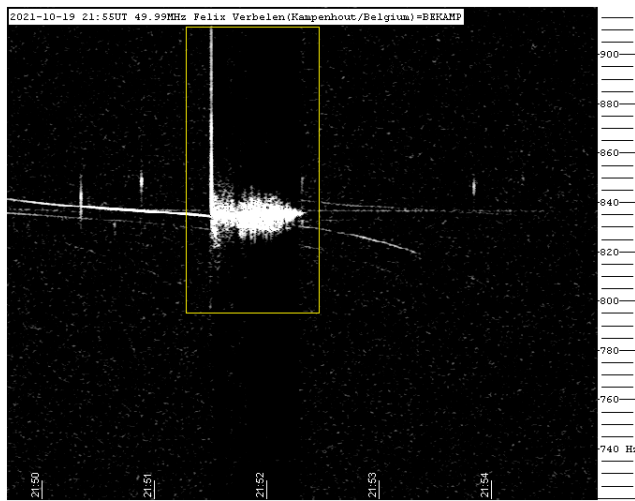
Figure 11 – Meteor reflection 19 October 2021, 21ʰ55ᵐ UT.
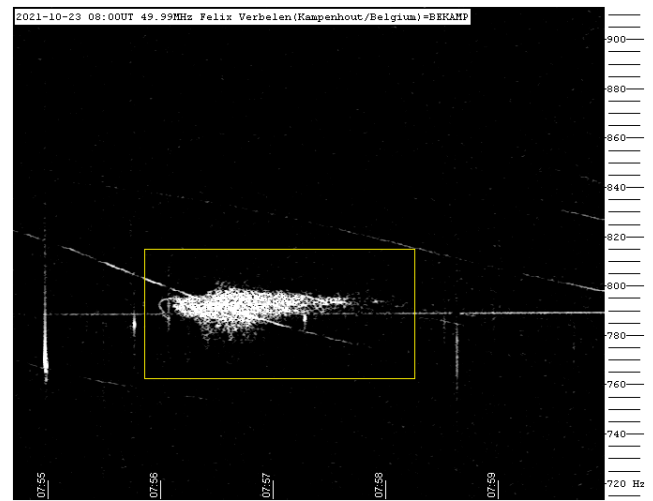
Figure 13 – Meteor reflection 23 October 2021, 08ʰ00ᵐ UT.
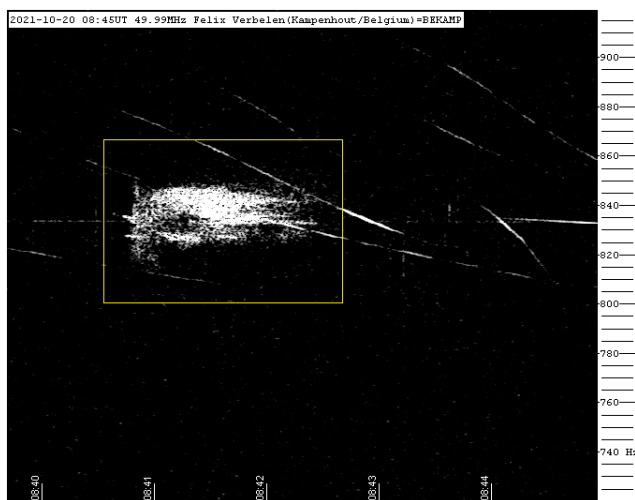
Figure 12 – Meteor reflection 20 October 2021, 08ʰ45ᵐ UT.

Radio meteors November 2021

Felix Verbelen

Vereniging voor Sterrenkunde & Volkssterrenwacht MIRA, Grimbergen, Belgium
`felix.verbelen@skynet.be`

An overview of the radio observations during November 2021 is given.

1 Introduction

The graphs show both the daily totals (*Figure 1 and 2*) and the hourly numbers (*Figure 3 and 4*) of "all" reflections counted automatically, and of manually counted "overdense" reflections, overdense reflections longer than 10 seconds and longer than 1 minute, as observed here at Kampenhout (BE) on the frequency of our VVS-beacon (49.99 MHz) during the month of November 2021.

The hourly numbers, for echoes shorter than 1 minute, are weighted averages derived from:

$$N(h) = \frac{n(h-1)}{4} + \frac{n(h)}{2} + \frac{n(h+1)}{4}$$

Local interference and unidentified noise remained moderate during most of the month and only on 4 days weak lightning activity was detected.

This month 18 reflections longer than 1 minute were observed here. A selection of these is shown in *Figures 5 to 14*.

In addition to the usual graphs, you will also find the raw counts in cvs-format[19] from which the graphs are derived.

The table contains the following columns: day of the month, hour of the day, day + decimals, solar longitude (epoch J2000), counts of "all" reflections, overdense reflections, reflections longer than 10 seconds and reflections longer than 1 minute, the numbers being the observed reflections of the past hour.

---

[19] https://www.meteornews.net/wp-content/uploads/2021/12/202111_49990_FV_counts.csv

Figure 1 – The daily totals of "all" reflections counted automatically, and of manually counted "overdense" reflections, as observed here at Kampenhout (BE) on the frequency of our VVS-beacon (49.99 MHz) during November 2021.

49.99MHz - RadioMeteors November 2021
daily totals of reflections longer than 10 seconds
Felix Verbelen (Kampenhout)

49.99MHz - RadioMeteors November 2021
daily totals of reflections longer than 1 minute
Felix Verbelen (Kampenhout)

Figure 2 – The daily totals of overdense reflections longer than 10 seconds and longer than 1 minute, as observed here at Kampenhout (BE) on the frequency of our VVS-beacon (49.99 MHz) during November 2021.

Figure 3 – The hourly numbers of "all" reflections counted automatically, and of manually counted "overdense" reflections, as observed here at Kampenhout (BE) on the frequency of our VVS-beacon (49.99 MHz) during November 2021.

49.99MHz - RadioMeteors November 2021
number of reflections >10 seconds per hour (weighted average)
Felix Verbelen (Kampenhout)

49.99MHz - RadioMeteors November 2021
hourly totals of overdense reflections longer than 1 minute
Felix Verbelen (Kampenhout/BE)

Figure 4 – The hourly numbers of overdense reflections longer than 10 seconds and longer than 1 minute, as observed here at Kampenhout (BE) on the frequency of our VVS-beacon (49.99 MHz) during November 2021.
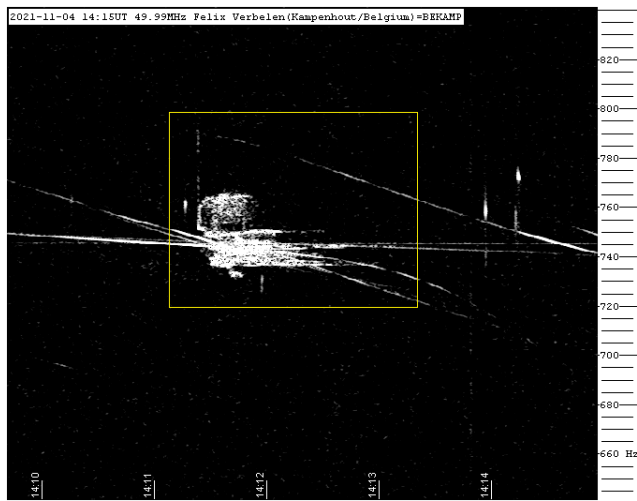
Figure 5 – Meteor reflection 4 November 2021, 14h15m UT.
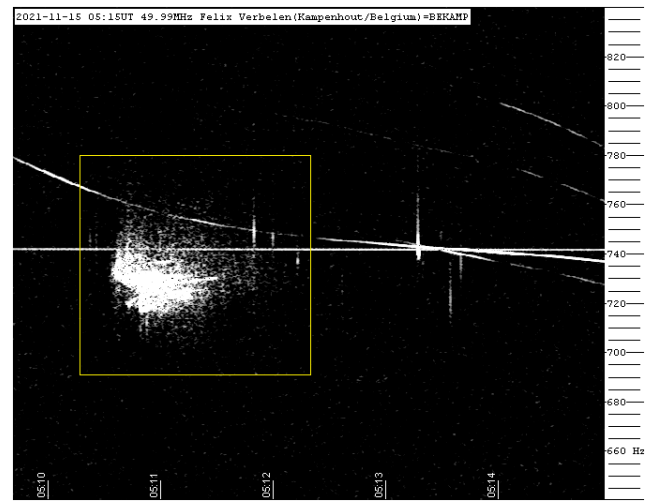
Figure 8 – Meteor reflection 15 November 2021, 05h15m UT.
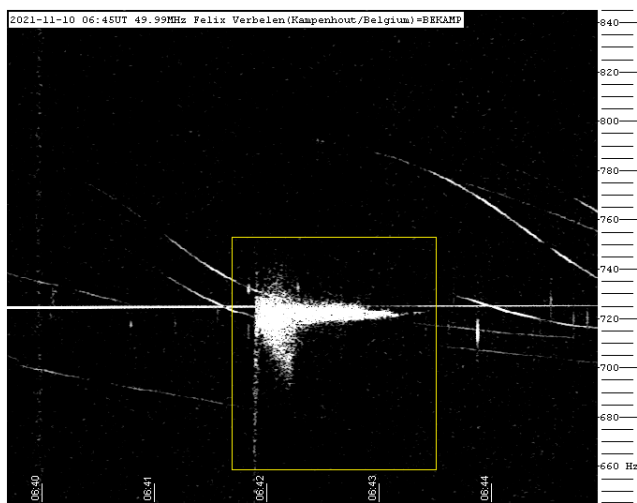
Figure 6 – Meteor reflection 10 November 2021, 06h45m UT.

Figure 9 – Meteor reflection 15 November 2021, 06h20m UT.
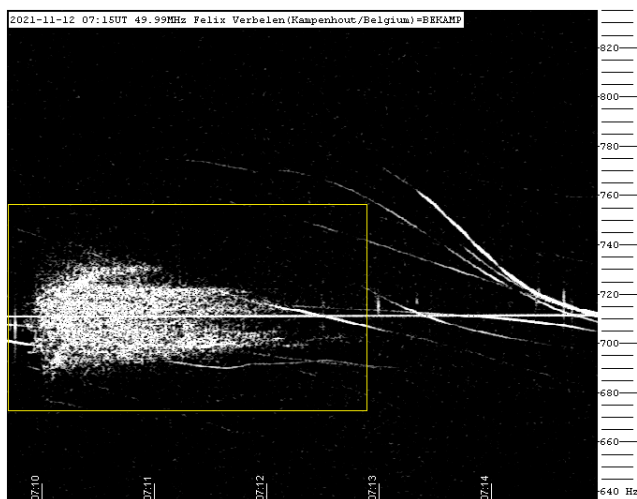
Figure 7 – Meteor reflection 12 November 2021, 07h15m UT.
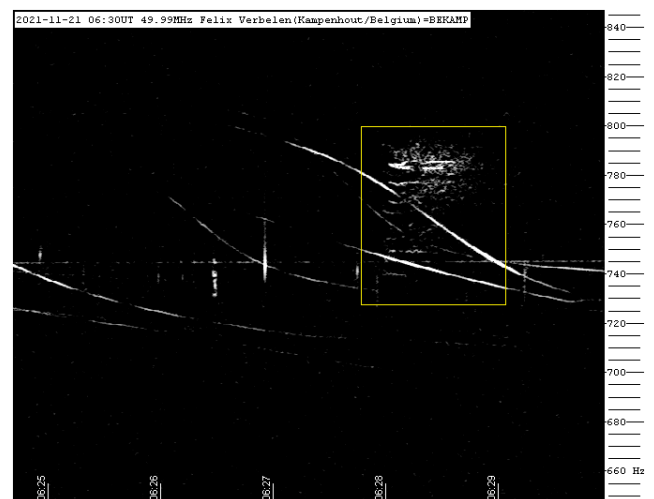
Figure 10 – Meteor reflection 21 November 2021, 06h30m UT.
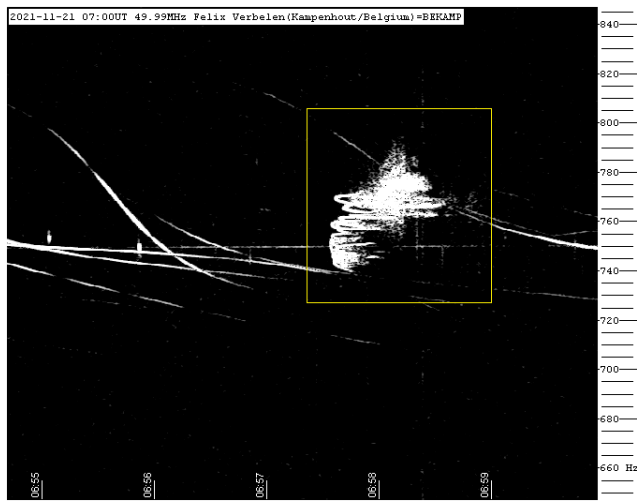
Figure 11 – Meteor reflection 21 November 2021, 07ʰ00ᵐ UT.
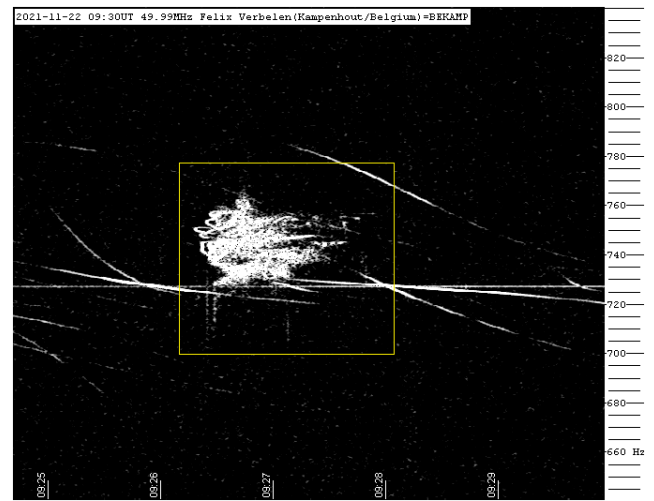
Figure 13 – Meteor reflection 22 November 2021, 09ʰ30ᵐ UT.
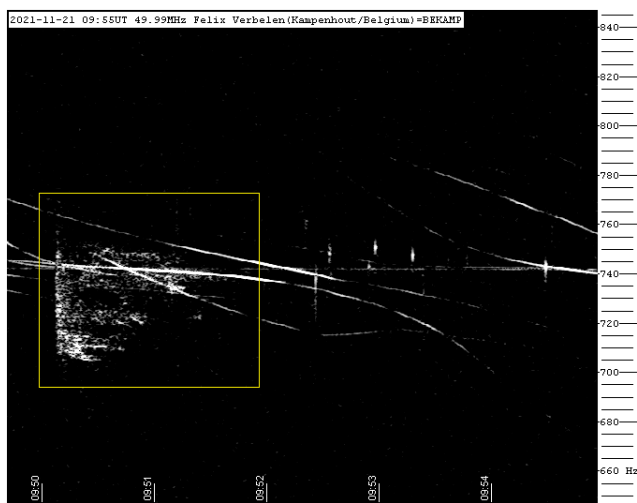
Figure 12 – Meteor reflection 21 November 2021, 09ʰ55ᵐ UT.
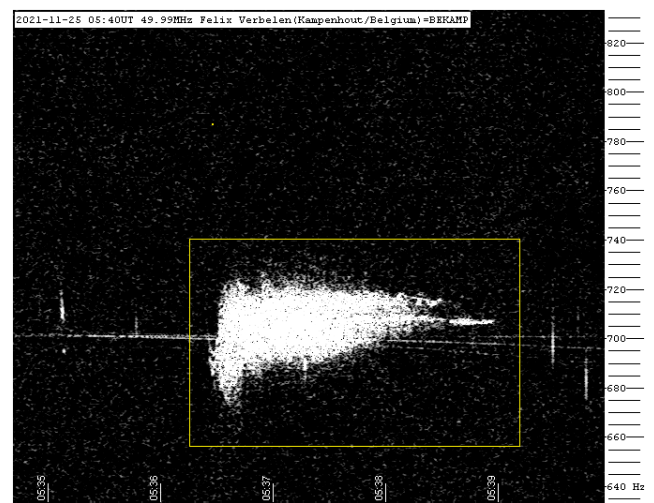
Figure 14 – Meteor reflection 25 November 2021, 05ʰ40ᵐ UT.

October 2021 report CAMS BeNeLux

Paul Roggemans

Pijnboomstraat 25, 2800 Mechelen, Belgium
paul.roggemans@gmail.com

A summary of the activity of the CAMS BeNeLux network during the month of October 2021 is presented. October 2021 had several clear nights and long-lasting clear spells at many other nights. A total of 51696 meteors has been recorded of which 62% was multi-station, resulting in 9669 good quality orbits.

1   Introduction

The long October nights with high meteor activity are probably the most promising month for the CAMS BeNeLux network. Unfortunately, most years it remains with "promising". Overcast and misty weather is most common during this autumn month in the BeNeLux. Would 2021 bring some good luck with October?

2   October 2021 statistics

Last year we got the worst-case weather scenario for the month October with not a single complete clear night for the entire network. Also 2019 had brought a poor month of October. October 2021 was a wet rainy month with a lot of cloud cover during the day, but with several clear nights and wide clear spells at night. For once we got lucky with this autumn month. 9669 orbits were collected (against 3305 in 2020) which is a new record for this month, doing slightly better than October 2018 when 9611 orbits were collected, including 1391 orbits in a single night with the Draconid outburst.

In total 51696 meteor detections were reported for all 94 operational cameras, 32268 of these could be used for a trajectory and orbit calculation, which is a multiple station score of 62%. A much better score than previous year when only 20135 meteors were detected of which 45% resulted in a trajectory solution. This month counted 23 nights with more than 100 orbits (12 in 2020). The best October night was 23–24 with as many as 926 orbits in a single night. Only two nights remained without any orbits, just like in 2020. The statistics of October 2021 are compared in *Figure 1* and *Table 1* with the same month in previous years since the start of CAMS BeNeLux in 2012. In 10 years, 257 October nights allowed to obtain orbits with a grand total of 38459 orbits collected during the month of October during all these years together.

Some CAMS stations were not operational due to technical problems or other reasons. October 2020 had a maximum of 90 cameras at 23 CAMS stations, 70.9 cameras on average available while October 2021 had 94 cameras at 26 CAMS stations and 82.2 cameras on average. The number of operational cameras increased thanks to a number of new

RMS cameras that were installed earlier this year. The advantage of these RMS cameras is that these are 100% automated and 7 on 7 operational.
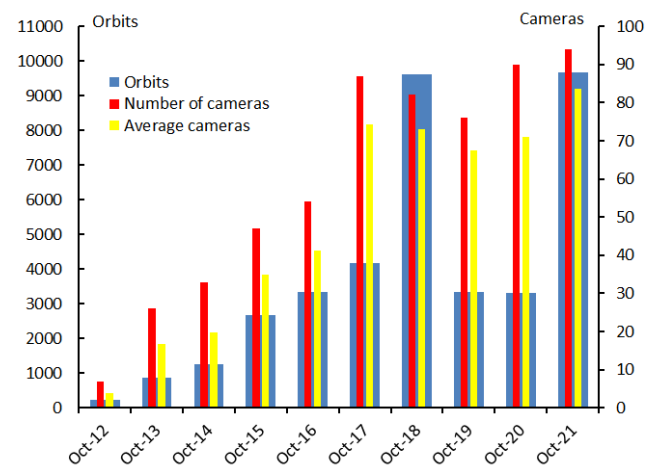
Figure 1 – Comparing October 2021 to previous months of October in the CAMS BeNeLux history. The blue bars represent the number of orbits, the red bars the maximum number of cameras running in a single night and the yellow bar the average number of cameras running per night.

Table 1 – October 2021 compared to previous months of October.

Year	Nights	Orbits	Stations	Max. Cams	Min. Cams	Mean Cams
2012	16	220	6	7	–	3.9
2013	20	866	10	26	–	16.8
2014	22	1262	14	33	–	19.7
2015	24	2684	15	47	–	34.8
2016	30	3335	19	54	19	41.3
2017	29	4163	22	87	45	74.4
2018	29	9611	21	82	52	73.0
2019	29	3344	20	76	47	67.5
2020	29	3305	23	90	52	70.9
2021	29	9669	26	94	70	82.2
Total	257	38459				

Again, no really perfect weather occurred for the Orionids apart from some partial clear sky 20–21–22 October, but CAMS BeNeLux could confirm the discovery by the Global Meteor Network of a new shortly active meteor shower (Vida et al., 2021).

3   Conclusion

The weather at night in October 2021 was in general favorable for CAMS BeNeLux. The large number of operational cameras, including several new RMS cameras combined with the favorable weather resulted in a new record number of orbits for the month of October.

References

Vida D., Šegon D., Roggemans P. (2021). "October zeta Perseid meteor shower (OZP#01131)". *eMetN*, **6**, 536–539.

---

[20] http://cams.seti.org/FDL/index-BeNeLux.html

November 2021 report CAMS BeNeLux

Paul Roggemans

Pijnboomstraat 25, 2800 Mechelen, Belgium
paul.roggemans@gmail.com

A summary of the activity of the CAMS BeNeLux network during the month of November 2021 is presented. 25832 meteors of which 14167 multiple station meteors were recorded. In total 4691 orbits were collected during this month, a third-best November month for CAMS BeNeLux.

1   Introduction

November is a typical autumn month with rather unstable weather over the BeNeLux. Completely clear nights are rare during this time of the year. However, during the long nights with 13 to 14 hours dark sky, it is also rare that clouds remain all night present. Very often clear gaps appear during which meteors can be registered. To be successful in a month like November is a matter of having enough cameras operational. With most stations running Auto CAMS seven days on seven, still a lot of double station meteors can be registered during periods with unexpected clear sky.

2   November 2021 statistics

CAMS BeNeLux detected 25832 meteors of which 14167 were multi-station (17241 in 2020 and 9339 in 2019), good for 4691 orbits (5441 in 2020, 3237 in 2019). This is less than previous year but still a much better result than in 2019. 2021 brought the third best month of November in ten years. AutoCams or RMS functioned at 24 camera stations, at 2 stations the cameras were only started when there was a chance for clear skies. Not all the camera stations could participate during the entire month.

This month counted 14 nights with more than 100 orbits (18 in 2020 and 10 in 2019). Two nights produced more than 500 orbits in a single night (2 in 2020 and 1 in 2019). The best November night in 2021 was 21–22 with as many as 1810 multi-station meteors, good for 578 orbits in this single night. Six nights remained without any orbits (2 in 2020). The statistics of November 2021 are compared in *Figure 1* and *Table 1* with the same month in previous years since the start of CAMS BeNeLux in 2012. In 10 years, 231 November nights allowed to obtain orbits with a grand total of 29927 orbits collected during November during all these years together.

While November 2020 had 88 cameras at best and 72.6 on average, November 2021 had 86 cameras at best and 81.6 on average. Since the last major expansion of CAMS BeNeLux in 2017, the number of operational cameras remained stable with a number of new cameras compensating the number of cameras that ceased participation in the CAMS network.
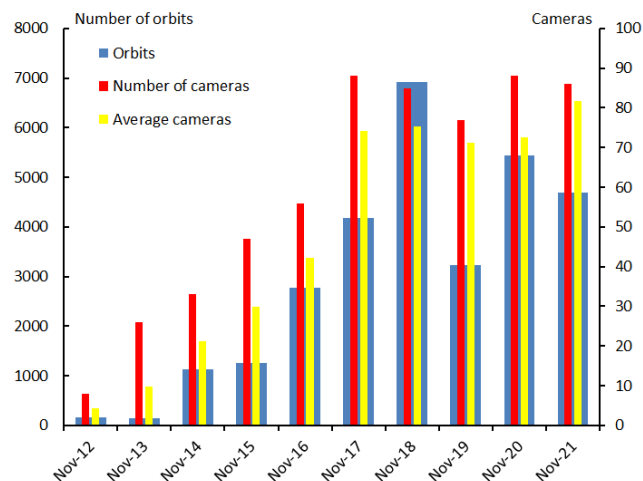

Figure 1 – Comparing November 2021 to previous months of November in the CAMS BeNeLux history. The blue bars represent the number of orbits, the red bars the maximum number of cameras running in a single night and the yellow bar the average number of cameras running per night.

Table 1 – November 2021 compared to previous months of November.

Year	Nights	Orbits	Stations	Max. Cams	Min. Cams	Mean Cams
2012	14	165	6	8	-	4.4
2013	13	142	10	26	-	9.8
2014	24	1123	14	33	-	21.1
2015	23	1261	15	47	10	29.8
2016	24	2769	19	56	19	42.2
2017	26	4182	22	88	57	74.2
2018	28	6916	21	85	59	75.3
2019	27	3237	20	77	60	71.1
2020	28	5441	23	88	57	72.6
2021	24	4691	26	86	74	81.6
Total	231	29927				

3   Conclusion

November 2021 brought fairly good autumn weather for the BeNeLux what resulted in a third-best November month during 10 years of CAMS BeNeLux.

Acknowledgment

---

[21] http://cams.seti.org/FDL/index-BeNeLux.html

The mission of MeteorNews is to offer fast meteor news to a global audience, a swift exchange of information in all fields of active amateur meteor work without editing constraints. MeteorNews is freely available without any fees. To receive a notification: https://www.meteornews.net/newsletter-signup/.

You are welcome to contribute to MeteorNews on a regular or casual basis, if you wish to. Anyone can become an author or editor, send an email to us. For more info read: https://meteornews.net/writing-content-for-emeteornews/

Contributing to this issue:

- *L. Barbieri*
- *H. Betlem*
- *B. Booz*
- *G. Brando*
- *Y. Harachka*
- *P. Jenniskens*
- *C. Johannink*
- *R. Kacerek*
- *K. Miskotte*

- *N. Moskovitz*
- *H. Ogawa*
- *J. Richert*
- *P. Roggemans*
- *I. Sergei*
- *S. Sposetti*
- *H. Sugimoto*
- *F. Verbelen*